Study on Development of Transmission Grid

INTERIM REPORT

- Sizing of System Rezerves in the Macedonian power systems for scenarios with large scale RES -

Carried out by:

Electricity Coordinating Center, Ltd.

Vojvode Stepe 412, Belgrade

March 2023

Issue and Revision Record

A	22 December 2022	Matija Kostic	Interim Report
		Predrag Miksa	
B	02 February 2023	Kliment Naumoski	
C	13 February 2023	Matija Kostic	
D	10 March 2023	Kliment Naumoski,	
		Stojan Malcheski	
		Zivorad Serafimoski	
E	16.03.2023.	Matija Kostic	
F	12.04.2023	Kliment Naumoski	

Information class: Standard

Contents

Contents i

Abbreviations ii

EXECUTIVE SUMMARY 3

1 INTRODUCTION 7

2 ANALYZED SCENARIOS 8

3 METHODOLOGY 12

3.1 Estimation of system (operating) reserves for power and frequency regulation 13
3.1.1 Sources of imbalances 15
3.1.2 Forecast errors and metrics 16
3.1.3 FRR sizing in MEPSO control area in case of higher level of VRE penetration 17

4 SYSTEM RESERVES RELATED ANALYSES 25

4.1 Input data analysis 25
4.1.1 Analysis of open-loop ACE 25
4.1.2 Load forecast error analysis 29
4.1.3 Wind forecast error analysis 32
4.1.4 Solar forecast error analysis 35
4.2 Balancing reserve dimensioning results 38
4.2.1 Green scenario 43
4.2.2 Rapid scenario 46
4.2.3 Slow scenario 49
4.3 Mid-term reserve provision analysis 52

5 CONCLUSIONS 55

6 REFERENCES 58

7 APPENDIX 59

7.1 Modeling of reserve in ANTARES software tool 59
7.2 Balancing reserve dimensioning detailed results 60

Abbreviations

ACE	- Area Control Error
ACEol	- Open Loop Area Control Error
aFRR	- Automatic Frequency Restoration Reserve
CBA	- Cost Benefit Analysis
CDF	- Cumulative probability density function
CGES	- Montenegrin Transmission System Operator
CY	- Climatic year
EMS	- Serbian Transmission System Operator
ENTSO-E	- European Network of Transmission System Operators for Electricity
ERAA	- European Resource Adequacy Assessment
FCR	- Frequency Containment Reserve
FOR	- Forced outage rate
FRR	- Frequency Restoration Reserve
LFC	- Load Frequency Control
MAPE	- Mean Absolute Percentage Error
MCY	- Monte Carlo year
MEPSO	- Macedonian Transmission System Operator
mFRR	- Manual Frequency Restoration Reserve
nRMSE	- Normalized mean root square error
NTC	- Net Transfer Capacity
PEMMDB	- Pan-European Market Modeling Database
Q-Q	- Quantile-quantile
RES	- Renewable Energy Sources
RR	- Replacement Reserve
SAFA	- Synchronous Area Framework Agreement
SI	- System imbalance
SMM	- Serbia-Macedonia-Montenegro (control block)
SO GL	- System Operation Guideline
TSO	- Transmission System Operator
TY	- Target Year
TYNDP	- Ten-Year Network Development Plan
VRE	- Variable renewable energy

EXECUTIVE SUMMARY

The presented study has investigated the impacts of different levels of VRE installed capacities in North Macedonia on the required secondary and tertiary reserve level, as well as the ability of the system to provide required reserve capacity, taking into account the cooperation with neighboring systems within SMM control block.

Based on the results, recommendations for improvements in MEPSO business processes that should enable more efficient RES integration while preserving safe and secure system operation have been proposed.

Scenarios and assumptions

In order to investigate the impacts of very high levels of variable renewable sources on required level of balancing reserve (secondary and tertiary) as well as on the power system operation and capability to provide required reserve capacity, three development scenarios (Green, Rapid and Slow) were analyzed, for three different target years (2025, 2030 and 2040). RES (i.e. wind and solar) installed capacities are shown in the following table:

	RES Development Scenarios for 2025, 2030 and 2040 [MW]								
Type	2025			2030			2040		
	Slow	Green	Rapid	Slow	Green	Rapid	Slow	Green	Rapid
Wind	50	170	460	170	410	944	446	750	1509
Solar	95	246	903	315	630	2228	806	1383	3941
Total	145	416	1363	485	1040	3172	1252	2133	5450

Total RES installed capacity is in relatively wide range, from 145 MW in 2025 (in case of Slow scenario of RES development) to 5450 MW in 2040 (in case of Rapid scenario of RES development). It should be emphasized that these values were selected by the MEPSO, based on expected RES applications. All differences between the numbers used in the report and those found in the Strategy are consequence of the fact that RES applications are coming very fast and are above RES targets on a long term in the Strategy. Therefore, in order to analyze the most critical case to the power system, figures listed in table above have been chosen.

Impact on required balancing reserve level

In order to estimate required secondary and tertiary reserve level that is sufficient for integration of planned VRE levels on long-term planning horizon (2025-2040), study-specific methodology has been developed for the MEPSO, based on general requirements and recommendations given in System Operation Guidelines, National Grid Code as well as ENTSO-E CE Synchronous Area Framework Agreement for Regional Group Continental Europe.

The proposed methodology is based on probabilistic approach, taking into account uncertainties in forecast of all components that cause system imbalances (load, wind, solar, thermal). It was demonstrated that the system imbalance can be decomposed into two components: forecast error component (stochastic imbalances) and noise component (deterministic imbalances). In order to forecast future system imbalances, depending on selected VRE penetration level, demand growth and other scenario-specific input assumptions, these two components were estimated separately. Forecast error component has been estimated using historical data of wind and solar forecast errors, provided by the MEPSO, as well as load forecast error taken from ENTSO-e Transparency Platform, while noise component has been estimated using hourly ramps of provided hourly time-series for load, wind and solar.

Total secondary and tertiary reserve (FRR) was determined as a 99th percentile of system imbalance in both positive and negative direction, while secondary reserve (aFRR) was determined as 99th percentile of corresponding noise component. The results of secondary and tertiary reserve dimensioning are presented on following diagrams, for different assumed levels of RES forecast error (4%, 6%, 8%, 10% and 12%). There are nine different points on all diagrams for one selected level of RES forecast error, representing three different target years and three different VRE development scenarios.

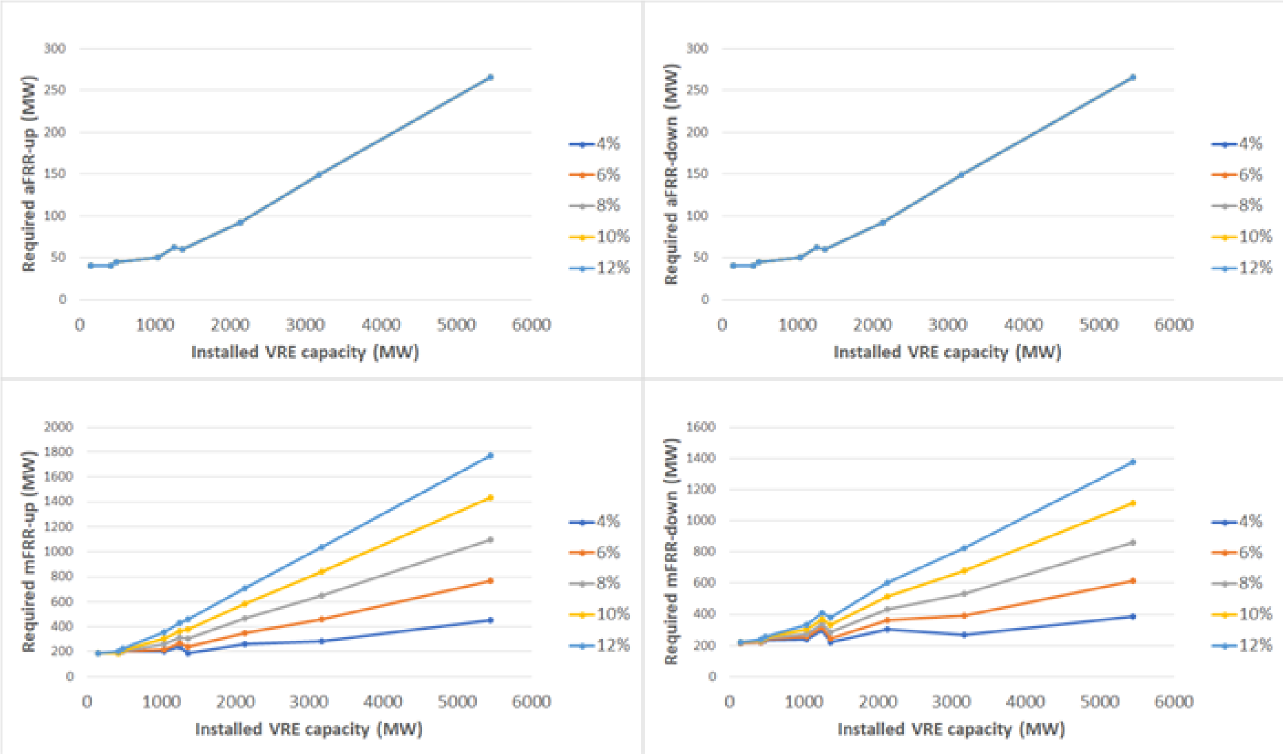

However, it should be noted, that according to assumed rule for dimensioning of secondary reserve, by definition aFRR does not depend on RES forecast error level, but only on corresponding ramps of load, wind and solar time-series.

Secondary reserve (aFRR) increases slowly at the beginning of the analyzed period as the installed VRE capacity grows, from the value of 41 MW, which is very close to the present aFRR level calculated based on deterministic methodology. Increase of installed VRE capacity up to 1363 MW leads to increase of required secondary reserve for 20 MW (in both directions since aFRR is symmetric). At the same time, an increase of tertiary reserve depend on assumed level of RES forecast error, and is around 16 MW in case of RES forecast error at level of 4% and 283 MW in case of RES forecast error of 12%.

Further increase of VRE installed capacity leads to increase of required secondary and tertiary reserve with more or less linear trend.

In addition, initial market simulations have been carried out in order to test the capability of Macedonian power system to provide required level of secondary and tertiary reserve in terms of required capacity (MW). This analysis has been carried out only for target year 2025 and Rapid scenario for 700 different MC years, in order to estimate the impact on power system operation on mid-term planning horizon. It was concluded that there are some critical periods in the year, when required level of secondary and tertiary reserve cannot be procured from local power plants in MEPSO control area. In such a situation it was assumed that up to 30% of required reserve capacity (by reserve product) can be imported from neighboring power systems within SMM control block. However, it was also concluded that there are critical MC years where allocated cross-border capacity reserve must be greater than 30% of reserve requirement.

Average of secondary reserve provision over all 700 simulated MC years is practically constant and equal approximately to the required value. On the other hand, in case of tertiary reserve, the situation is a little different, since inability of Macedonian system to procure required reserve level is reduced. The main reason for this behavior lies in the fact that that maintenance period for thermal units in MEPSO market area is assumed to be during the summer. Average of tertiary reserve provision is depicted on following two diagrams.

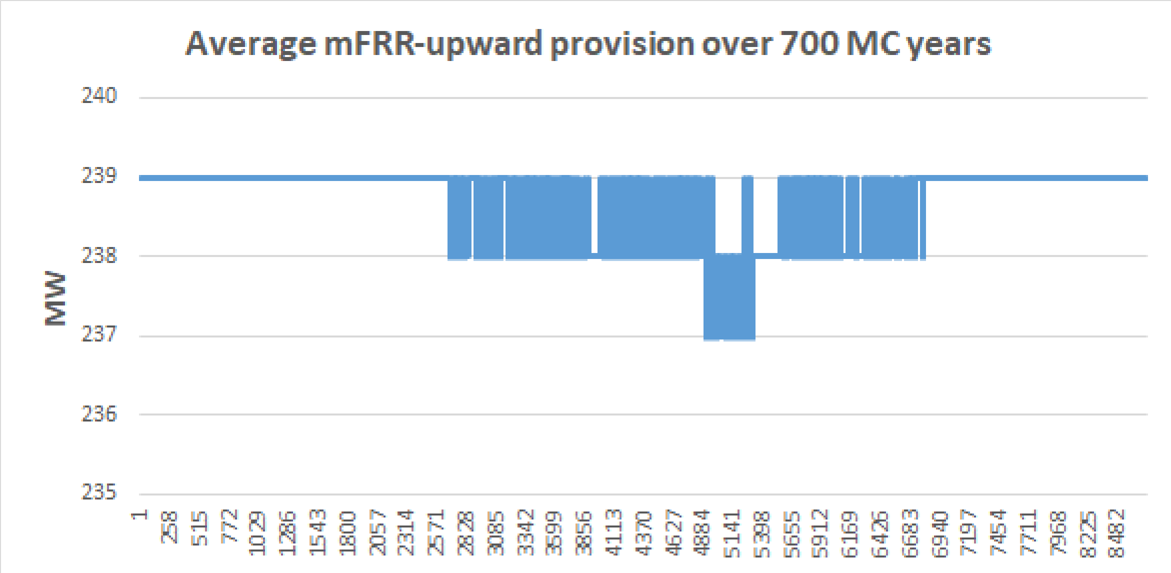

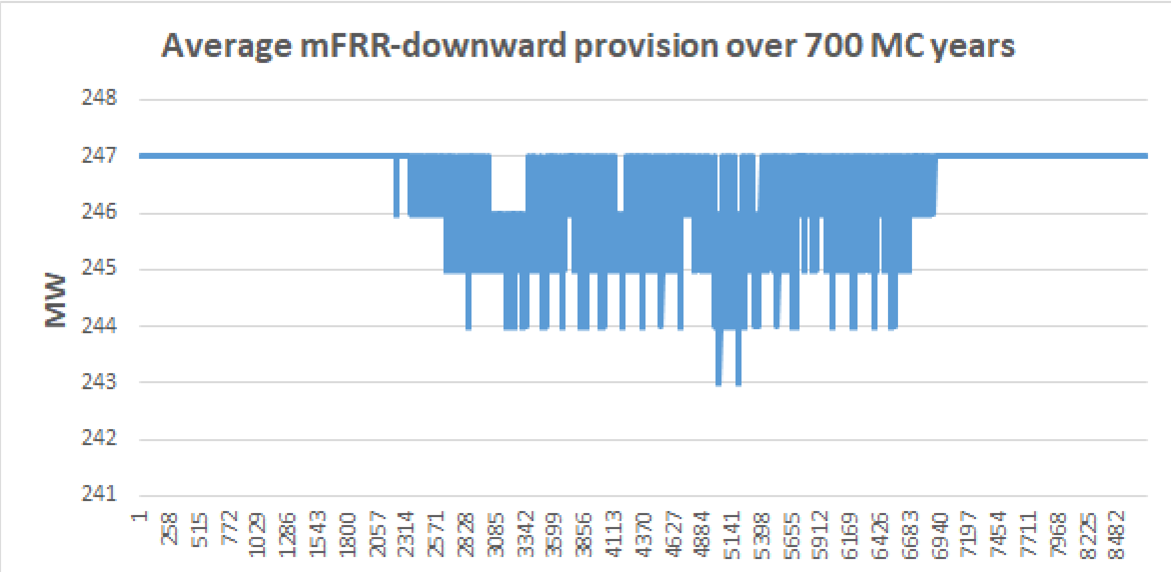

Recommendations for improvements of MEPSO core business processes related to RES integration

In order to get more accurate results related for reserve sizing in the future, it is recommended that all necessary data from history should be stored by the MEPSO and accompany quality analysis of data should be performed. In order to achieve that, the following information should be stored:

- 15-min (or hourly) load forecast and realization
- 15-min (or hourly) wind and solar forecast and realization
- 1-min (or 15-min) Area Control Error (ACE)
- 15-min (or hourly) balancing reserve activation
- Unavailable power due to forced outages of thermal power plants

All these data should be statistically analyzed and processed in order to obtain all necessary information for balancing reserve sizing on short-term horizon by the MEPSO in the future.

Other planning and operational measures that can decrease required balancing reserve level are:

- Better quality of load, wind and solar forecasts
- Common dimensioning in SMM control block
- Moving to 15-min dispatch interval in the future

Measures that can increase available capacity for balancing reserve are:

- Installation of additional battery storage systems (for PV peak shaving)
- Demand side response
- Construction of pumped storage power plant Cebren

DISCLAIMER:

It should be emphasized that all the results presented here which depict the impact of VRE on secondary and tertiary reserve required level depends on many input assumptions and quality of provided input data. Therefore, the goal of the study is to estimate an expected level of required reserve for analyzed scenarios as well as to develop the methodology for reserve sizing. Therefore, all results presented here are general results for future system state calculated on long-term planning horizon. All analyses should be repeated with more precise data on mid and short-term horizon in order to estimate more realistic values. In other words, at least, 15-min data should be provided for VRE and load realizations, while in case of open-loop ACE, 1-min data should be provided as well as in order to get a better quality of performed calculations. In addition, the analyses should be repeated sequentially after addition of a few MW in VRE, for instance when additional X MW of VRE capacity are installed. Using this method, the input assumptions will be corrected. Finally, time granularity related to input data is also of interest.

1 INTRODUCTION

According to energy law, the MEPSO as a Transmission System Operator (TSO) is responsible for long-term development planning of transmission system in Republic of North Macedonia.

According to the Grid Code for electricity transmission (Grid Code), MEPSO plans the development of the electricity transmission network in a way that will ensure its safe and economically justified operation in the interest of all users. The basic document in which the directions for the development of the transmission network are defined and the optimal plan for development activities, interventions and projects is prepared is **Transmission Network Development Study (Study).**

The goal of the Study is to define a clear concept, principles and strategy for the development of 110 kV and 400 kV voltage level in the national transmission network, as well as the role of individual lines in the transmission of electricity. In order to achieve that goal, various network and market analyses and calculations should be carried out.

According to the Terms of Reference (i.e. the project technical specification) the following tasks should be conducted as a part of market analyses:

1. **Indicators for estimation of system (operating) reserves for power and frequency regulation**
2. Indicators for assessing the adequacy of the system,
3. Benefits and indicators for applying the CBA project evaluation methodology.

This report describes task No.1 under the study and contains the description of analyzed scenarios of RES development in MEPSO control area, developed methodology for balancing reserve sizing on long-term planning horizon, as well as the results of balancing reserve sizing and the impact to system operation.
All necessary input data were provided by the MEPSO or obtained from publicly available sources, such as ENTSO-E Transparency platform. The methodology for secondary and tertiary reserve sizing was developed in coordination with MEPSO.

NOTE: All input data regarding the rest of the interconnection, used in the analysis of reserve provision, were taken from ENTSO-E PEMMDB database used for TYNDP 2022. The modeled region and the way of modeling of individual countries are shown on the following figure.

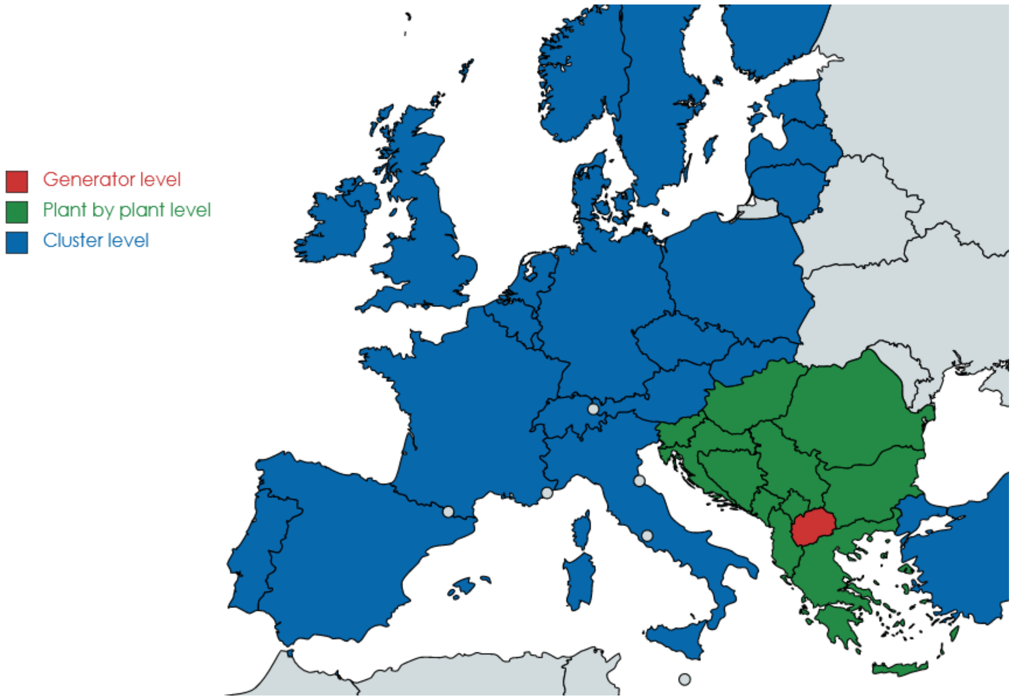

Figure 1.1 – Geographical scope of modeled systems

2 ANALYZED SCENARIOS

This chapter describes the input data for MEPSO market area. All data were provided by the MEPSO in PEMMDB format (version 3.5) and encompasses thermal power plants data, renewables data (by power plant), hydro power plants data, NTC values towards neighboring systems as well as demand forecast and distribution by transmission network bus bars.

Forecasted final electricity consumption in MEPSO market areas as well as corresponding peak demand are presented in tables below. All data presents an average over all 35 climatic years (1982-2016) and are in accordance with publicly available data from ENTSO-E TYNDP 2022 and ERAA 2021.

Table 2.1 – Macedonian demand forecast (TWh)

Market Node	2025	2030	2040
MK00	8.1	8.9	11.0

Table 2.2 – Macedonian peak demand (MW)

Market Node	2025	2030	2040
MK00	1562	1686	2092

Demand forecast on country level has been provided by the MEPSO within *„A00_DevelopmentStudyLDC.xlsm"* excel file, for all 35 climatic years. All provided time-series for 2025 and 2030 are in accordance with ERAA 2022 study, while the data for 2040 were estimated by the MEPSO. Demand growth rate is the highest in 2025, with 2022 as a reference year, and is equal to 5.5%. Demand growth rate in 2030 compared to 2025 is 5.2%, while in 2040 growth rate is 4.3%.

Input data related to thermal power plants are presented in the following table. It can be seen that only lignite and gas fired power plants are present in Macedonian generation mix in period 2025-2040. All power plants parameters were provided within „Main and Thermal" excel file in PEMMDB format. It should be emphasized that efficiency and corresponding heat rates are the same as in generic ENTSO-E data. Therefore, there is no information about heat rate at minimum and maximum generation level.

In addition, heat rate of steam unit (ST) in TETO Skopje was estimated according to the following relation:

$$HR_{GT} = \left(1 + \frac{P_{ST}^{max}}{P_{GT}^{max}}\right) \cdot HR_{CCGT}$$

Table 2.3 – Macedonian thermal capacities (TWh)[1]

Generating unit name	Commissioning date	Decommissioning date	Fuel type	Net maximum generating capacity (MW)	Net minimum stable generation (MW)	Efficiency	Forced outage rate (ratio)	Forced outage duration (days)	Min-down time (h)	Min up time (h)	VO&M (EUR/MWh)
Bitola G1-110	01/01/1984	31/12/2024	Lignite	150	100	0.4	0.1	45	11.0	11.0	3.7
Bitola G2-400	01/01/1984	31/12/2024	Lignite	150	100	0.4	0.1	45	11.0	11.0	3.7
Bitola G3-400	01/01/1988	31/12/2024	Lignite	150	100	0.4	0.1	45	11.0	11.0	3.7
TPP Oslomej	01/01/1950	01/01/2019	Lignite	120	70	0.4	0.1	1	11.0	11.0	3.7
TPP Negotino	01/01/1978	01/01/2020	Heavy oil	200	160	0.4	0.1	1	3.0	3.0	3.7
TETO-GT	01/01/2010	31/12/2100	Gas	199	6	0.6	0.1	30	2.0	2.0	1.4
TETO-ST	01/01/2010	31/12/2100	Gas	51	11	0.6	0.1	30	2.0	2.0	1.4
Energetika	01/01/2000	31/12/2100	Gas	30	2	0.4	0.1	1	5.0	5.0	1.4
Kogel	01/01/2000	31/12/2100	Gas	30	18	0.4	0.1	1	5.0	5.0	1.4
Bitola Gas	01/01/2025	31/12/2100	Gas	250	6	0.6	0.1	30	2.0	2.0	1.4
Skopje Gas	01/01/2028	31/12/2100	Gas	200	6	0.6	0.1	30	2.0	2.0	1.4

[1] Forced outage durations of thermal units were assumed to be one day, according to agreement with the MEPSO.

On the other hand, forced outage rates and durations are given per generating unit. As a consequence, thermal availability time-series within the model were generated stochastically.

Data related to hydro power plants were provided for tree scenarios (Green, Rapid and Slow), within „Renewables“ excel file in PEMMDB format. Installed capacities by power plant and type are presented in following three tables for all three scenarios.

It should be emphasized here that according to the MEPSO Network Code as well as the implemented solution, all power plants have technical capability to contribute in provision of secondary and tertiary reserve.

Table 2.4 – Macedonian hydro capacities (2025-2040) – Green scenario

Power plant	Commissioning date	Power plant type	Net maximum generating capacity (MW)	Net minimum stable generation (MW)
HPP Vrutok	existing	Reservoir	172.0	10.0
HPP Vrben	existing	Run of River	17.2	8.0
HPP Raven	existing	Run of River	24.3	12.0
HPP Globocica	existing	Reservoir	41.6	8.0
HPP Spilje	existing	Reservoir	84.0	15.0
HPP Tikves	existing	Reservoir	116.0	15.0
HPP Kozjak	existing	Reservoir	88.0	31.0
HPP Sv Petka	existing	Reservoir	37.0	6.0
HPP Veles	01/01/2030	Reservoir	93.0	19.0
HPP Gradec	01/01/2030	Reservoir	76.0	16.0
HPP Globocica G3	01/01/2030	Reservoir	21	8.0
PSHPP Cebren	01/01/2040	Open Loop Pumping	332.9	25.0
HPP Dubrovo	01/01/2040	Run of River	29.6	4.0
HPP D.Kapija	01/01/2040	Run of River	24.7	4.0
HPP Krivolak	01/01/2040	Run of River	19.8	4.0
HPP Babuna	01/01/2040	Run of River	9.8	4.0
HPP Zgropolci	01/01/2040	Run of River	14.0	4.0
HPP Gradsko	01/01/2040	Run of River	16.6	4.0
HPP Kukurecani	01/01/2040	Run of River	16.6	4.0
HPP Miletkovo	01/01/2040	Run of River	22.2	6.0
HPP Gjavato	01/01/2040	Run of River	18.4	4.0
HPP Gevgelija	01/01/2040	Run of River	16.8	4.0

Table 2.5 – Macedonian hydro capacities (2025-2040) – Rapid scenario

Power plant	Commissioning date	Power plant type	Net maximum generating capacity (MW)	Net minimum stable generation (MW)
HPP Vrutok	existing	Reservoir	172.0	10.0
HPP Vrben	existing	Run of River	17.2	8.0
HPP Raven	existing	Run of River	24.3	12.0
HPP Globocica	existing	Reservoir	41.6	8.0
HPP Spilje	existing	Reservoir	84.0	15.0
HPP Tikves	existing	Reservoir	116.0	15.0

Power plant	Commissioning date	Power plant type	Net maximum generating capacity (MW)	Net minimum stable generation (MW)
HPP Kozjak	existing	Reservoir	88.0	31.0
HPP Sv Petka	existing	Reservoir	37.0	6.0
HPP Veles	01/01/2030	Reservoir	93.0	19.0
HPP Gradec	01/01/2030	Reservoir	76.0	16.0
HPP Globocica G3	01/01/2030	Reservoir	21	8.0
PSHPP Cebren	01/01/2040	Open Loop Pumping	332.9	25.0
HPP Dubrovo	01/01/2040	Run of River	29.6	4.0
HPP D.Kapija	01/01/2040	Run of River	24.7	4.0
HPP Krivolak	01/01/2040	Run of River	19.8	4.0
HPP Babuna	01/01/2040	Run of River	9.8	4.0
HPP Zgropolci	01/01/2040	Run of River	14.0	4.0
HPP Gradsko	01/01/2040	Run of River	16.6	4.0
HPP Kukurecani	01/01/2040	Run of River	16.6	4.0
HPP Miletkovo	01/01/2040	Run of River	22.2	6.0
HPP Gjavato	01/01/2040	Run of River	18.4	4.0
HPP Gevgelija	01/01/2040	Run of River	16.8	4.0

It can be seen that total installed capacity is currently around 600 MW and that input data for Green and Rapid scenarios are the same. In case of these two scenarios three hydro storage power plants start to operate till 2030 (Veles 93 MW, Gradec 76 MW and Globocica 21 MW), while in 2040 pumped storage power plant Cebren of 333 MW turbining capacity starts to operate as well as a lot of Run of River hydro power plants with total installed capacity around 189 MW.

Table 2.6 – Macedonian hydro capacities (2025-2040) – Slow scenario

Power plant	Commissioning date	Power plant type	Net maximum generating capacity (MW)	Net minimum stable generation (MW)
HPP Vrutok	existing	Reservoir	172.0	10.0
HPP Vrben	existing	Run of River	17.2	8.0
HPP Raven	existing	Run of River	24.3	12.0
HPP Globocica	existing	Reservoir	41.6	8.0
HPP Spilje	existing	Reservoir	84.0	15.0
HPP Tikves	existing	Reservoir	116.0	15.0
HPP Kozjak	existing	Reservoir	88.0	31.0
HPP Sv Petka	existing	Reservoir	37.0	6.0
PSHPP Cebren	01/01/2040	Open Loop Pumping	332.9	25.0

On the other hand, in case of Slow scenario, only pumped storage hydro power plant Cebren enters in operation till 2040.

Renewables installed capacities (wind, solar and biomass) for tree analyzed scenarios (Green, Rapid and Slow) are presented in following tables.

In case of Green scenario, total installed capacity in wind power plants grows from 170 MW in 2025 to 750 MW in 2040, while solar installed capacities coming from distributed rooftop sources goes from 70 MW to 400 MW in 2040. On the other hand, installed capacity in solar PV farms dramatically grows up from 193 MW in 2025 to 1000 MW in 2040.

Table 2.7 – Renewables installed capacity in North Macedonia (2025-2040) – Green scenario

Technology	2025	2030	2040
Wind Onshore	170	410	750
Solar Rooftop	70	217	400
Solar PV	176	413	983
Small Biomass	31	31	31

In case of Rapid scenario, installed capacities are significantly higher, even for year 2025. Total installed capacities in VRE in 2040 will be above 5.4 GW which is more than two times higher installed capacity compared to situation in Green scenario.

Table 2.8 – Renewables installed capacity in North Macedonia (2025-2040) – Rapid scenario

Technology	2025	2030	2040
Wind Onshore	460	944	1509
Solar Rooftop	105	300	600
Solar PV	798	1928	3341
Small Biomass	31	31	31

Finally, in case of Slow scenario installed RES capacities are lower, reaching 1.3 GW in 2040.

Table 2.9 – Renewables installed capacity in North Macedonia (2025-2040) – Slow scenario

Technology	2025	2030	2040
Wind Onshore	50	170	446
Solar Rooftop	35	100	200
Solar PV	60	215	606
Small Biomass	31	31	31

In addition, hourly capacity factors per climatic year were provided for wind and solar. Average values of capacity factors are presented on following diagrams.

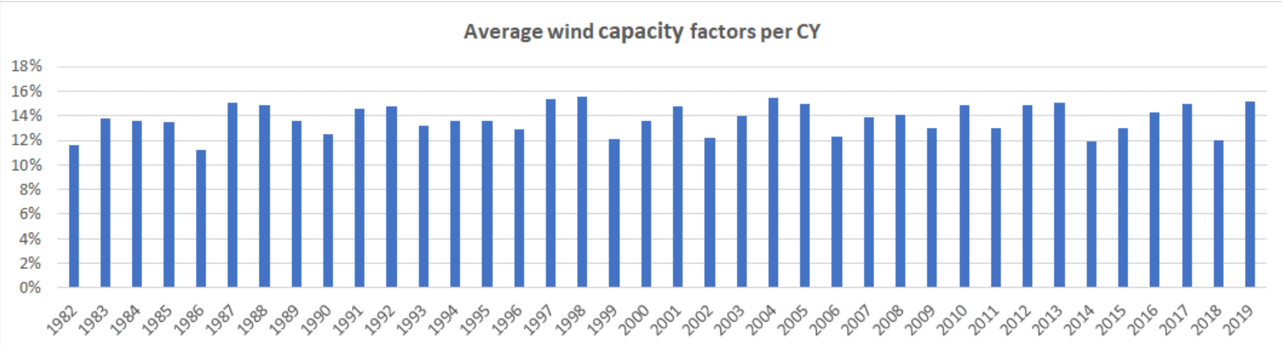

Figure 2.1 – Wind onshore average capacity factors (2025-2040)

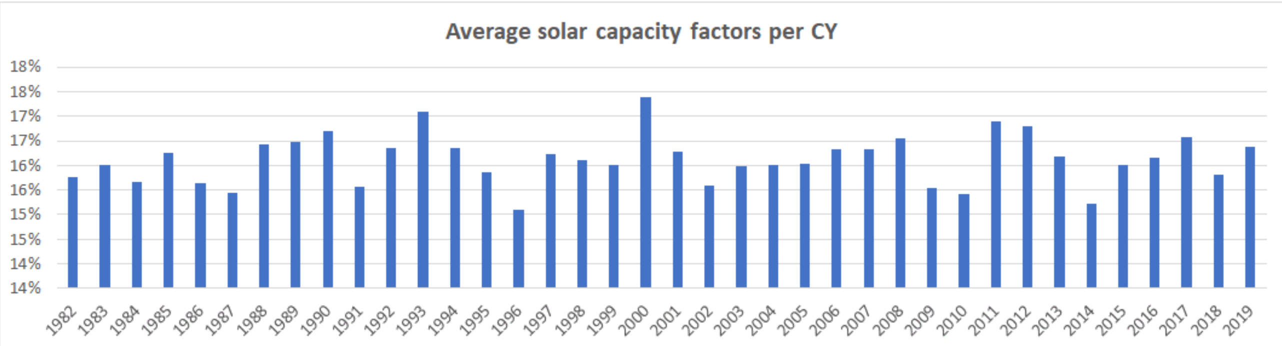

Figure 2.2 – Solar average capacity factors (2025-2040)

It should be emphasized that in input data there is no difference between categories, such as „Solar“ and „Solar PV". Therefore, one set of input data for solar has been used in all calculations and simulations.

Finally, transfer capacities between MEPSO and other surrounding market areas are shown in following table. All data have been provided by the MEPSO in PEMMDB format. It should be emphasized that only one set of data was provided for the entire analyzed period.

Table 2.10 – Macedonian transfer capacities (2025 – 2040)

Border	NTC (MW)
BG00-MK00	500
MK00-BG00	400
MK00-GR00	850
GR00-MK00	1100
MK00-AL00	500
AL00-MK00	500
MK00-RS00	600
RS00-MK00	630

3 METHODOLOGY

Reserve sizing is a crucial aspect of power system planning and operation, as it ensures the ability to maintain reliable and secure system operation in the face of unexpected events such as equipment failures or sudden changes in demand. Balancing reserves play a critical role in this process, as they provide the necessary flexibility to respond to these events and maintain the balance between supply and demand.

The process of balancing reserve sizing involves a complex set of calculations and considerations, taking into account a variety of factors such as the size and characteristics of the system, the nature of the loads and generation resources, and the likelihood and impact of potential contingencies. To ensure accurate and effective reserve sizing, a well-defined and rigorous methodology is required, one that considers not only technical and operational factors, but also economic and regulatory considerations.

This chapter will provide an overview of the key principles and methodologies for balancing reserve sizing, including the different types of reserves, the methods for estimating reserve requirements, and the factors that influence reserve sizing decisions. We will explore the role of probabilistic methods in reserve sizing, as well as the importance of considering uncertainties and risks in reserve planning. Additionally, we will discuss the practical considerations for implementing reserve sizing methodologies in real-world power systems.

3.1 Estimation of system (operating) reserves for power and frequency regulation

In a power systems active power should be generated and consumed in the same time, since the system frequency must be maintained close to its nominal value of 50 Hz in Europe. It is important to maintain the frequency close to the nominal value because the generators can trip off and cascade of generators tripping can occur leading to the so called “system collapse” which result in a blackout. Each TSO contributes in the balancing mechanism and is responsible for the balance of its control area.

System imbalances (SI) may occur due to different issues, such as outage of generation units or unexpected variations of load and the production from renewables (wind and solar). On the other hand, variation in coal quality can cause unexpected imbalance of thermal power plants. All these imbalances cause the frequency deviation, but at the same time regulating units perform automatic so-called primary control and the balance between generation and demand is re-established.

The System Operation Guideline (SO GL) defines four types of reserve products which can be grouped under three processes. The reserve categories are: Frequency Containment Reserve (FCR), Frequency Restoration Reserve (FRR) and Replacement Reserve (RR).

The following table summarize frequently used terms and describes the products with more detail:

Table 3.1 - Terminology related to reserve products and time of response

	Frequency containment process	Frequency restoration process		Reserve replacement process
Operational reserves defined by SO GL	Frequency Containment Reserve (FCR)	Automatic Frequency Restoration Reserve (aFRR)	Manual Frequency Restoration Reserve (mFRR)	Replacement Reserve (RR)
ENTSO-E CE Operation handbook	Primary Control	Secondary Control Reserve	Fast Tertiary Control Reserve	Slow Tertiary Control Reserve
Time of response	Up to 30 seconds	Up to 5/7.5 min	Up to 15 min	30 minutes

The secondary control is applied only to selected generators in the power plants, where its behavior over the time is associated with proportional-integral characteristic of the secondary controller. The automatic activation of the Frequency Restoration Process is based on the so-called Area Control Error (ACE, equivalent to the FRCE Frequency Restoration Control Error), that can be calculated using the following formula:

$$ACE = P_{meas} - P_{prog} + K \cdot (f_{meas} - f_0)$$

where:

P_{meas} is the sum of the instantaneous measured active power on tie-lines;
P_{prog} is the exchange program with all neighboring control areas;
K is the K-factor of the control area (a constant MW/Hz set on the secondary controller);
$f_{meas} - f_0$ is the difference between measured system frequency and set-point.

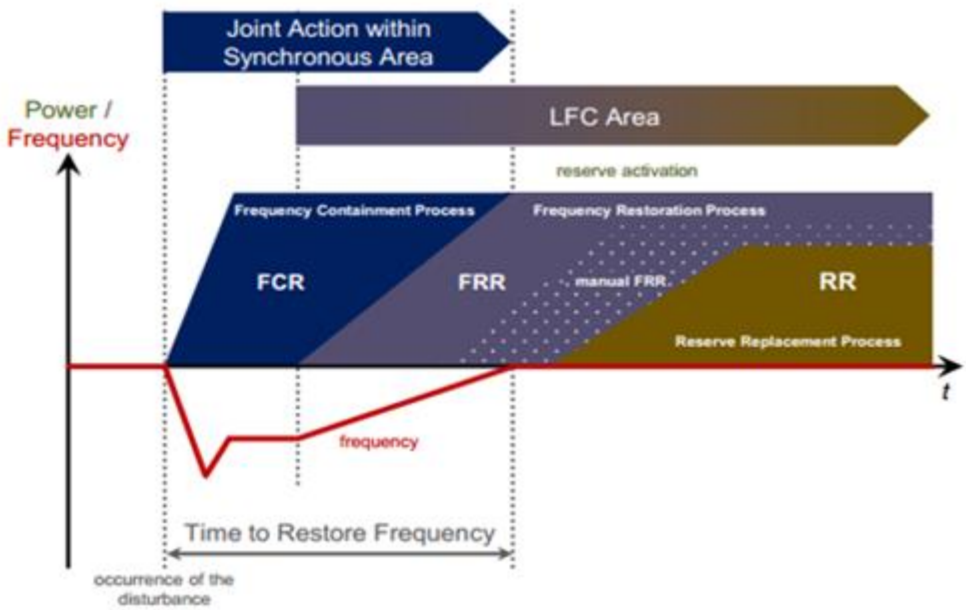

Figure 3.1: Reserve activation

On the other hand, by the concept of open-loop ACE, it is defined as a difference of measured ACE (the value on hourly or 15 min basis) and the amount of activated secondary and tertiary reserve:

$$OLACE_i = ACE_i - aFRR_{activated,i} - mFRR_{activated,i} - RR_{activated,i}$$

The goal of this task is the sizing of the secondary and tertiary reserve, while the primary reserve is sized according to the ENTSO-E rules on annual basis (according to the participation coefficients calculated based on net generation and consumption in its control area). Sizing of the balancing reserve should be done by the TSO, while required balancing capacity depends on the following factors:

- The expected system imbalance in real/time
- The amount of non-constricted flexibility
- The activation strategy of the TSO

Sizing of reserves is mainly covered by the SO GL, where dimensioning rules for FCR, FRR and RR are described in Articles 153, 157 and 160. Regarding sizing of FRR, the geographic scale for dimensioning is the LFC block. Per LFC block TSO is required to determine the ratio between aFRR and mFRR, while the complete FRR should not be less than the reference incident, which by definition shall be the largest imbalance that may result from instantaneous change of active power of a single power generating module, single demand facility or single HVDC interconnector or from a tripping of an AC line within the LFC block. On the other hand, FCR should cover all imbalances (based on probabilistic assessment) for at least 99% of time, based on the historical records (considering respective direction, positive or negative).

3.1.1 Sources of imbalances

Total system imbalance (SI) represents the difference between instantaneous measured active power on tie-lines and corresponding exchange program with all neighboring control areas without any control. In fact, this is ΔP part of area control error (ACE) reduced for activated balancing energy:

$$\Delta P = P_{meas} - P_{prog} - P_{activated}$$

where:

ΔP is system imbalance (SI) in observed control area,
P_{meas} is the sum of the instantaneous measured active power on tie-lines,
P_{prog} is the exchange program with all neighboring control areas,
$P_{activated}$ is activated reserve within control area.

On the other hand, since the market area's balance within the observed time interval can be calculated as the difference between total system generation and total system load, total system imbalance can be written as a sum of few components:

$$\Delta P = \Delta P_L + \Delta P_W + \Delta P_S + \Delta P_T + \Delta P_H$$

where:

ΔP_L is deviation of instantaneous measured load from scheduled value,
ΔP_W is deviation of instantaneous measured wind generation from scheduled value,
ΔP_S is deviation of instantaneous measured solar generation from scheduled value,
ΔP_T is deviation of instantaneous measured thermal generation from scheduled value,
ΔP_H is deviation of instantaneous measured hydro generation from scheduled value.

System imbalances may have different origins. According to the standard categorization from the literature we can distinguish stochastic from deterministic processes. In other words, control area imbalance is the sum of these deterministic and stochastic imbalances. Stochastic processes are unplanned outages of generating units as well as forecast errors, while the deterministic processes are related to the deviations between stepwise schedules and continuous (realized) values, as it is shown in the following figure.

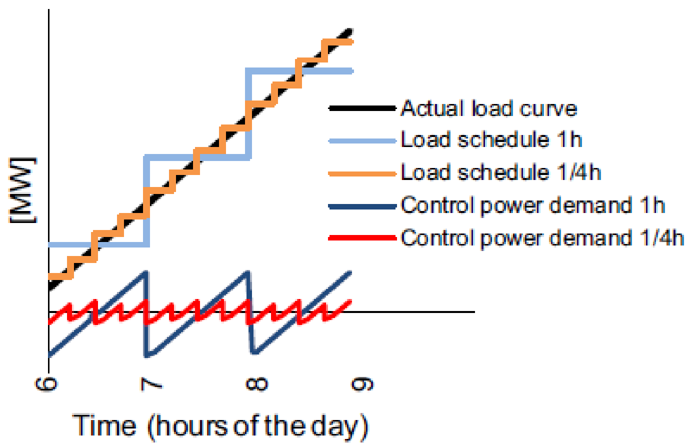

Figure 3.2: Deterministic imbalances caused by discrete schedules

In other words, deterministic imbalances can be written in the following form:

$$e(t) = p(t) - \bar{P}$$

where $p(t)$ is continuous signal (usually in practice with 1-min resolution), while $\bar{P}$ is average value of signal within dispatch interval (1-hour or 15-min, depending on the market design).

Deterministic imbalances can be forecasted very easily, while stochastic imbalances are more complicated. The probability of unplanned outages of power plants or transmission lines depends on characteristics of the equipment. On the other hand, operational measures should be also taken into account.

Deterministic imbalances are connected to the way contracts are designed in liberalized electricity markets. Schedules are usually defined as discrete step functions with duration of typically one hour or 15 min. On the other hand, in reality the change of demand and supply in time is continuous function. These differences between physical and scheduled values are called *schedule leaps*.

Therefore, we can distinguish two-time scales for imbalances: one is the deviation of mean value during the dispatch interval from the scheduled value (forecast error) and variations around the mean value within dispatch interval ("noise"):

$$\Delta P = \varepsilon_L + \varepsilon_W + \varepsilon_S + \varepsilon_T + \varepsilon_H + e_L + e_W + e_S + e_T + e_H$$

All five sources result in both forecast errors ($\boldsymbol{\varepsilon}$) and noise (e). It should be emphasized that forecast error and corresponding noise related to hydro power plants are usually neglected in practice. Therefore, we are dealing only with load, wind and solar forecast errors and noise, as well as with unavailable power caused by thermal units forced outages.

3.1.2 Forecast errors and metrics

Load forecast errors are often treated as a normally distributed, while wind and solar forecast errors are related to more complicated probability density functions (PDF). Therefore, it can be assumed that the load forecast error distribution is a Gaussian distribution given with the following formula:

$$f(\varepsilon) = \frac{1}{2\pi\sigma} e^{-\frac{1}{2}\left(\frac{\varepsilon-\mu}{\sigma}\right)^2}$$

where, ε is the forecast error, while σ is standard deviation and μ is the mathematical expectation.

In case of wind and solar forecast error, the situation is a little complicated. Wind forecast error is usually assumed as Normal distribution. However, in many research papers and literature it can be found that wind forecast error can be modeled using hyperbolic, beta, Laplace distribution or even combinations of these distributions. The similar situation is with solar forecast errors. In addition, in many research papers related to forecast errors it is stated that wind and solar forecast errors are weakly negative correlated. However, in many RES integration studies Gaussian distribution is still used as a god approximation.

Regarding the wind and solar forecast error, the main indicator of quality of forecast is normalized mean root square error (nRMSE), which is defined as follows:

$$nRMSE = \frac{\sqrt{\sum_{i=1}^{n}(y_i - \hat{y}_i)^2/n}}{y_{max}}$$

where y_i is realized (measured) value and $\hat{y}_i$ is forecasted value, while n is the number of samples and y_{max} is the maximum value of the sample.

If the nRMSE of historic/simulated time-series is different from the nRMSE of scenario for which the control reserve is sized, the time-series of historic forecast error should be multiplied by so-called nRMSE factor defined as:

$$nRMSE\ factor = \frac{nRMSE_{scenario}}{nRMSE_{time-series}}$$

On the other hand, Mean Absolute Percentage Error (MAPE) has been widely used in regression problems and by the renewable energy industry to evaluate forecast performance::

$$MAPE = \frac{1}{n}\sum_{i=1}^{n}\left|\frac{y_i - \hat{y}_i}{y_{max}}\right|$$

3.1.3 FRR sizing in MEPSO control area in case of higher level of VRE penetration

The approach for reserve sizing which is proposed relies on a statistical method which aims at determining the sufficient amounts of balancing reserves adjusted to the projected integration levels of variable renewable energy sources. This proposal is completely in line with SO GL.

The proposed method considers system imbalance caused by wind, solar, and demand, including planned integration of variable renewables (VRE). It also takes into account forced outages of thermal generating units.

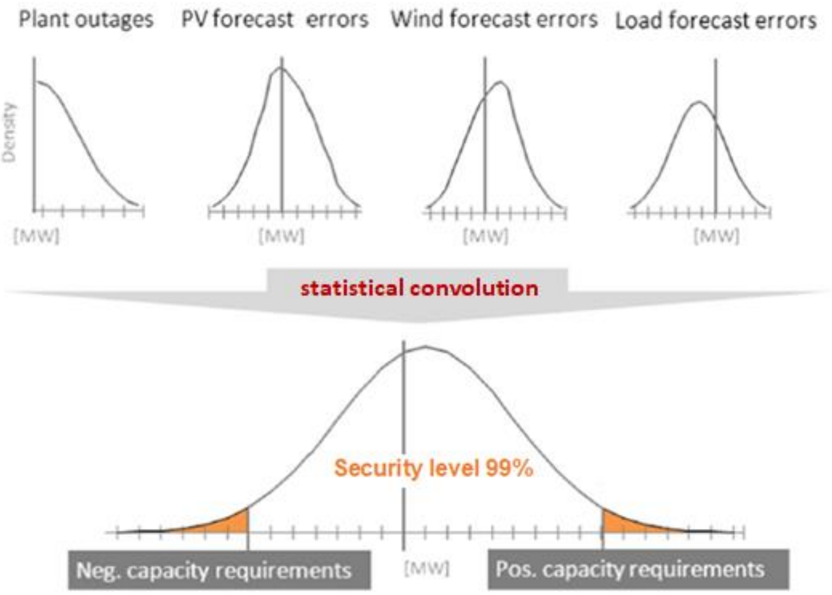

Figure 3.3 – Schematic representation of proposed FRR sizing in MEPSO control area

The probabilistic approach for FRR sizing, according to SO GL (Article 157) requires that for both positive and negative direction it should be sufficient to cover 99% of the imbalances based on the historical (in this case forecasted) imbalance records, while there is no clear recommendation regarding aFRR sizing.

3.1.3.1 Sizing of aFRR

According to SO GL, Article 157(2), it is proposed that all TSO's within the LFC block should define aFRR level, mFRR level as well as full activation time for aFRR and mFRR that shoud not be longer than time to restore the frequency (15 min).

According to the European practice (Belgian TSO), aFRR needs are determined to cover 79% of 15-min absolute system imbalance variations[2] (absolute value is taken since aFRR is symmetric). System imbalance variations are calculated according to the following formula:

$$var(SI)_t = SI_t - SI_{t-1}$$

In addition, section B-6-2-2-1-5 in SAFA document (Annex 1) recommends the following approach.

The amount of the aFRR that is needed typically depends on the size of load variations, schedule changes and generating unit outages. In this respect, the recommended minimum amount of aFRR has to ensure:

- that the positive aFRR is larger than the 1st percentile of the difference of the 1-minute average ACEol and the 15-minute average ACEol of the LFC Block of the corresponding quarter of hour, and
- that the negative aFRR is larger than the 99th percentile of the difference of the 1-minute average ACEol and the 15-minute average ACEol of the LFC Block of the corresponding quarter of hour.

[2] According to "Methodology for the dimensioning of the aFRR needs – Elia"

It should be noted here, that 1-minute ACEol should be known in order to apply this method for aFRR sizing. In addition, since market design in North Macedonia implies hourly dispatch interval, it seems reasonable that previously listed requirements should be applied on difference between 1-hour average ACEol and 1-min average ACEol. However, obtaining ACEol with 1-min resolution is complicated yet within the entire SMM block. Therefore, the difference between 1-hour average ACEol and 15-min average ACEol has been used as a first approximation of nosie component for aFRR sizing on long-term planning horizon.

Finally, according to the deterministic method that can be found in ENTSO-e operation handbook, the amount of secondary reserve (aFRR) is determined using the following formula:

$$aFRR = \sqrt{a \cdot L_{max} + b^2} - b$$

where L_{max} is the maximum load in the observed control area, while a and b are empirically determined constants (typical value used in France is $a = 10$ and $b = 150$). This deterministic approach is based on empiric noise management and can be used to obtain the recommended minimum value of aFRR.

3.1.3.2 Sizing of mFRR

Tertiary reserve is determined as a difference between calculated total secondary and tertiary reserve (FRR) and calculated secondary reserve (aFRR). In other words, tertiary reserve (upward and downward), is calculated as follows:

$$mFRR_{up/down} = FRR_{up/down} - aFRR$$

3.1.3.3 Estimation of imbalances

According to deterministic approach, FRR should not be smaller than reference incident, separate for positive and negative direction. In other words, when we are talking about upward FRR capacity it is determined as a capacity of the largest unit in the system while in case of the downward reserve, the crucial is the outage of the largest consumer in the system.

The main task related to balancing reserve sizing within this study was to estimate system imbalance for analyzed target years and scenarios. In order to estimate the system imbalance in the future the following methodology has been proposed. First of all, all components that participate in system imbalance were forecasted, respecting the nature of these quantities as well as all input data and marked design. These are load, wind and solar forecast errors as well as imbalance caused by thermal units forced outages and finally noise component for all three sources.

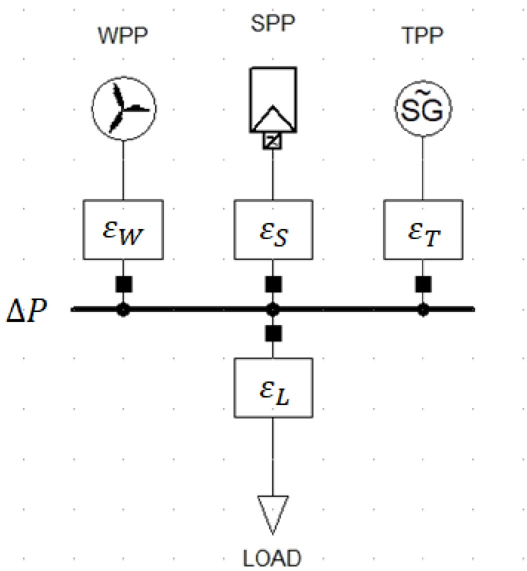

Figure 3.4 – Forecast error modeling (simplified)

Total system imbalance in the practical situation can be represented by following equation:

Simulated in ANTARES

$$\Delta P = \boxed{\varepsilon_L + \sum_{k=1}^{N_W} \varepsilon_{W,k} + \sum_{k=1}^{N_S} \varepsilon_{S,k}} + \boxed{\sum_{k=1}^{N_T} \varepsilon_{T,k}} + \boxed{e_L + e_W + e_S}$$

Estimated out of ANTARES

where:

ε_L is load forecast error in the observed scenario,
$\varepsilon_{W,k}$ is forecast error of kth wind power plant in the system,
$\varepsilon_{S,k}$ is forecast error of kth solar power plant in the system,
$\varepsilon_{T,k}$ is imbalance caused by forced outage kth thermal unit in the system,
N_W, N_S, N_T are total numbers of wind, solar and thermal power plants in the system, respectively,
e_L, e_W, e_S are deterministic imbalances (noise) of load, wind and solar power plants, respectively.

Individual components of the previous equation were explained with more detail in 3.1.1.

Forecast errors for wind, load and solar, as well as imbalances caused by thermal units forced outages were generated using ANTARES software tool (Time-Series generator).

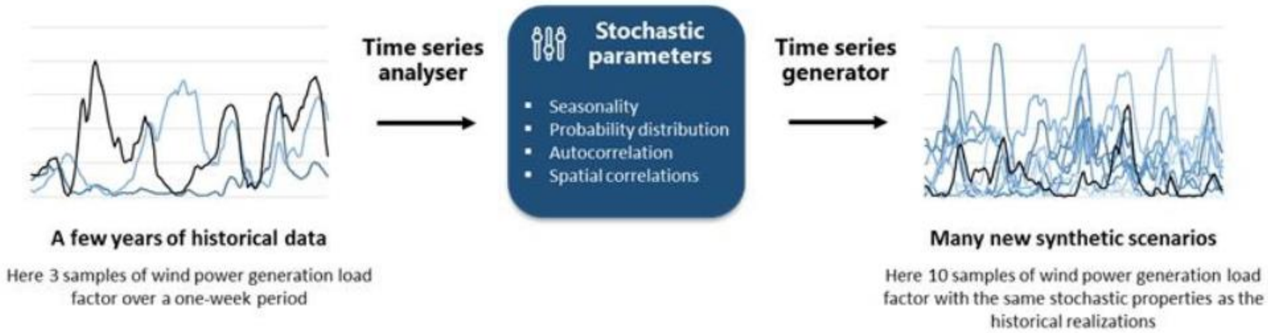

Figure 3.5 – Working principle of the ANTARES time series analyzer and time series generator

The time series analyzer learns from external data (i.e. from historical data) intrinsic characteristics of their stochastic behavior:

> their seasonality (e.g. daily and yearly climatic cycles impacting PV generation)
> their probability distribution functions,
> their autocorrelation functions
> and their spatial correlations - e.g. correlations between wind regimes of adjacent areas.

The time series generator randomly draws new samples of stochastic processes based on given values of the aforementioned characteristics. The generated set respects the same global characteristics as the learning sample, but each generated time series has its own specificities, for instance a low wind generation which occur during a day when the wind was always high in the learning sample.

The combined use of these two modules allows to enrich the Monte-Carlo approach with new situations that did not occur in past records but could possibly happen in the future. These two modules are independent and can also be run separately. For instance, the time-series generator can be supplied with stochastic parameters obtained with another source than the time series analyzer.

3.1.3.4 Estimation of imbalances due to forecast error of load, wind and solar

All necessary parameters for time-series generation have been previously calculated by ANTARES module, called Time-series Analyzer. Historical data, i.e. load, wind and solar forecast errors annual time-series were used as an input in order to obtain parameters such as monthly standard deviations and average values (to preserve seasonality), as well as autocorrelation coefficients and daily shape profiles. These parameters were imported in ANTARES simulator in order to generate forecast errors for load, wind and solar, considering normal distribution (Gaussian) for all three kinds of forecast errors.

All forecast errors were generated on plant by plant level, considering the ratio between installed capacity of observed wind and solar power plants and existing power plants used as an input (so called c-factor). The similar approach was applied in case of load, where maximum annual load has been used to scale the load forecast error. It was assumed that forecast errors corresponding to wind and solar power plants from different locations are not correlated. Correlation between individual wind farms' forecast errors is a very important issue and has the potential to significantly increase the overall uncertainty that the system is exposed to from wind capacity. However, it should be noted that this correlation is distinct from the correlation between individual wind farms' forecasted outputs, which do not expose the system to greater levels of uncertainty. It has been shown in some research papers that the correlation between wind power forecast errors of individual wind farms is strongly dependent on the distance between the wind farms. The similar situation is in case of solar power plants.

Finally, aggregation of wind or solar forecast error was achieved by using of Monte-Carlo simulation. In fact, synthetically generated 100 time-series (100 time-series per power plant) were combined randomly in order to get overall system hourly imbalance (i.e. the forecast error). This number was selected in order to achieve better convergence of the results.

Since forecast errors of all individual power plants were assumed to be independent random variables with normal distribution, total nRMSE by technology (wind and solar) due to aggregation can be easily estimated using the following analytic formula:

$$nRMSE = \sqrt{\alpha^2 \left(\frac{\sigma}{P_0}\right)^2 + \left(\frac{\mu}{P_0}\right)^2} \cdot 100\%$$

where:

σ is standard deviation of historical wind/solar forecast error

μ is average value of historic wind/solar forecast error

P_0 is nominal capacity of referent wind/solar power plant with historic forecast error time-series

α is coefficient defined by following formula:

$$\alpha = \frac{\sqrt{\sum_{k=1}^{N} P_k^2}}{\sum_{k=1}^{N} P_k}$$

This coefficient should be calculated depending on the observed scenario and target year, i.e. respecting corresponding renewables generation mix. On the other hand, if it is assumed that an increase of renewables installed capacity is linear, for instance by constantly adding incremental capacity ΔP (within n iterations), α coefficient can be calculated as:

$$\alpha = \frac{1}{\sqrt{n}}$$

Therefore, it can be concluded that increase of VRE installed capacity in general leads to decrease of normalized root mean square error (nRMSE) at country level. However, depending on value of coefficient **α**, it is also possible to have greater nRMSE for greater VRE installed capacity.

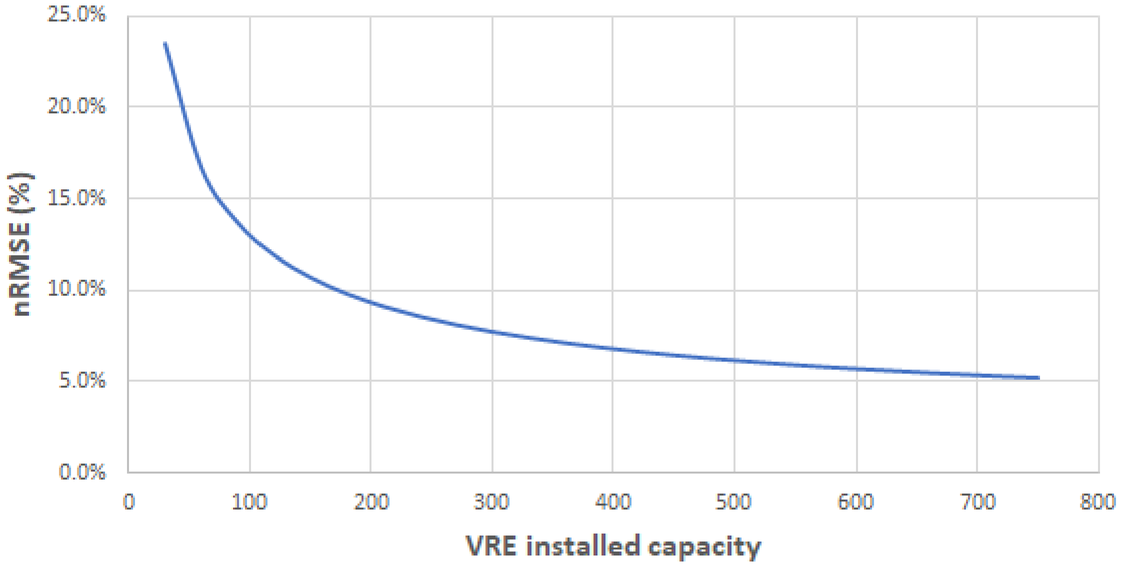

Figure 3.6 – Illustration of VRE nRMSE decrease with linear installed capacity increase

3.1.3.5 Estimation of imbalances due to forced outage of thermal units

Unavailability of thermal units due to forced outages has been simulated in ANTARES using the following approach. First of all, one MC year has been arbitrary selected from the initial market simulation for planned system state (2025, 2030 and 2040), with corresponding hourly thermal generation dispatch by generating units. These time-series should represent day-ahead schedule for thermal units in the future, reflecting all scenario specific impacts, such as lower thermal generation schedule due to high-RES penetration etc. In addition, forced outages of thermal units have been simulated in ANTARES software tool, stochastically generated based on forced outage rates (FOR) of thermal units provided by MEPSO within market questionnaires. Since forced outages were simulated for large number of MC years (100 in this case), it was not necessary to extract more than one MC year for initial dispatch of thermal units.

The difference between scheduled power and available power of thermal units was used to determine thermal system imbalance component. In addition, one thermal unit of capacity 200 MW has been introduced in the model in order to reflect the RR process (i.e. slow tertiary control). The balance equation of simulated optimization problem is:

$$\sum_{k=1}^{N_T} P_{T,k}(t) - \sum_{k=1}^{N_T} P_{k,h}^{sch}(t) + P_{RR}(t) + \varepsilon_T(t) = 0$$

where maximum capacities of thermal units are limited to their scheduled values from day-ahead market simulation.

In order to model correctly the effect of reserve replacement process (RR) one additional linear constraint related to integer variable $NODU \in \{0,1\}$ (i.e. the number of dispatched units) was added to the model:

$$NODU_{RR}(t+1) - NODU_{RR}(t) - \varepsilon_T(t) \leq 0$$

Therefore, it should be only one hour with imbalance due to thermal unit forced outage, as it is depicted on Figure 3.7.

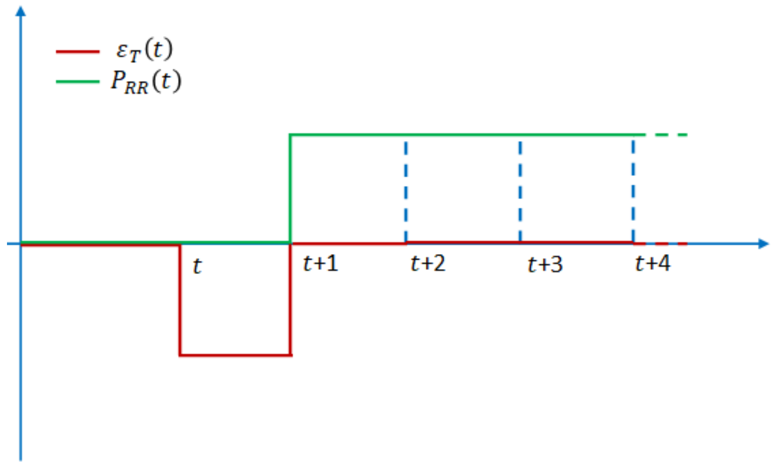

Figure 3.7 – Illustration of replacement reserve activation modeling in ANTARES

One hour time-lag was selected using consultant assessment as well as the analysis of provided ACE open-loop in order to catch the imbalances caused by thermal power plant forced outages. Finally, it should be emphasized that corresponding penalty prices should be properly selected in order to model correctly the activation of replacement reserve.

Considering all these assumptions, load, wind, solar and thermal forecast error components were simulated within ANTARES and aggregated on country level. Total forecast error has been estimated for all analyzed scenarios and target years on hourly basis.

3.1.3.6 Estimation of imbalances due to noise

However, the goal of the analysis was to predict total system imbalance for different scenarios and target years on 15-min resolution in order to determine the balancing reserve requirements depending on VRE penetration level. The key assumption that was implemented is that the electricity market and corresponding generation and load schedule in North Macedonia will be based on 1-hour scheduling interval in the future, as it is the case in the present. That means that all day-ahead nominations are determined on hourly basis. As a consequence, 15-min interval can be used for system imbalances and noise component representation. For instance, 15-min load imbalance can be expressed as a difference between scheduled (hourly) value and realized value. By adding and subtracting hourly average, load imbalance can be decomposed on two terms by the following formula:

$$\Delta P_L(i,h) = \underbrace{P_L^{for}(h) - P_L^{avg}(h)}_{stohastic\ component} + \underbrace{P_L^{avg}(h) - P_L(i,h)}_{deterministic\ component} = \varepsilon_L(i,h) + e_L(i,h)$$

Where discrete time $t(i,h)$ is assumed, represented by hour h and i^{th} 15-min interval (1 to 4).

On the other hand, it can be easily shown that hourly average load (or hourly energy) can be calculated as:

$$P_L^{avg}(h) = \frac{1}{4}\sum_{i=1}^{4} P_L(i,h)$$

As a consequence of the previous equation, defined noise component $e_L(t)$ always has zero mean value. Completely similar approach as described above can be applied for solar and wind generation.

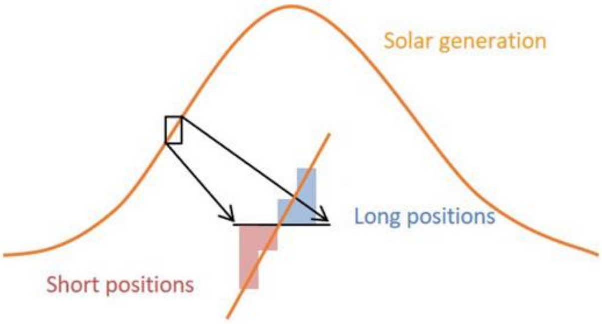

Figure 3.8 – Illustration of solar generation within-hour deviations (noise)

The main goal here is to estimate deterministic component of imbalance i.e. the noise. The noise as a continual function can be expanded in Taylor series about one point, for instance the middle of 1-hour dispatch interval, where the noise value is around zero:

$$e(t) = e(t_0) + \frac{e'(t_0)}{1!}(t - t_0) + \frac{e''(t_0)}{2!}(t - t_0)^2 + \cdots + \frac{e^{(n)}}{n!}(t - t_0)^n + \cdots$$

Keeping only first two terms, and knowing that that noise component first-order derivative is equal to the continuous function derivative (load, solar, wind) within the observed hourly interval, the noise component can be expressed as follows:

$$e(t) \approx e(t_0) + p'(t_0)(t - t_0)$$

In case of 15-min intervals resolution and 1-hour dispatch interval, this approximation can be written in the following form[3]:

$$e(i, h) = \pm\frac{2i - 5}{16}[P(h + 1) - P(h - 1)]$$

where central *finite difference method* is used to estimate first-order derivative of the observed function (continuous load, solar or wind generation). In other words, hourly ramps from forecasted load, wind or solar time-series can be used to estimate noise. This is a good approximation in case when observed function is slow changing, what is the case for load and solar generation (see Figure 3.8). In case of wind the situation is more complicated, since there can be unpredictable deviations inside 1-hour interval, while in case of load and solar this transition inside one-hour interval is more or less linear.
Deterministic imbalances (i.e. the noise), for load, solar and wind were estimated for Belgium and compared with realized 15-min values from ENTSO-E Transparency Platform in order to test the methodology. All results are presented on following three diagrams.

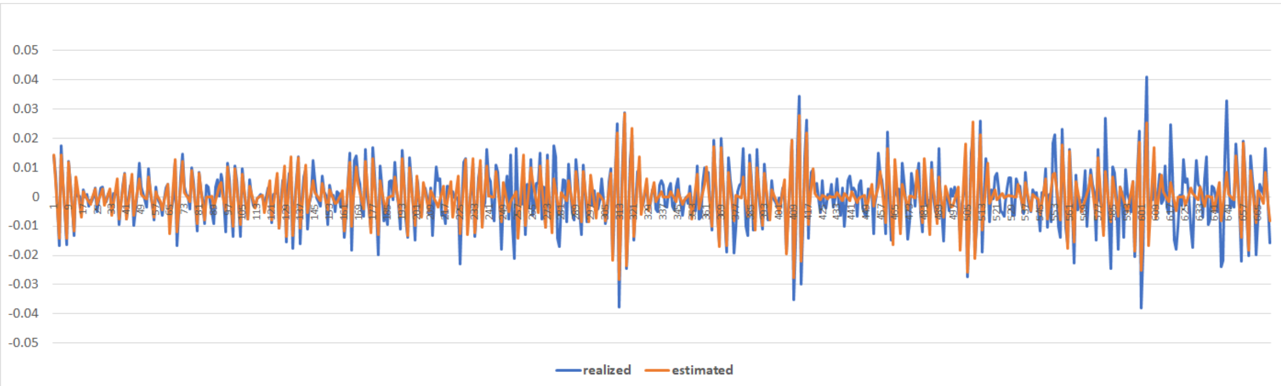

Figure 3.9 – Weekly load noise component for Belgium – proof of concept (ENTSO-E Transparency Platform)

[3] Negative sign is used in case of load noise.

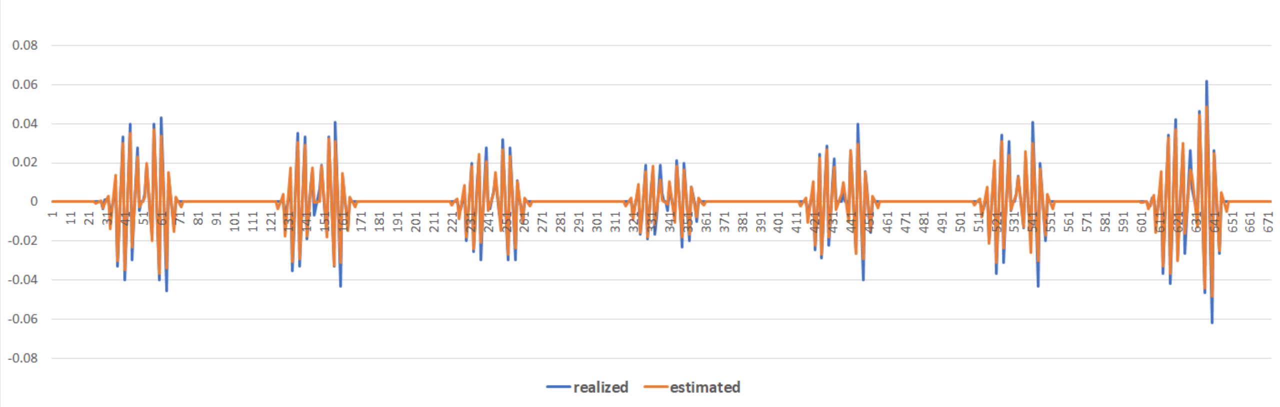

Figure 3.10 – Weekly solar noise component for Belgium - proof of concept (ENTSO-E Transparency Platform)

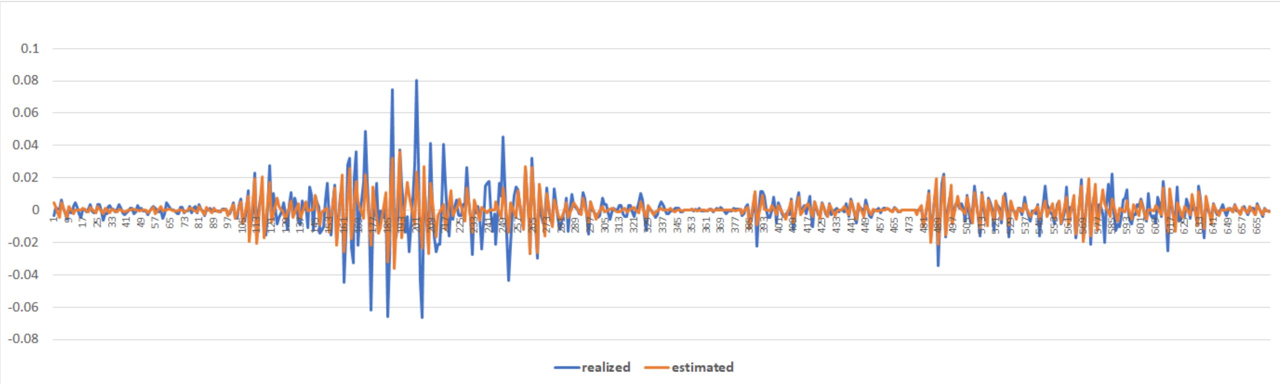

Figure 3.11 – Weekly wind noise component for Belgium - proof of concept (ENTSO-E Transparency Platform)

Standard deviation of deterministic imbalances (load, wind and solar) can be estimated from hourly ramps as follows:

$$\sigma_{noise} = \sqrt{\frac{1}{35040}\sum_{i=1}^{4}\sum_{h=1}^{8760}\left(\frac{2i-5}{16}\right)^2 [P(h+1) - P(h-1)]^2}$$

Comparing the results for observed example, it was concluded that estimated standard deviation for load is about 80% of realized value, while in case of solar and wind it is 92% and 70% of realized value, respectively.

Finally, in case of VRE (wind and solar), hourly capacity factors are usually known on planning horizon instead of hourly generation time-series. Therefore, total wind/solar noise component for all power plants within country and in timestamp $t(i,h)$ can be calculated as follows:

$$e(i,h) = P_n \times \frac{2i-5}{16} \cdot [\overline{CF}(h+1) - \overline{CF}(h-1)]$$

where:

$$P_n = \sum_{k=1}^{N} P_{n,k}$$ is total installed wind/solar capacity

$$\overline{CF} = \frac{\sum_{k=1}^{N} P_{n,k} \cdot CF_k}{\sum_{k=1}^{N} P_{n,k}}$$ are weighted (by rated power) wind/solar capacity factors, i.e. capacity factors on country level, calculated taking into account all individual power plant's location specific characteristics.

4 SYSTEM RESERVES RELATED ANALYSES

Results of FRR (aFRR and mFRR) dimensioning for analyzed three scenarios (Green, Rapid and Slow), as well as for three analyzed years are presented in this chapter.

Required secondary and tertiary levels (aFRR and mFRR) on a long-term planning horizon were determined according to developed methodology and input data presented in previous chapters. Historical load and VRE forecast errors were used as an input in order to model the future system imbalance for observed scenarios and target years, using ANTARES simulator and auxiliary calculations in excel, while historical system imbalance (open-loop ACE) was used in order to compare the results and test the validity of applied methodology.

4.1 Input data analysis

Following subchapters describes relevant input data needed for balancing reserve sizing. All data were collected and provided by the MEPSO or downloaded from publicly available databases such as ENTSO-E Transparency Platform as well as from the regional study related to common reserve dimensioning within SMM block. All input data were presented and analyzed in detail in order to emphasize the impact of initial assumption to obtained results at the end of this report.

4.1.1 Analysis of open-loop ACE

In order to assess the adequacy of the amount of operational reserves the behavior of each control area should be analyzed by the responsible TSO. In this respect the ACE_{ol} representing the overall sum of imbalances within a control area is of special significance. ACE_{ol} is related to the overall need of reserves (FRR and RR) of a control area. The following rule applies in general: the higher the ACE_{ol} of a control block - the higher is the need for operational reserves. Values of historical 15-min time series of Area Control Error (ACE) and corresponding hourly activated secondary and tertiary reserve were taken from the study *„Studija zajedničkog dimenzionisanja FRR rezerve u okviru SMM kontrolnog bloka“*, and were used for proof of concept.

System open-loop ACE and its derivative ACE_{ol}'– defined as the change of the ACE_{ol} from the previous time stamp – can be analyzed. In relation to the ACE these two parameters give insight into the intrinsic behaviour of the analyzed system. In addition, difference between ACE_{ol} and its average on dispatch interval, 1-hour or 15-min interval, depending on the market design, is usually analyzed as well. Figure 4.1 shows decomposition of 15-min open-loop ACE to average value (i.e. 1 hour open-loop ACE) and corresponding noise component for one arbitrary chosen day in January 2021 (09.01.2021).

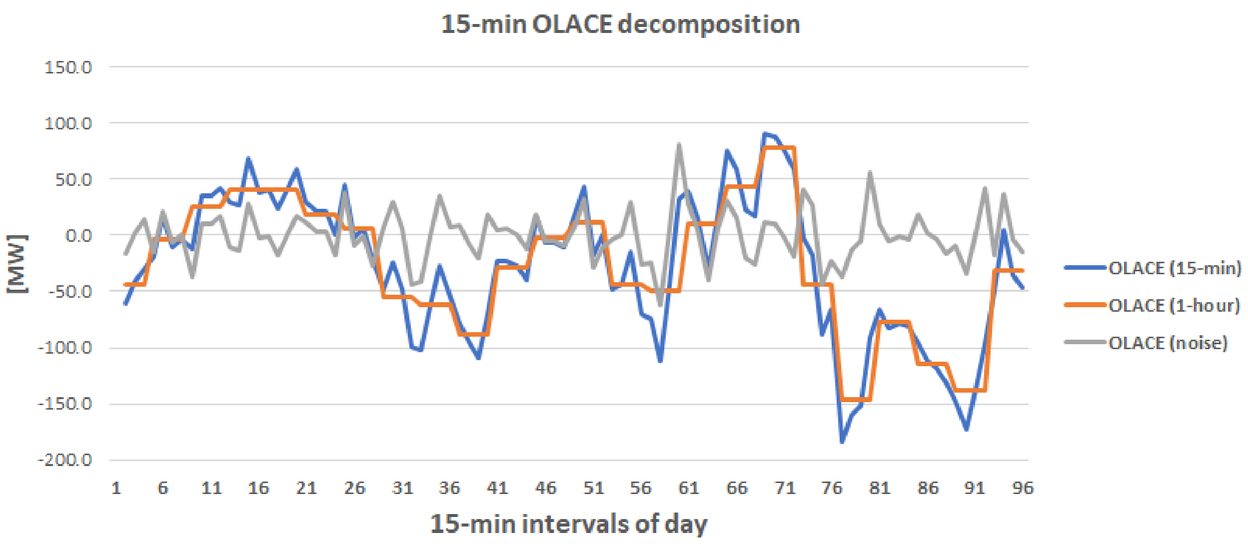

Figure 4.1 – MEPSO control area 15-min open-loop ACE decomposition

The following table (Table 4.1) shows numerical characteristics of open-loop ACE in 15-min and 1-hour resolution as well as the corresponding noise component in MEPSO control area in 2021. It can be seen that average value of the system imbalance is negative, around -16 MW, while at the same time the average load forecast error is strictly positive, indicating that the difference between these two values (around 25.4 MW) corresponds to unavailability of thermal units due to forced outages as well as to RES forecast error.

Table 4.1 – MEPSO control area open-loop ACE and its components numerical characteristics in 2021

Parameter	ACE_{ol} (15-min)	ACE_{ol} (1-hour)	ACE_{ol} (noise)
μ [MW]	-16.0	-16.0	0.0
σ [MW]	61.7	59.4	16.7
Max [MW]	237.6	195.1	117.4
P99- [MW]	-191.1	-181.9	-50.1
P99+ [MW]	148.3	142.0	53.8

On the other hand, standard deviation of 15-min open-loop ACE is around 62 MW which is very close to standard deviation of hourly average. As a consequence, total FRR can be determined approximately using hourly open-loop ACE instead 15-min values. It should be noted that following relation is valid:

$$\sigma_{15-min} = \sqrt{\sigma_{1-hour}^2 + \sigma_{noise}^2} = 61.7\ MW$$

indicating that these two random variables are independent.

P99 values for both negative and positive samples of 15-min open-loop ACE are equal to -191 MW and 148 MW, indicating that required upward/downward FRR level. On the other hand, it can be seen that P99 values 1-hour average ACEol and 15-min average ACEol are very close each other since the noise component is less dominant in total standard deviation (according to addition rule described above).

The following diagram shows empirical histogram of 15-min open-loop ACE, as well as corresponding normal distribution probability density function. It can be seen that this theoretical function is a good approximation for empirical.

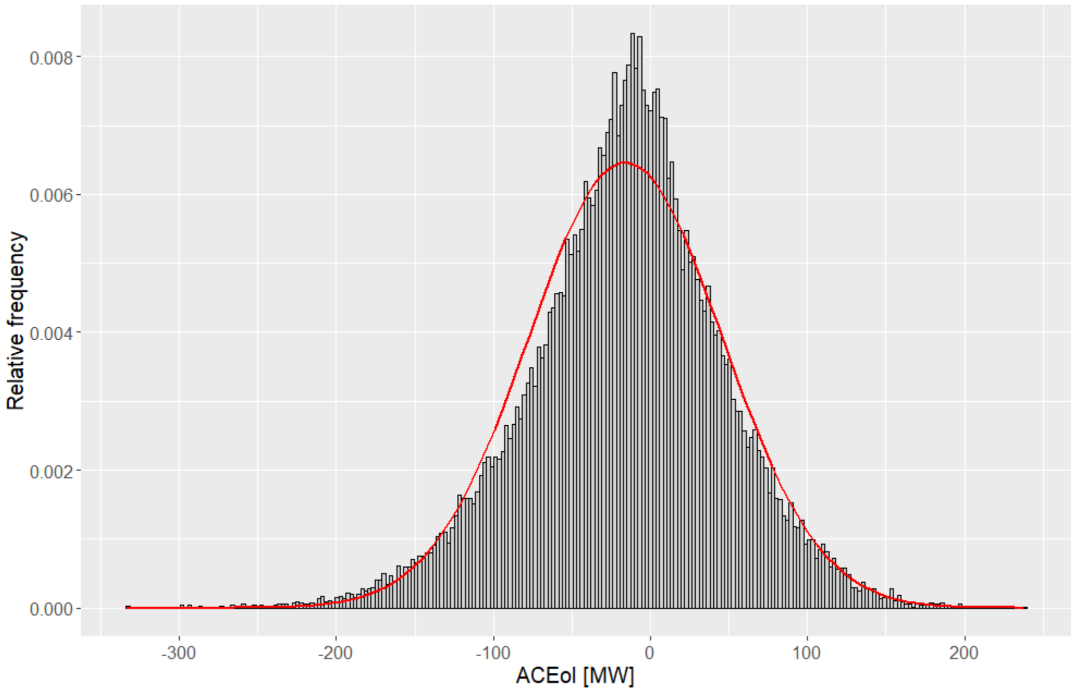

Figure 4.2 – Comparison of MEPSO control area 15-min open-loop ACE histogram with normal distribution

On the other hand, in order to test if hypothesized distribution is proper or not, quintile-quantile (Q-Q) diagrams can be constructed (Figure 4.3) by plotting the quantiles from hypothesized theoretical distribution against observed quantiles from empirical distribution. It can be seen from the Q-Q diagram that, empirical distribution is very close to the normal distribution. A significant difference lies in the region of negative system imbalances, indicating that theoretical value of total FRR, determined for a given security level (99% for instance) will be a little different compared to value obtained from the empirical cumulative probability density function (CDF), presented in (Figure 4.3).

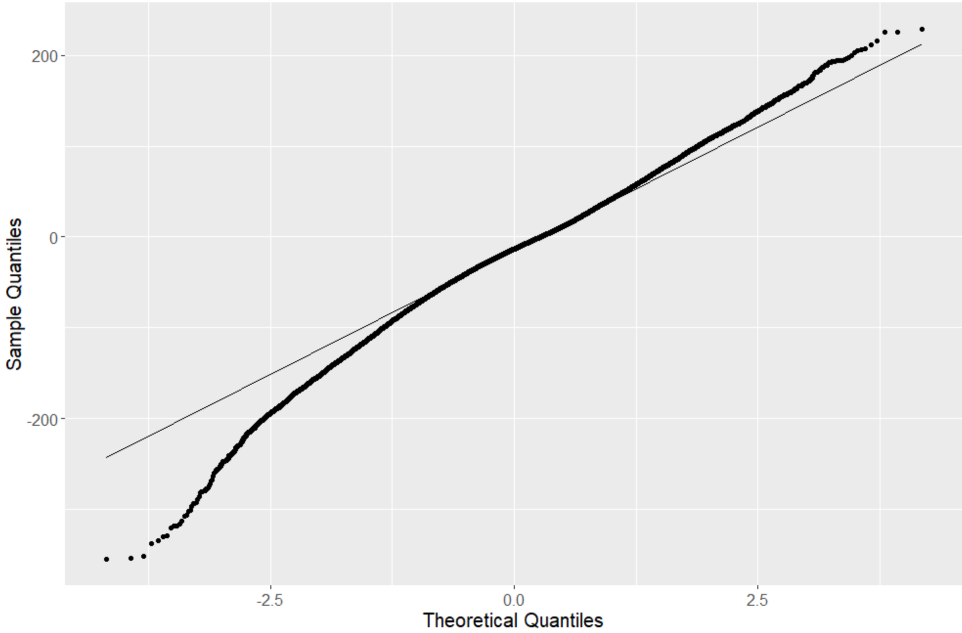

Figure 4.3 – A normal quantile-quantile plot of the distribution of MEPSO control area open-loop ACE

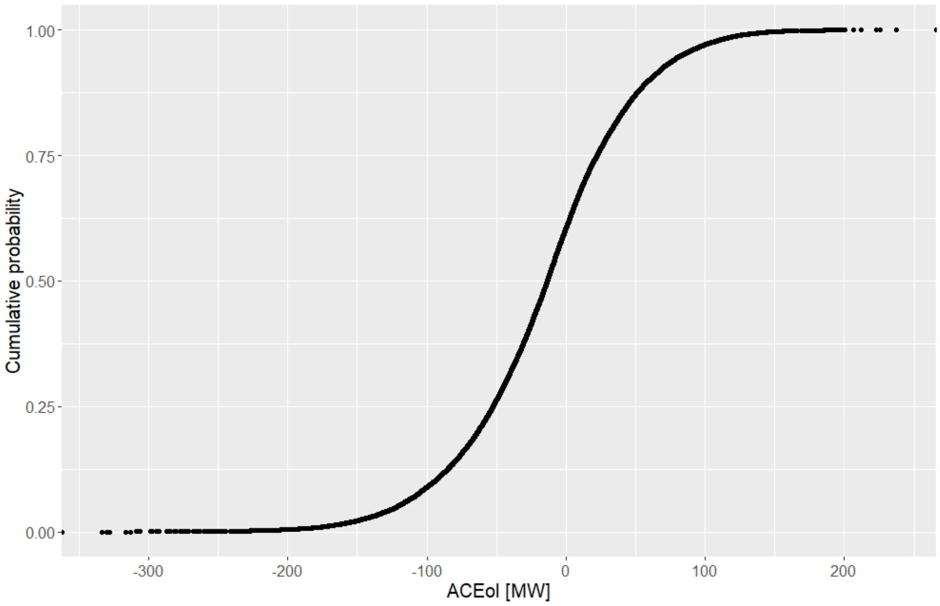

Figure 4.4 – Empirical cumulative distribution function of MEPSO control area open-loop ACE

When plotting ACE against ACE_{ol} in its quarterly hour dependency the following distribution is assumed to be typical (Figure 4.4). While assuming no interrelation between the ACE and being independently distributed according to a Gaussian distribution no patterns are recognizable (i.e. no statistical dependency). In this diagram Figure 4.5, the x–axis represents the "influence of the market" whereas the y–axis represents the result of the TSO control activities.

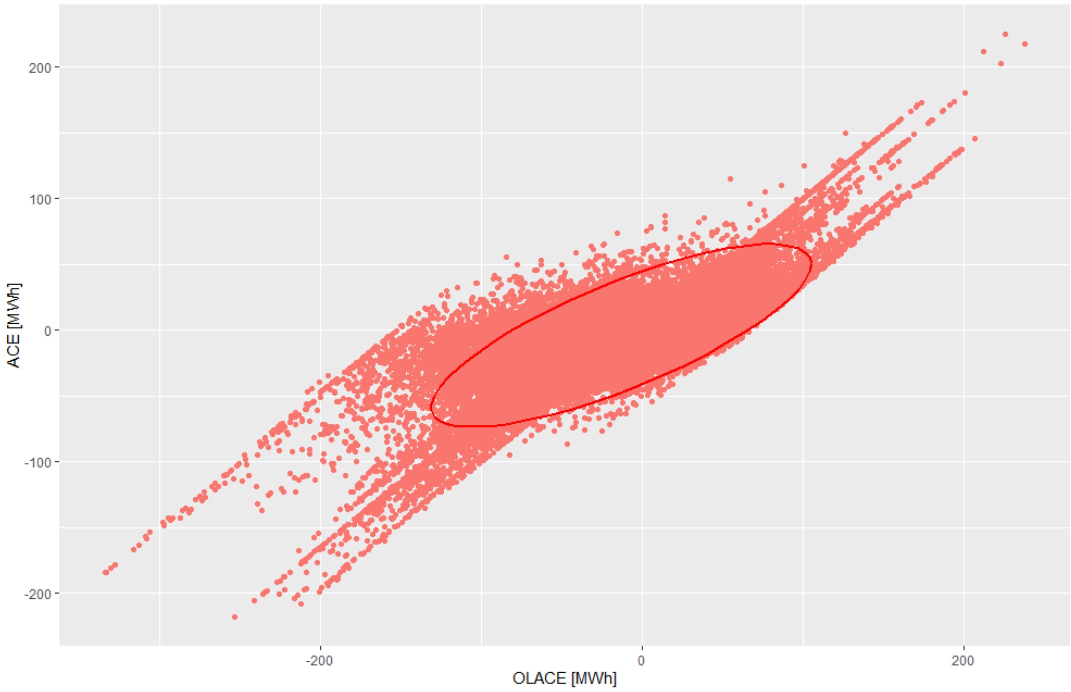

Figure 4.5 –Empirical ACE_{ol}/ACE point distribution for MEPSO control area

A histogram of open-loop ACE noise is presented on Figure 4.6. It can be seen that the noise is symmetric and practically between 50 MW in 99% of time. Average value is equal to zero. Therefore, corresponding normal distribution is centered.

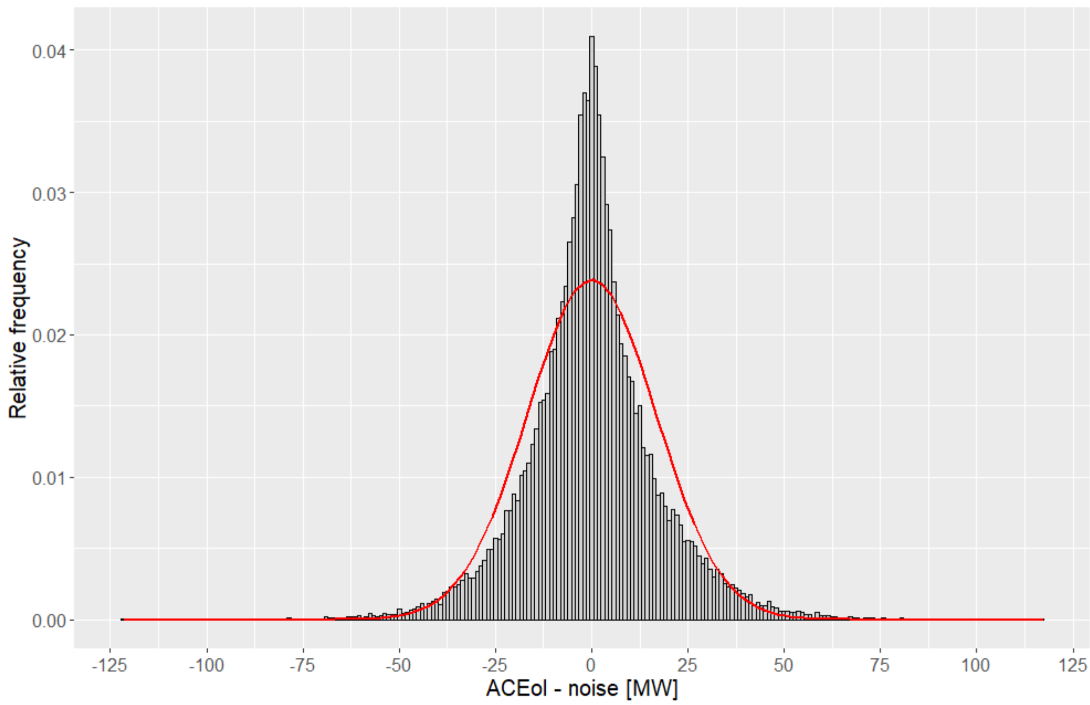

Figure 4.6 – Comparison of MEPSO control area 15-min open-loop ACE noise histogram with normal distribution

Following diagrams (Figure 4.7 and Figure 4.8) shows Q-Q diagrams of open-loop ACE noise component, and empirical cumulative density function.

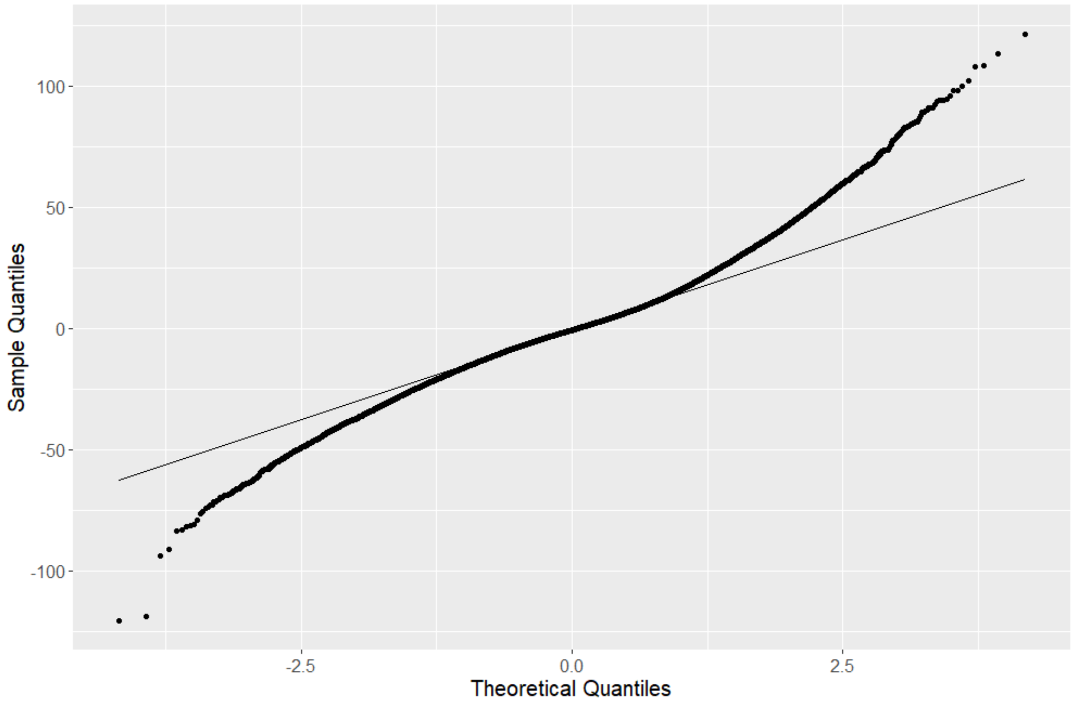

Figure 4.7 – A normal quantile-quantile plot of the distribution of MEPSO control area open-loop ACE noise

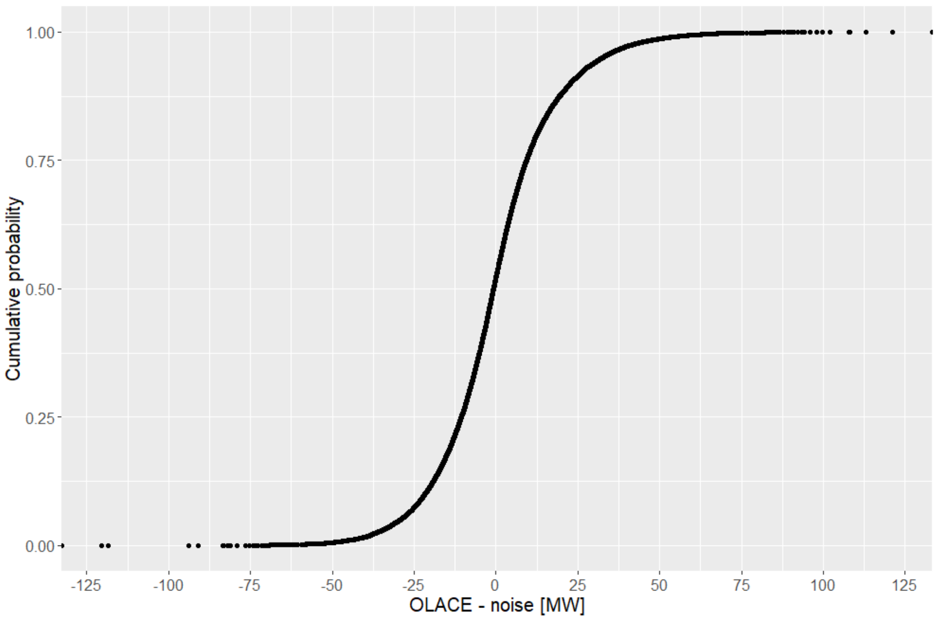

Figure 4.8 – Empirical cumulative distribution function of observed open-loop ACE noise

4.1.2 Load forecast error analysis

The MEPSO provided necessary input data for balancing reserve sizing, such as historical wind and solar forecast errors, including load forecast for observed target years (2025, 2030 and 2040), as well as wind and solar hourly capacity factors. On the other hand, historical load time-series (Day ahead forecast and realization) were taken from ENTSO-E Transparency Platform for the period 2015-2021.

The following Table 4.2 shows numerical characteristics, such as mean value, standard deviation of load forecast error in analyzed period 2015-2021. It should be emphasized here that for almost all years (all except year 2020) data for MEPSO market area on ENTSO-E Transparency Platform are only partially populated.

Therefore, missing data were replaced with best available data, i.e. with the data from previous/next day. This may have an impact on all parameters presented in the table.

Table 4.2 – Historical load forecast error numerical characteristics (ENTSO-E data)

	2015	2016	2017	2018	2019	2020	2021
Lmax [MW]	1559	1406	1460	1388	1423	1401	1419
σ [MW]	85.8	44.4	42.5	56.0	77.9	62.2	62.8
μ [MW]	-16.7	27.4	19.2	35.7	42.3	35.9	37.4
P99- [MW]	-482.8	-217.2	-99.7	-256.0	-156.9	-273.2	-179.0
P99+ [MW]	130.0	143.1	210.0	180.0	339.5	186.1	227.5

It should be noted that mean value is strictly positive from 2016 to 2021 and is greater than 50% of standard deviation, indicating that load forecast overestimates the consumption in operational practice. 99th percentile of load forecast error for both directions, positive and negative were calculated only as an illustration of demand imbalance level in history.

The following table shows main numerical characteristics of load forecast error in year 2020, such as monthly normalized mathematical expectation (μ) and monthly normalized standard deviation (σ). This year has been selected as a referent since it gives us typical representation of system performance for the last decade as well as due to missing values in other years. All values are normalized to annual peak load value of 1401 MW, which occurs during December. The input data were taken from the ENTSO-E Transparency Platform, in form of hourly time series of forecasted and realized hourly load. It can be seen that relative numerical characteristics of forecast error are pretty much constant during the year, with exception of April. On the other hand, normalized root mean square forecast error (nRMSE) is between 2% and 10% during the year, with its peak in April.

Table 4.3 – Load forecast error numerical characteristics (ENTSO-E Transparency Platform)

Month	μ	σ	nRMSE [%]	Pmax [MW]
January	0.0427	0.0422	6.0%	1305
February	0.0224	0.0456	5.1%	1289
March	0.0231	0.0431	4.9%	1174
April	0.0336	0.0902	9.6%	1169
May	0.0377	0.0325	5.0%	870
June	0.0198	0.0396	4.4%	852
July	0.0208	0.0318	3.8%	960
August	0.0382	0.0288	4.8%	919
September	0.0207	0.0221	3.0%	904
October	0.0149	0.0340	3.7%	1073
November	0.0112	0.0374	3.9%	1343
December	0.0215	0.0356	4.2%	1401

It should be added that normalized standard deviation of load forecast error for MEPSO control area (relative to the peak demand) is above the value calculated for EMS control area in 2020 and below the value calculated for CGES control area in 2020. Therefore, it is difficult to compare these parameters since the peak demand has a significant impact to normalized value.

The following diagram (Figure 4.9) shows typical daily profiles of normalized load forecast error for arbitrary chosen several days of 2020. Typical daily profiles by months have been used within ANTARES Time-Series Analyzer and Time-Series generator in order to preserve typical daily patterns. Therefore, all synthetic forecast errors time-series reflects these typical patterns.

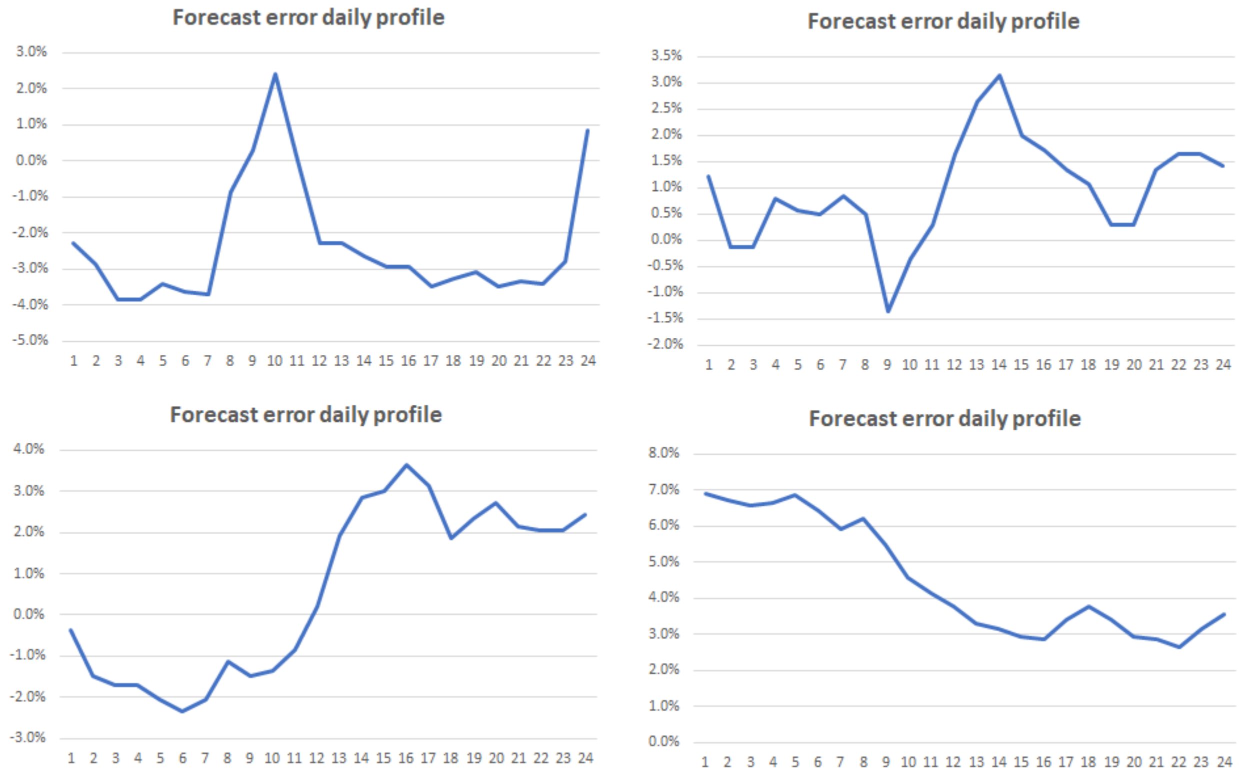

Figure 4.9 – Normalized load forecast error daily profile (ENTSO-E Transparency Platform)

Empirical histogram of load forecast error, as well as corresponding Normal distribution probability density function are shown on Figure 4.10. It can be seen that load forecast error probability density function in 2021 is positively shifted.

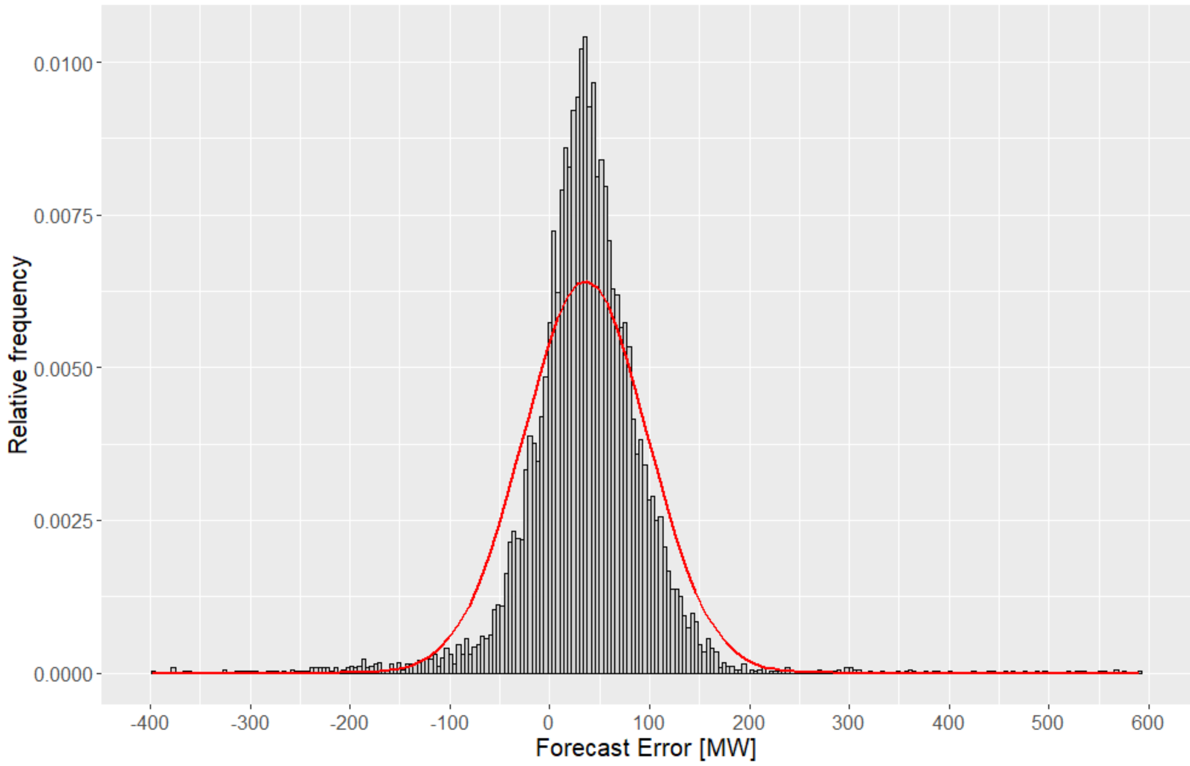

Figure 4.10 – Comparison of hourly load forecast error histogram with normal distribution

On the other hand, in order to test if hypothesized distribution is proper or not, quantile-quantile (Q-Q) diagrams can be constructed by plotting the quantiles from hypothesized theoretical distribution against observed quantiles from empirical distribution (Figure 4.11 and Figure 4.12). It can be seen from the Q-Q diagram that, empirical distribution is very close to the normal distribution in wider interval around the mean value. However, significant discrepancy is present in the region of extreme forecast errors (both positive and negative).

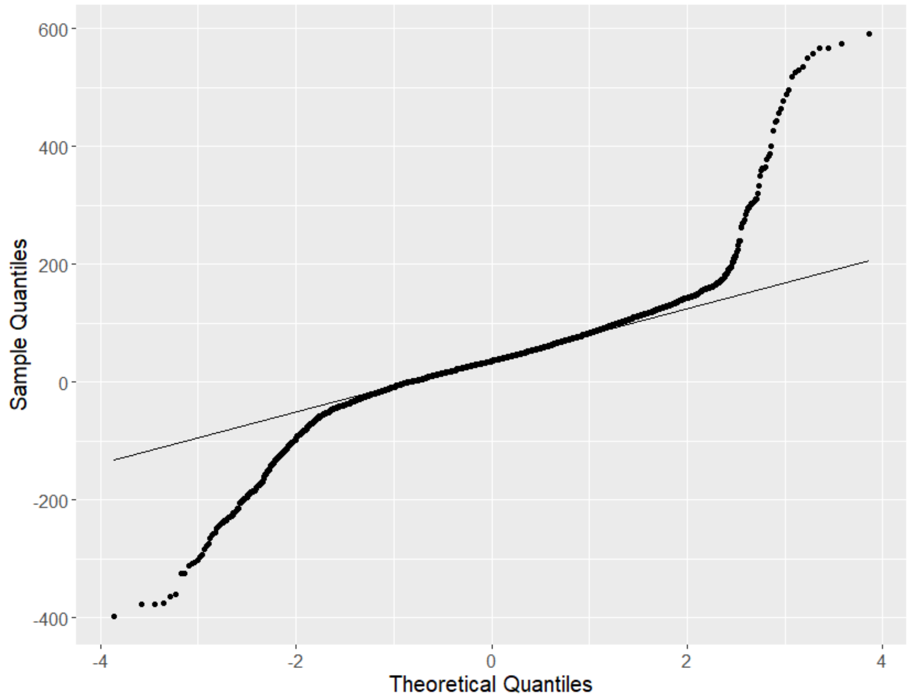

Figure 4.11 – A normal quantile-quantile plot of the distribution of day-ahead load forecast error

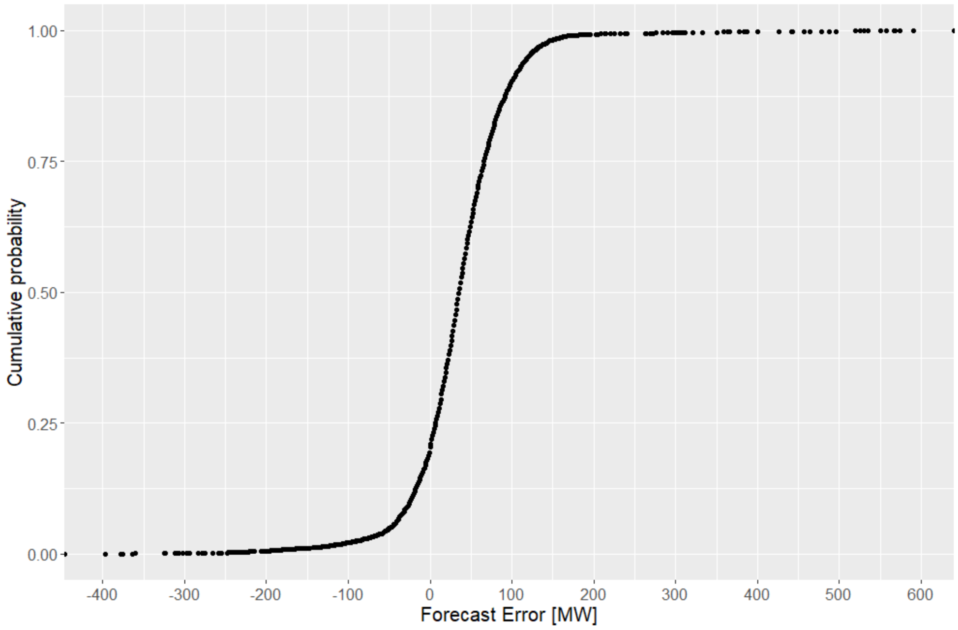

Figure 4.12 – Empirical cumulative distribution function of observed load forecast error

4.1.3 Wind forecast error analysis

Regarding the wind forecast error, MEPSO provided hourly day-ahead forecast and realization for 2021. Data correspond to the only one existing wind power plant in North Macedonia, i.e. for WPP Bogdanci with 36.8 MW of installed capacity. Wind forecast errors of planned wind power plants were generated using ANTARES

Time-Series generator based on provided data as well as corresponding numerical characteristics, such as mean value and standard deviation by months. The results are shown in the following table.

Table 4.4 – Wind forecast error numerical characteristics (MEPSO data)

Month	μ	σ	nRMSE [%]
January	0.0402	0.2067	21.1%
February	-0.0570	0.1938	20.2%
March	-0.0701	0.1965	20.9%
April	-0.0053	0.1986	19.9%
May	0.0030	0.2317	23.2%
June	-0.1173	0.3364	35.6%
July	-0.0810	0.2367	25.0%
August	-0.0619	0.2861	29.3%
September	-0.0079	0.1677	16.8%
October	-0.0096	0.2154	21.6%
November	0.0494	0.1971	20.3%
December	0.0305	0.2174	22.0%

Wind forecast error (normalized) typical daily profiles, for a few days in 2021 are shown on Figure 4.13. It can be seen that the forecast error profiles are different for different days. However, there are hours within a day with practically zero forecast error. This is due to the fact that wind forecast error is a consequence of forecasted wind speed, since generation forecast is determined by prognosed wind speed and transfer function (i.e. the wind turbine power curve). Therefore, if forecasted wind speed is in interval between rated and cut-off wind speed of turbine, wind speed forecast error does not have a significant impact on generation forecast, since generation is always around nominal value. The similar situation is for the region below cut-in wind speed as well as the region for wind speed above cut-off wind speed, where the wind turbine generation should be at zero. The highest wind generation forecast errors are expected if forecasted wind speed is at the edge of nominal power generation as well as inside the region between cut-in and rated wind speed.

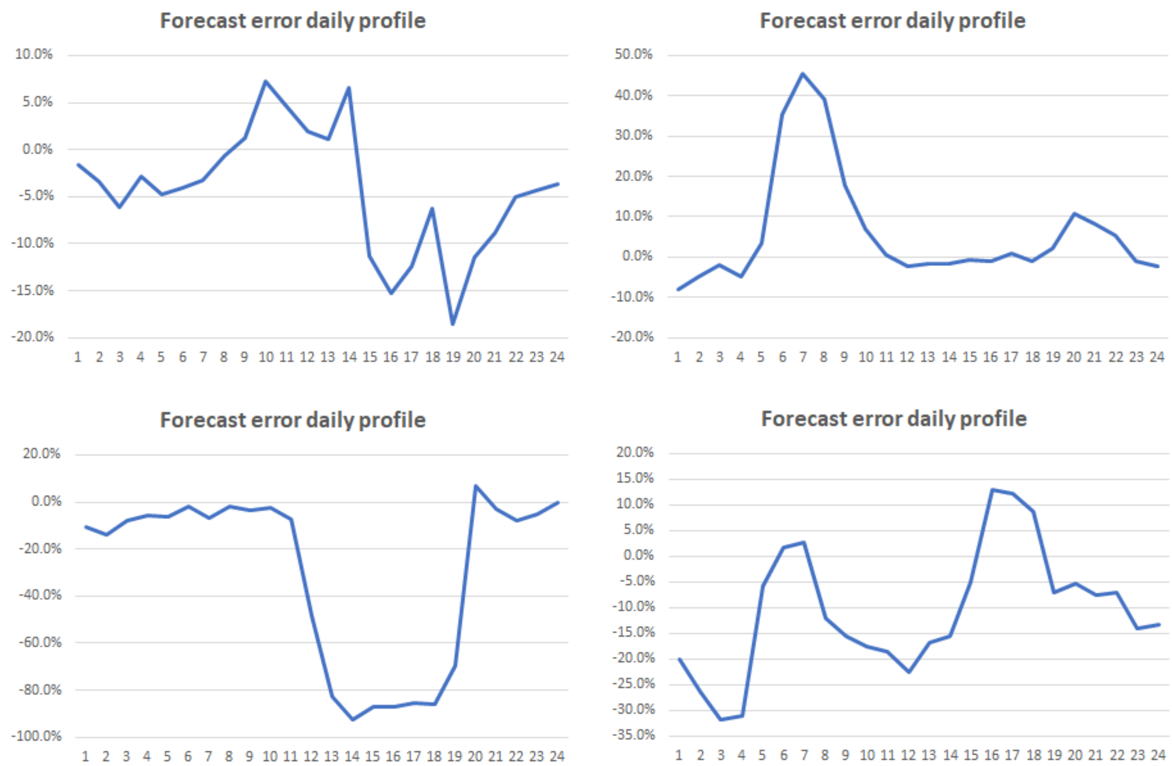

Figure 4.13 – Normalized wind forecast error daily profile (MEPSO data)

Typical daily profiles by months have been used within ANTARES Time-Series Analyzer and Time-Series generator, in order to preserve typical daily patterns. Therefore, all synthetic wind forecast errors time-series reflect these typical daily patterns.

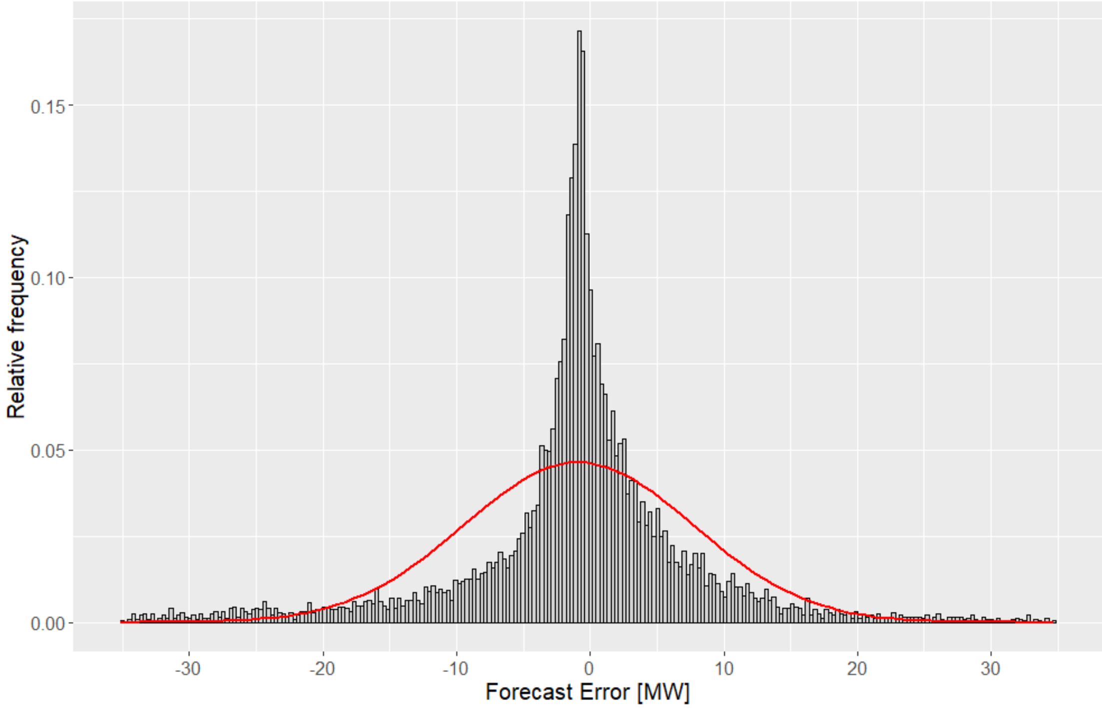

Figure 4.14 – Comparison of hourly wind forecast error histogram with normal distribution

Empirical histogram of wind forecast error, as well as corresponding Normal distribution probability density function are shown on Figure 4.14. According to previously described facts (related to wind turbine power curve), it is easy to conclude that wind forecast error could be equal to zero over an extended period of time, which happens in a high probability. Therefore, wind forecast error PDF converged in the peak, and it is almost centered.

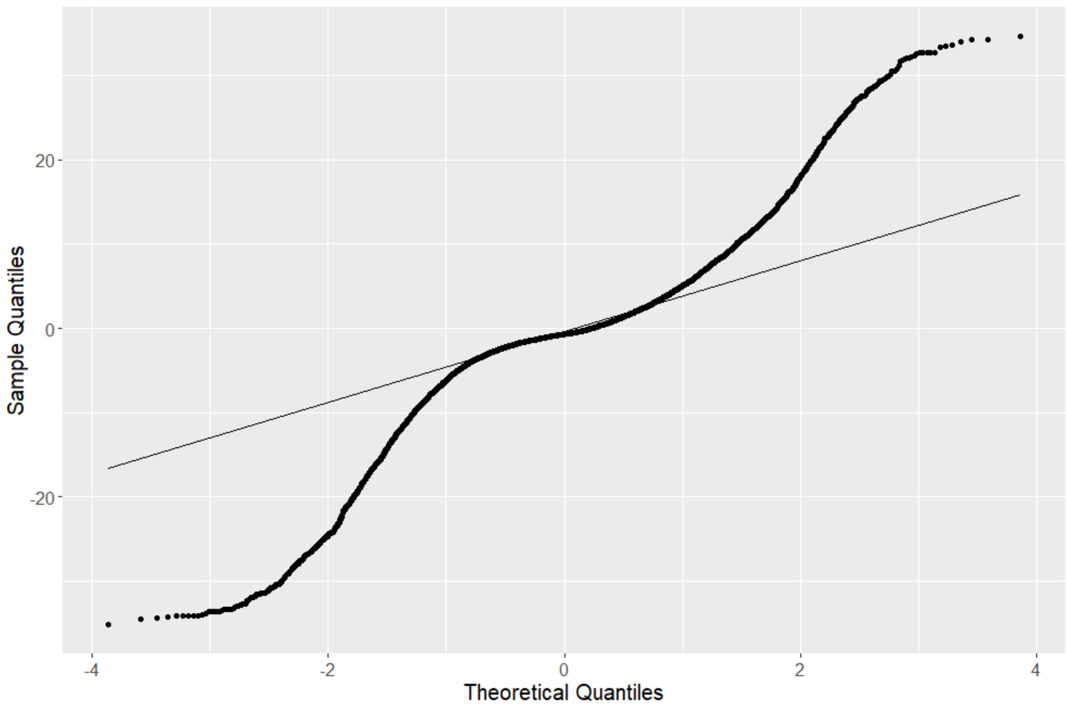

Figure 4.15 – A normal quantile-quantile plot of the distribution of day-ahead wind forecast error

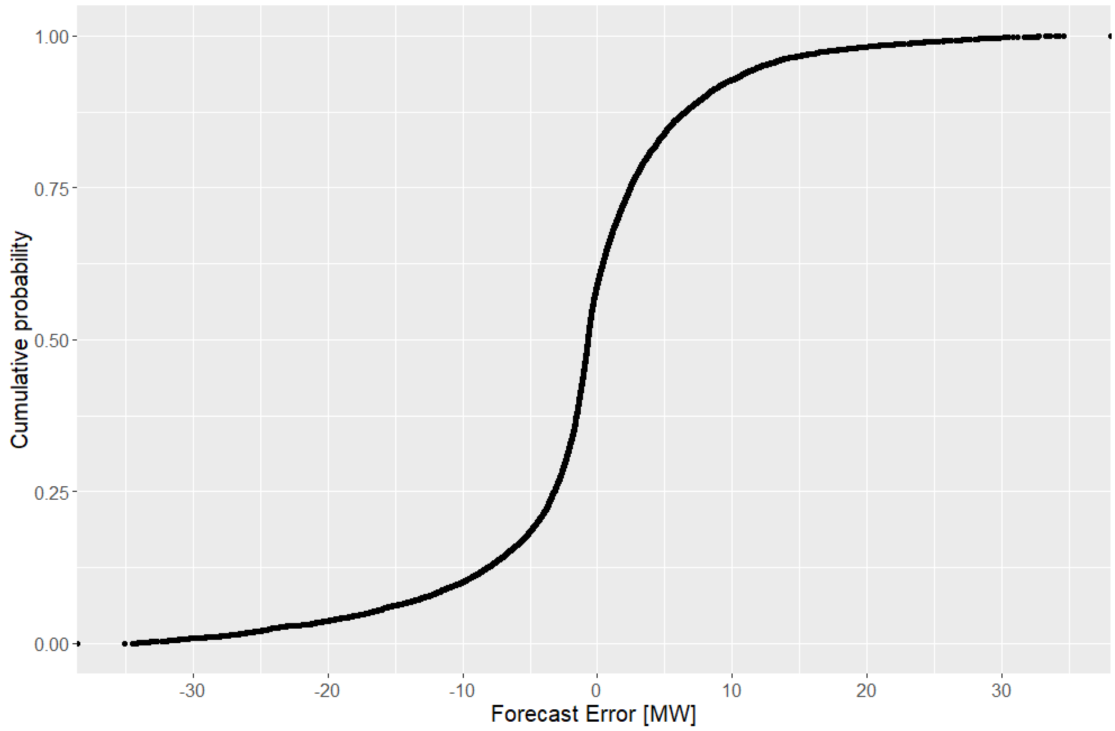

Figure 4.16 – Empirical cumulative distribution function of observed wind forecast error

A normal Q-Q diagram of hourly wind forecast error distribution is shown on Figure 4.15. It can be concluded that normal distribution cannot fit the PDF of observed forecast error very well in all cases. However, for the purpose of long-term planning, and according to the approach applied in many RES integration studies, Gaussian distribution has been used in all calculations. It should be emphasized here that ANTARES Time-Series generator takes into account other coefficients related to daily profile and autocorrelation, making synthetical time-series and corresponding “empirical” distribution more realistic. Finally, empirical cumulative distribution function of observed wind forecast error is shown on Figure 4.16.

4.1.4 Solar forecast error analysis

The MEPSO provided hourly day-ahead forecast of solar generation as well as realization for 2021. Data correspond to aggregated forecasts of distributed solar power plants generation in North Macedonia, with total installed capacity around 44 MW.

Table 4.5 – Solar forecast error numerical characteristics (MEPSO data)

Month	μ	σ	nRMSE [%]
January	-0.0164	0.0390	4.2%
February	-0.0186	0.0361	4.1%
March	-0.0190	0.0438	4.8%
April	-0.0095	0.0301	3.2%
May	-0.0087	0.0274	2.9%
June	-0.0156	0.0335	3.7%
July	0.0002	0.0509	5.1%
August	-0.0096	0.0188	2.1%
September	-0.0107	0.0260	2.8%
October	-0.0089	0.0349	3.6%
November	-0.0141	0.0507	5.3%
December	-0.0165	0.0365	4.0%

On the other hand, solar forecast errors of planned solar power plants were generated using ANTARES Time-Series generator based on provided input data by scenarios as well as corresponding numerical characteristics of historical forecast errors, such as mean value and standard deviation by months. The results are shown in Table 4.5.

Normalized root mean square forecast error for solar (nRMSE) is around 3.9% in 2021. It can be seen that nRMSE is above average annual level in March, July and November, while in May, August and September is below average value. Minimum is reached in August (around 2.1%).

Typical daily profiles of normalized solar forecast error are shown on Figure 4.17, for arbitrary chose four days of year 2021. It can be seen that the pattern is more or less similar. In fact, since the solar generation is more predictable compared to wind for instance, forecast error is more predictable as well, in sense of hours when forecast error is different than zero. It is clear that forecast error is expected only in part of the day between sunrise and sunset, which a consequence of analyzed year period as well as geographical position of country (latitude and longitude) and location specific topography. in other words, when we are estimating solar forecast error, window function should be considered. Other causes of forecast error within allowed interval are related to daily weather conditions, such as nebulosity. Typical daily profiles by months have been used within ANTARES Time-Series Analyzer and Time-Series generator, in order to preserve typical daily patterns. Therefore, all synthetic solar forecast errors time-series reflect these typical daily patterns.

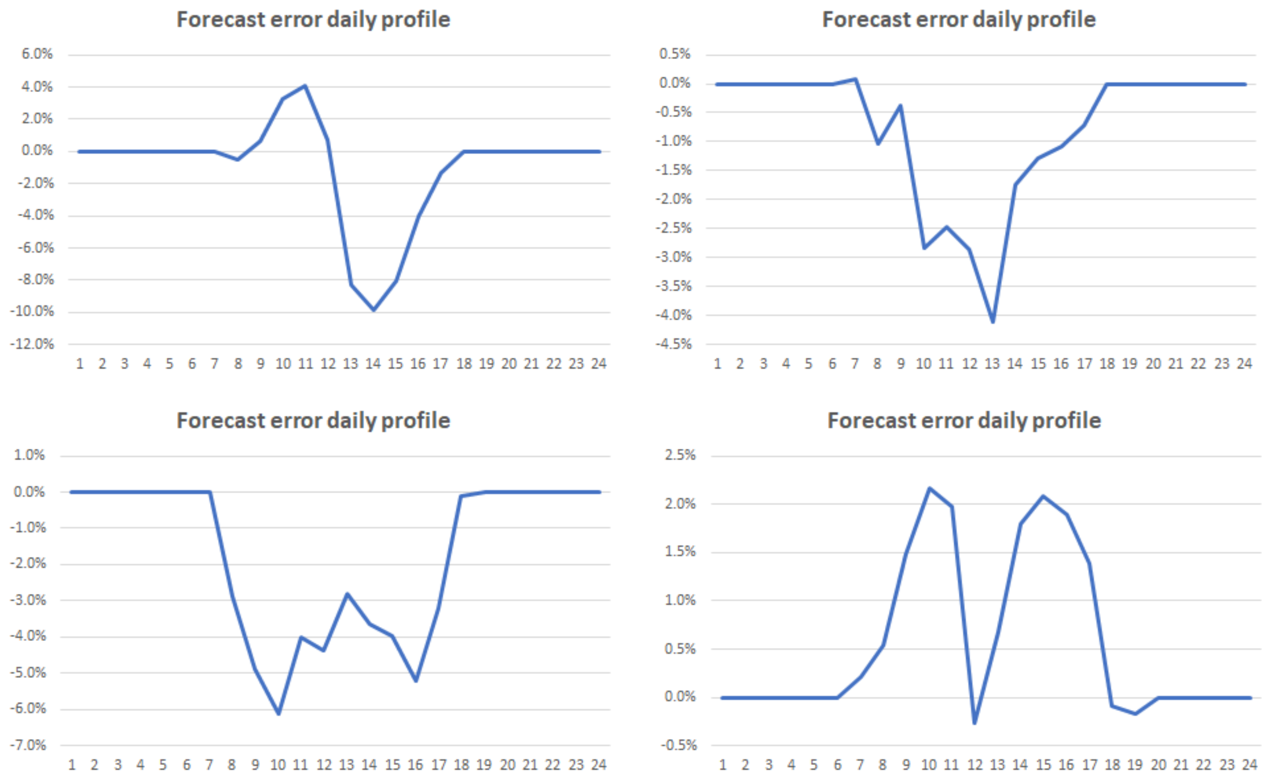

Figure 4.17 – Normalized solar forecast error daily profile (MEPSO data)

Empirical histogram of solar forecast error, as well as corresponding Normal distribution probability density function are shown and the following diagram (Figure 4.18). According to previously explained facts, related to nature of solar generation, it is easy to know that solar forecast error could be equal to zero over an extended period of time, which happens in a high probability. Therefore, solar forecast error is almost centered, with relatively small skew (negatively).

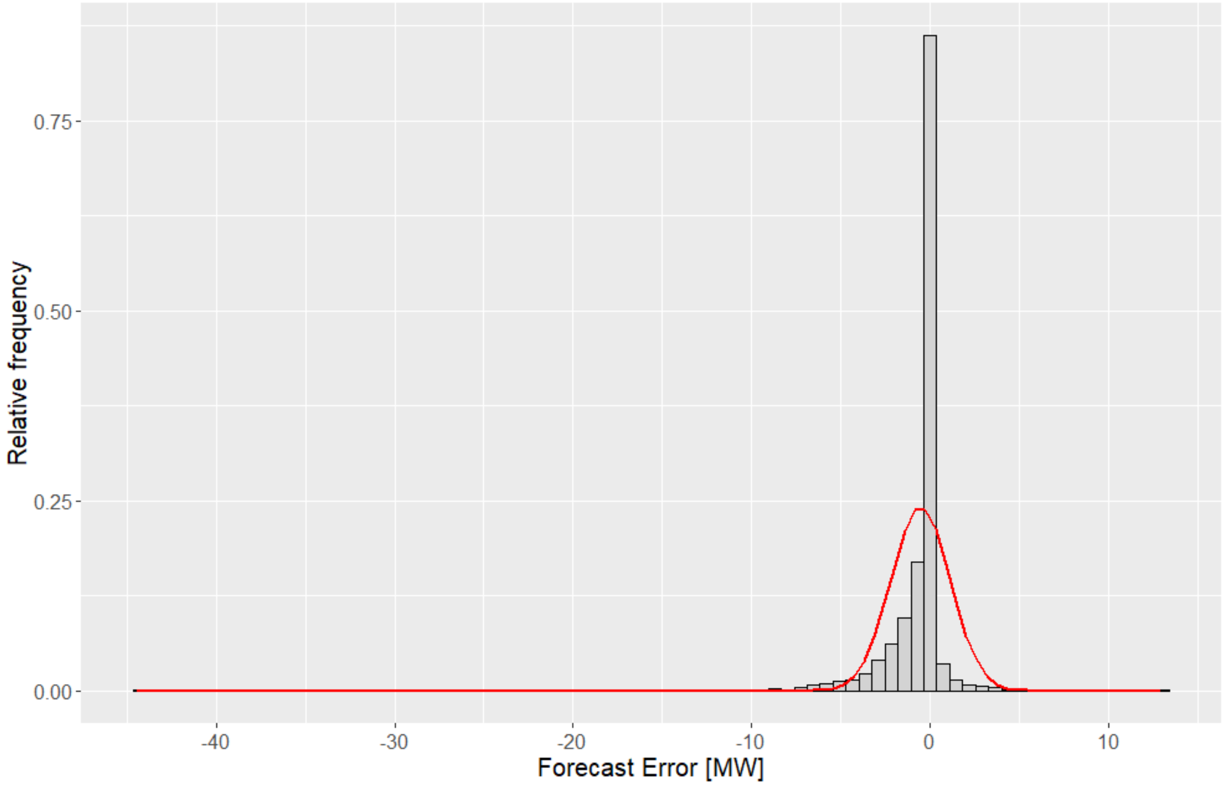

Figure 4.18 – Comparison of hourly solar forecast error histogram with normal distribution

The following figure (Figure 4.19) shows Q-Q diagram of solar forecast error distribution. It can be seen that in relatively narrow interval around the mean (i.e. zero) we have good approximation, while in case of larger errors there is a larger deviation from theoretically assumed Gaussian distribution.

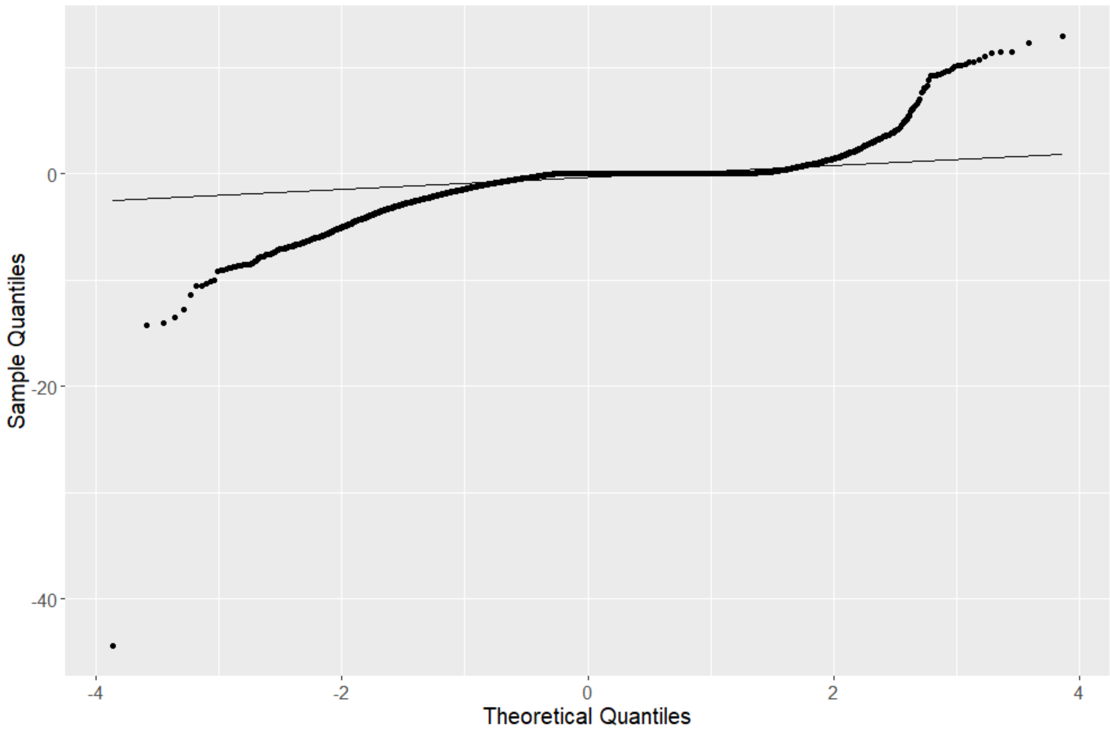

Figure 4.19 – A normal quantile-quantile plot of the distribution of day-ahead solar forecast error

However, for the purpose of long-term planning and according to the approach applied in many RES integration studies, Gaussian distribution has been used in all calculations. It should be emphasized here that ANTARES Time-Series generator takes into account other coefficients related to daily profile and autocorrelation, making synthetical time-series and corresponding "empirical" distribution more realistic. Finally, empirical cumulative distribution function of observed solar forecast error is shown on Figure 4.20.

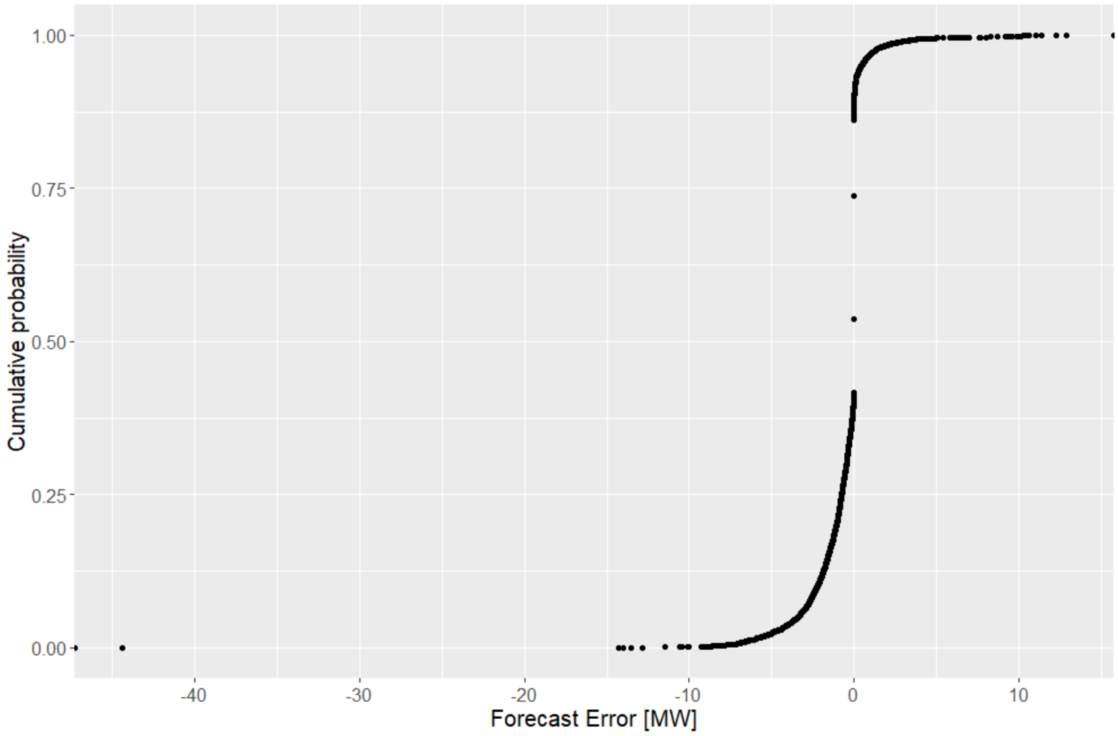

Figure 4.20 – Empirical cumulative distribution function of observed solar forecast error

4.2 Balancing reserve dimensioning results

Here are presented general results of reserve dimensioning for analyzed target years and VRE development scenarios. More detailed results by scenarios and target years area presented in separate subchapters below.

Installed VRE (i.e. wind and solar) capacities for analyzed three scenarios (Green, Rapid and Slow) and target years (2025, 2030 and 2040) are presented in Table 4.6.

Table 4.6 – North Macedonia installed VRE capacities evolution

Scenario	Year	WPP [MW]	SPP [MW]	VRE [MW]
Slow	2025	50	95	145
Green	2025	170	246	416
Slow	2030	170	315	485
Green	2030	410	630	1040
Slow	2040	446	806	1252
Rapid	2025	460	903	1363
Green	2040	750	1383	2133
Rapid	2030	944	2228	3172
Rapid	2040	1509	3941	5450

Load forecast error has been scaled up in order to reflect an impact of consumption increase on load forecast error increase, while VRE forecast error was aggregated using estimated time-series for all individual power plants in the system for analyzed development scenario. Change of normalized root mean square forecast error as a function of installed VRE capacity is presented on following figure (Figure 4.21).

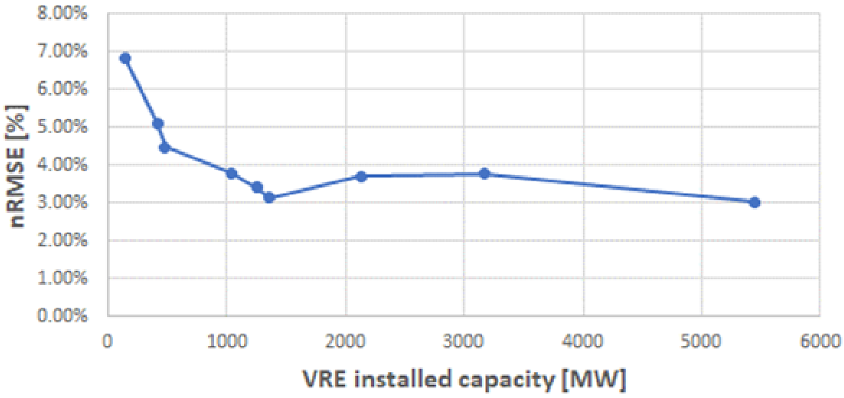

Figure 4.21 – VRE nRMSE as a function of installed VRE capacity

It can be concluded that permanent decrease of nRMSE is expected with increase of VRE installed capacity in the system. This is due to fact that installed VRE capacity increases linearly while aggregated absolute forecast error does not increase linearly, that can be expected according to analytic formula given in chapter 3.1.3.4. Initial level was estimated at the level of 7% with significant decrease up to the level of 3% for the first 1000 MW of VRE installed capacity. The results show that additional increase of VRE installed capacity does not significantly reduce the aggregated VRE nRMSE.

However, it should be noted that during the estimation of VRE forecast error impact on system imbalances in the future, nRMSE and other numerical characteristics of individual wind and solar power plants have been assumed to be the same as in the present (conservative approach). In other words, there were no assumed improvements in RES forecasting in the future.

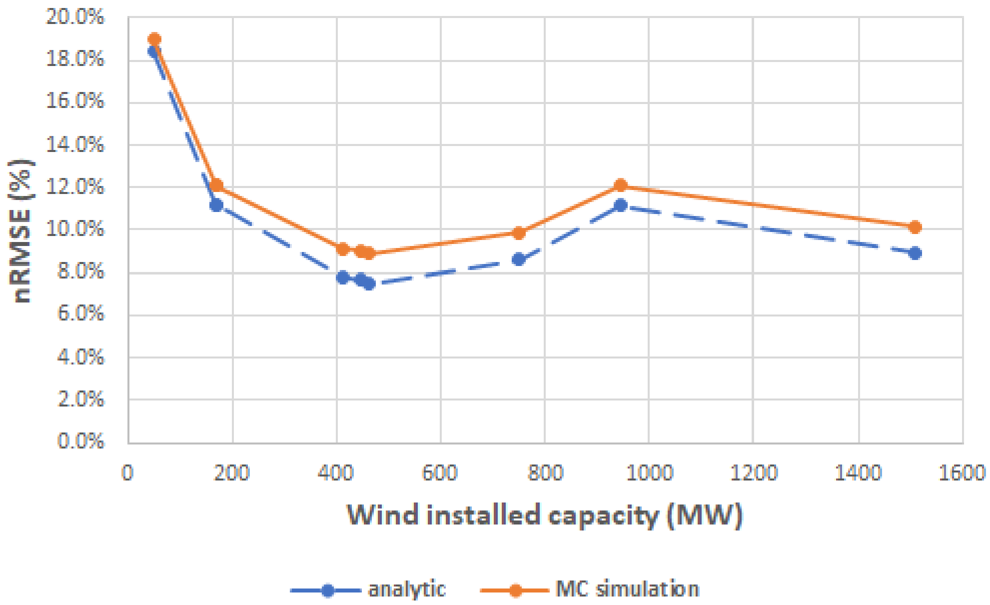

Figure 4.22 – Wind nRMSE as a function of installed capacity

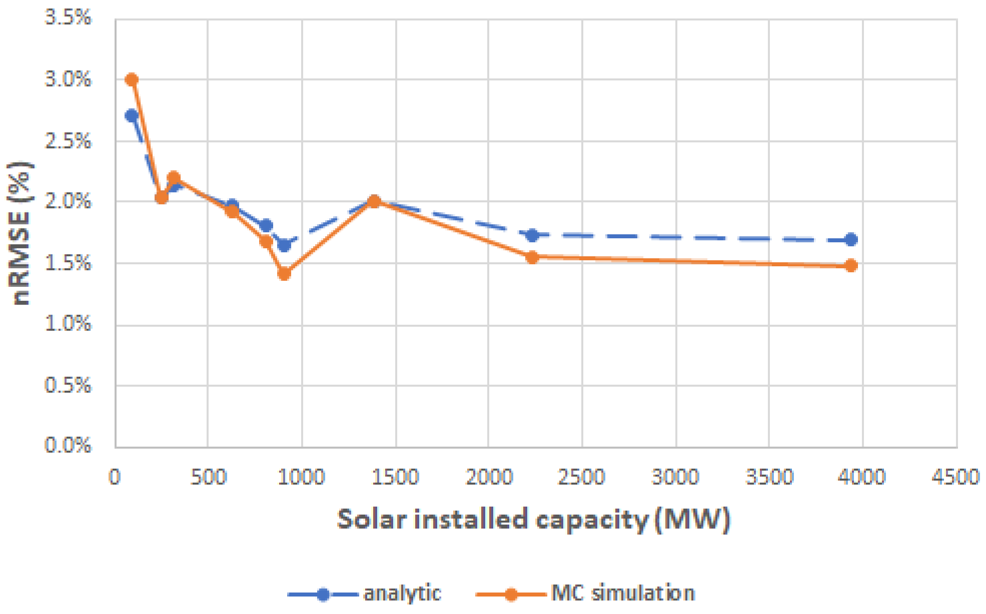

Figure 4.23 – Solar nRMSE as a function of installed VRE capacity

In order to distinguish the influence of wind and solar forecast error to total VRE forecast error, following two diagrams are presented (Figure 4.22 and Figure 4.23). On each figure, two different curves are shown. One with results of Monte Carlo simulation, based on synthetic forecast error data and one related to nRMSE calculated using analytic formula proposed in chapter 3.1.3.4. It can be concluded that these two curves are very close. Therefore, the analytic formula can be used for explanation of forecast error change with increase of VRE installed capacity.

At the beginning, for relatively low installed wind capacities, nRMSE decreases rapidly with addition of new wind power plants in the system up to the one limiting point. On the other hand, for a large wind installed capacity levels even a small increase of nRMSE is expected. These deviations from an inverse square root law can be explained by the impact of nRMSE coefficient alpha, described in chapter 3.1.3.4, that highly depends on installed capacities of individual power plants. The similar explanation can be applied to solar power plants.

It should be emphasized that both options for aFRR dimensioning mentioned in the previous chapters were tested[4]:

- The method base on 79th percentile of absolute system imbalance variation
- The method based on 99th percentile of absolute value of system imbalance noise component (with 15-min resolution)

After the initial analysis of results, the second method was adopted as referent. However, since still there is no unique rule for aFRR dimensioning, all results related to aFRR dimensioning should be taken with a grain of salt.

All the results related to reserve dimensioning presented here were calculated considering so-called "natural" forecast error for VRE. The results are presented in following subchapters by scenarios for analyzed target years 2025, 2030 and 2040. However, in order to compare the results between analyzed years and scenarios estimated VRE forecast errors were scaled up and down to match the referent nRMSE targets of 6%, 8%, 10% and 12%. These results were calculated based on original results taking into account so-called nRMSE factor[5].

[4] See subchapter 3.1.3.1

[5] See the definition in subchapter 3.1.2

Therefore, required reserve level as a function of installed VRE capacity and for different levels of VRE nRMSE is presented on following diagrams. It should be noted that the results correspond to 9 points calculated for three target years (2025, 2030 and 2040) as well as for three analyzed scenarios (Green, Rapid and Slow) described in Table 4.6. All these combinations take into account different load forecast error. Therefore, these diagrams do not represent only an impact of VRE installed capacity, but also the load and all other scenario/target year specific input data.

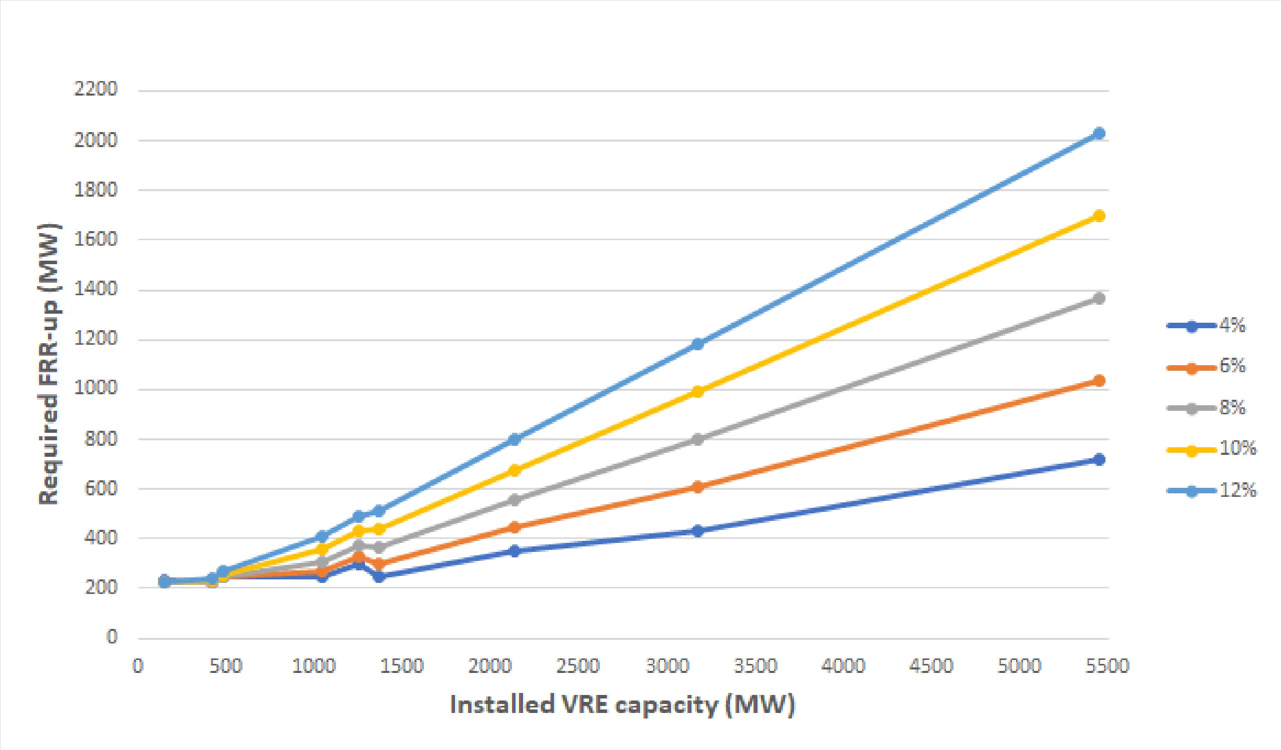

Figure 4.24 – Required level of upward FRR as a function of installed VRE capacity

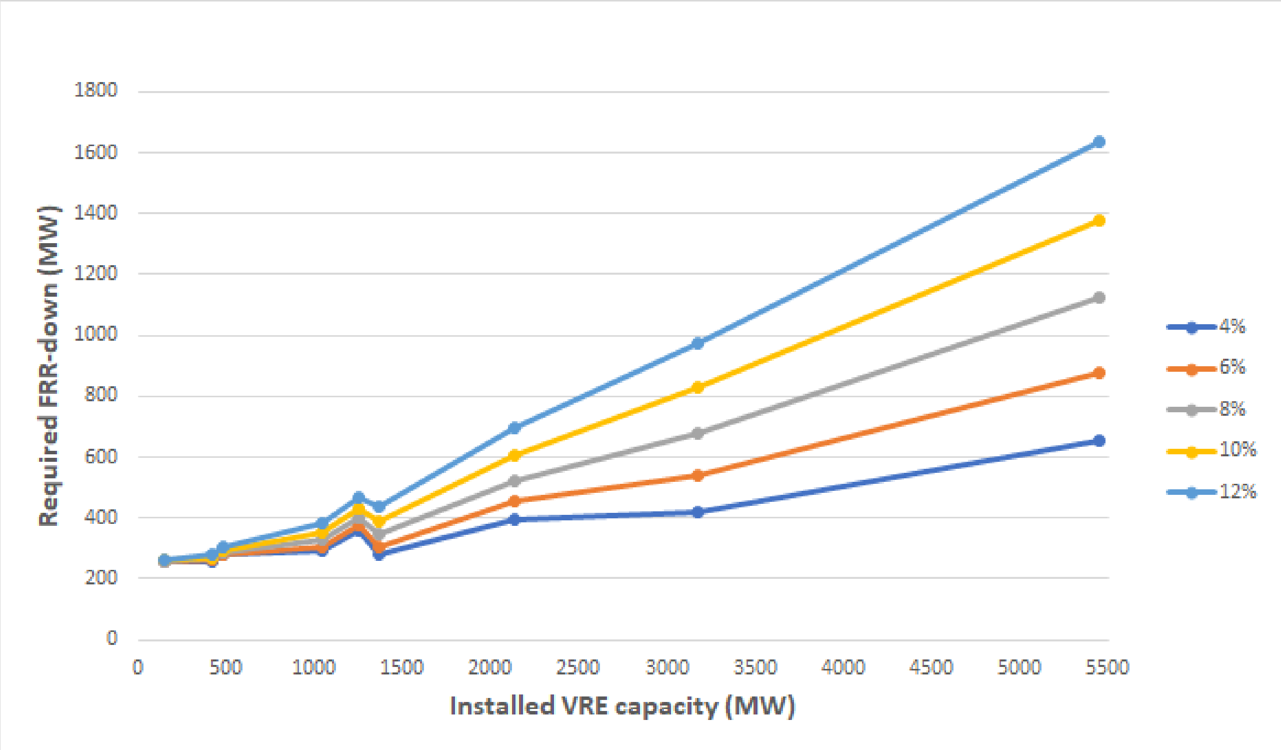

Figure 4.25 – Required level of downward FRR as a function of installed VRE capacity

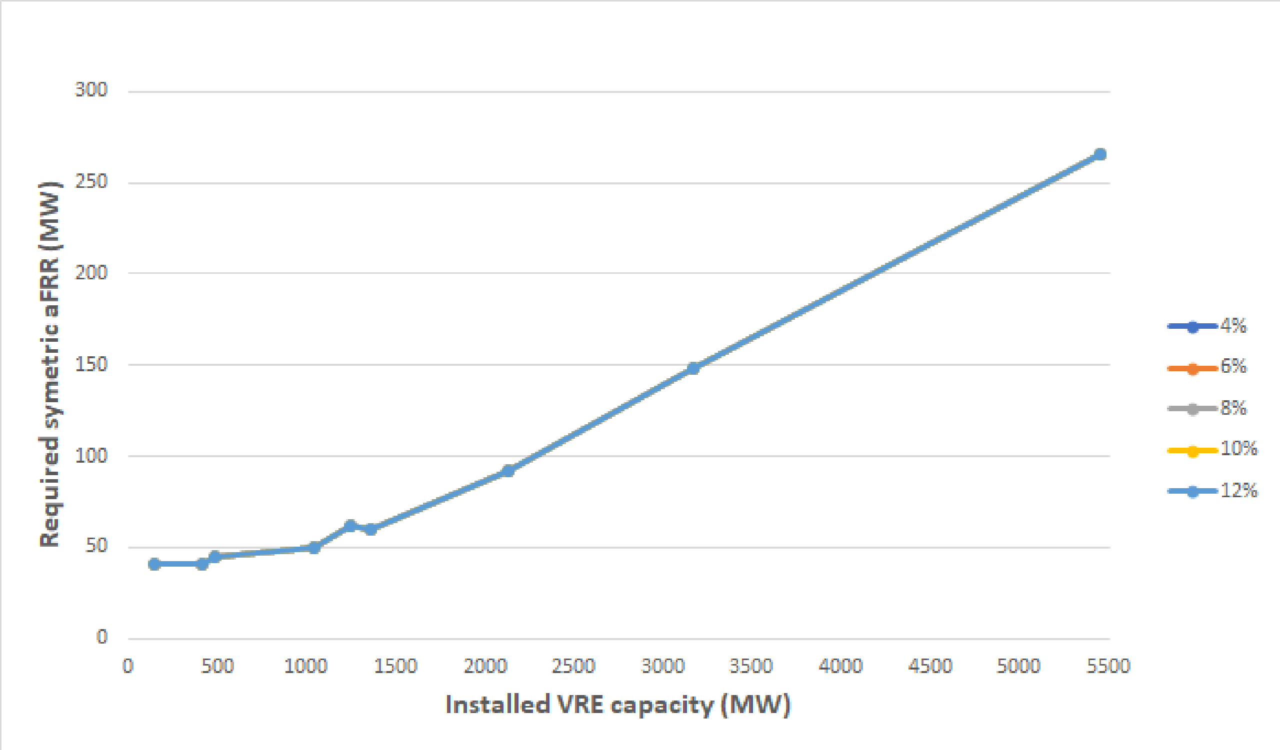

Figure 4.26 – Required level of symmetric aFRR as a function of installed VRE capacity

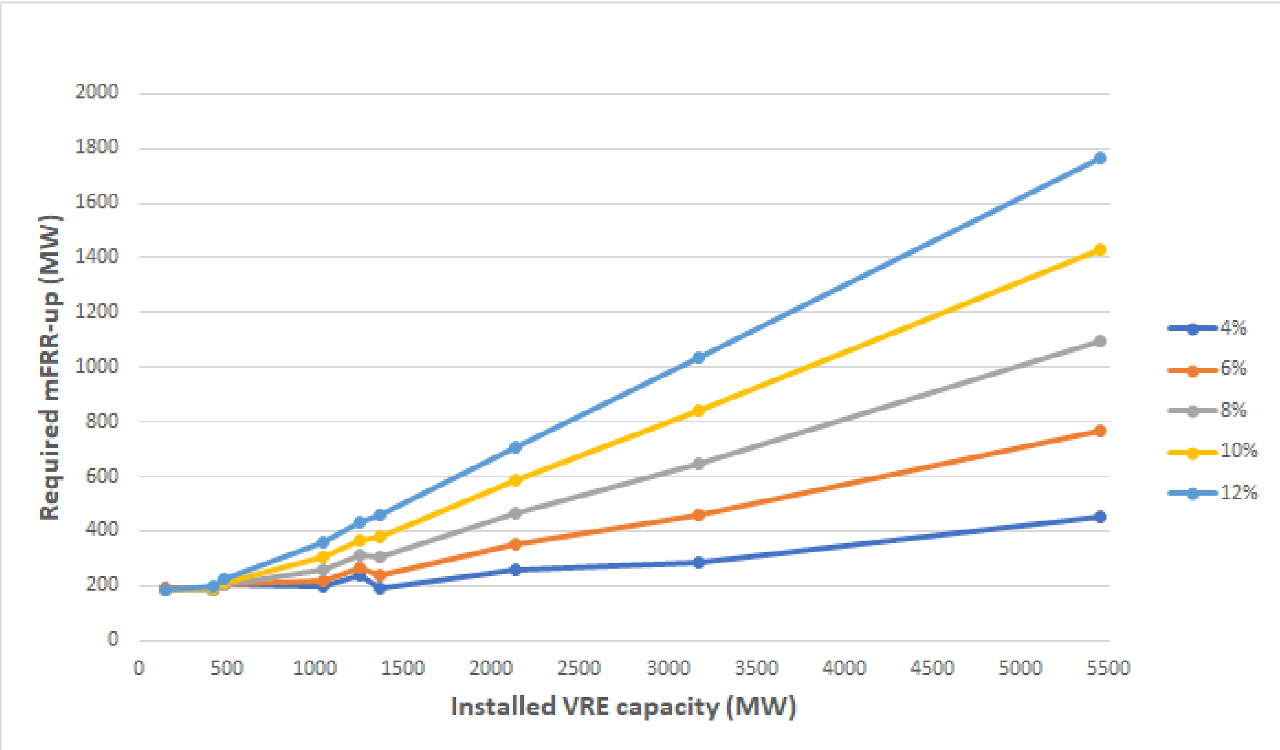

Figure 4.27 – Required level of upward mFRR as a function of installed VRE capacity

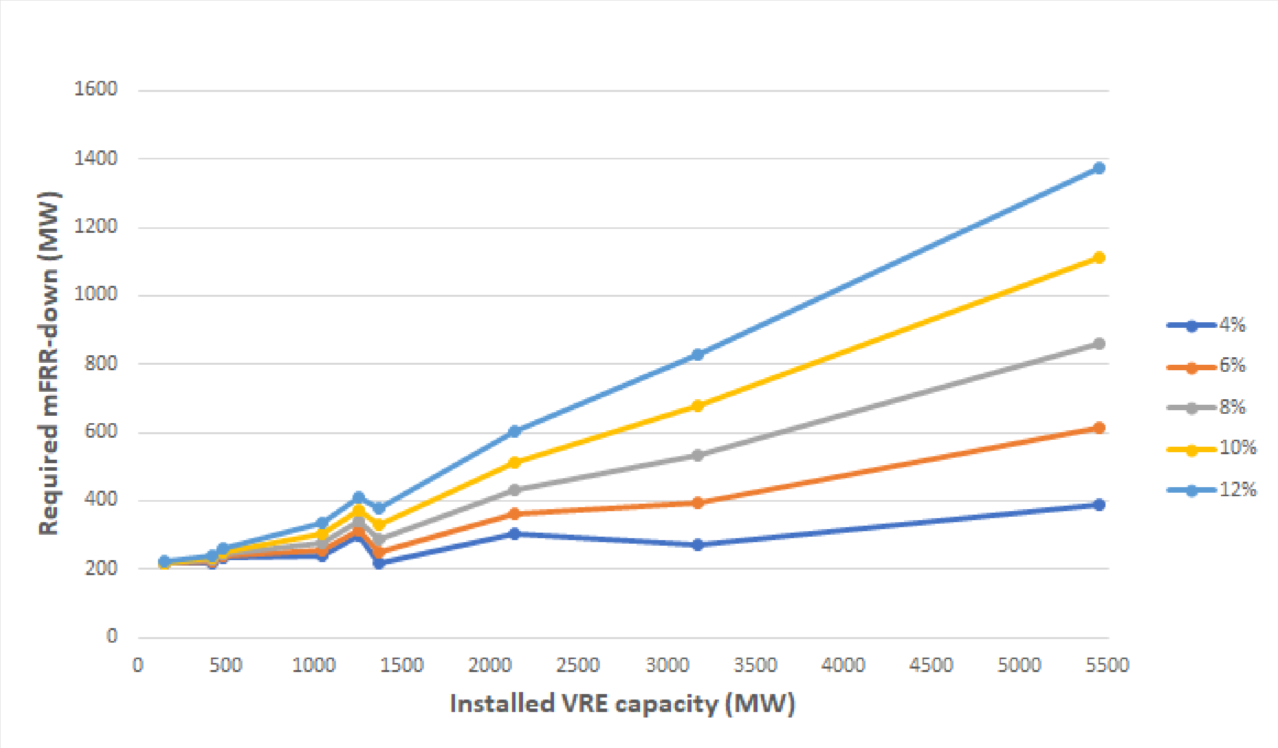

Figure 4.28 – Required level of downward mFRR as a function of installed VRE capacity

4.2.1 Green scenario

Balancing reserve dimensioning (aFRR and mFRR) results for Green scenario of development are presented in this subchapter, for all three analyzed years 2025, 2030 and 2040. In 2025 forecasted peak load in MEPSO market area is around 1562 MW (average on 35 climatic years, data provided by the MEPSO) while total VRE (wind and solar) installed capacity is 416 MW. The results of secondary (aFRR) and tertiary (mFRR) reserve dimensioning, as well as the total FRR level are presented in Table 4.7. The expected value for the reserve (i.e. the average over all simulated MC years) is given in the first column. It can be seen that total FRR in upward direction is 226 MW, while FRR downward is 261 MW, indicating the impact of assumed positively shifted load forecast error. On the other hand, a symmetric aFRR (upward and downward) is around 41 MW, which is less than the value calculated using the empiric formula (45.2 MW). All other typical values are presented in the table, such as minimum and maximum value among all simulated MC years, as well as the median (P50) and P95 value.

Table 4.7 – Secondary and tertiary reserve forecast – Green scenario (2025)

Product	EXP	MIN	MAX	P95	P50
FRR-up	**226**	149	302	285	222
FRR-down	**261**	215	319	311	257
aFRR-up	**41**	39	42	41	41
aFRR-down	**41**	39	42	41	41
mFRR-up	**186**	109	262	244	182
mFRR-down	**220**	176	278	269	217

The convergence of the obtained results is depicted on following diagrams (Figure 4.29). It can be seen that incremental average converges to the expected value practically for 35 MC years. However, in order to get the better convergence of results, 100 MC years were considered in all calculations. Aggregated "natural" VRE forecast error for the observed scenario and year is also depicted on the same figure.

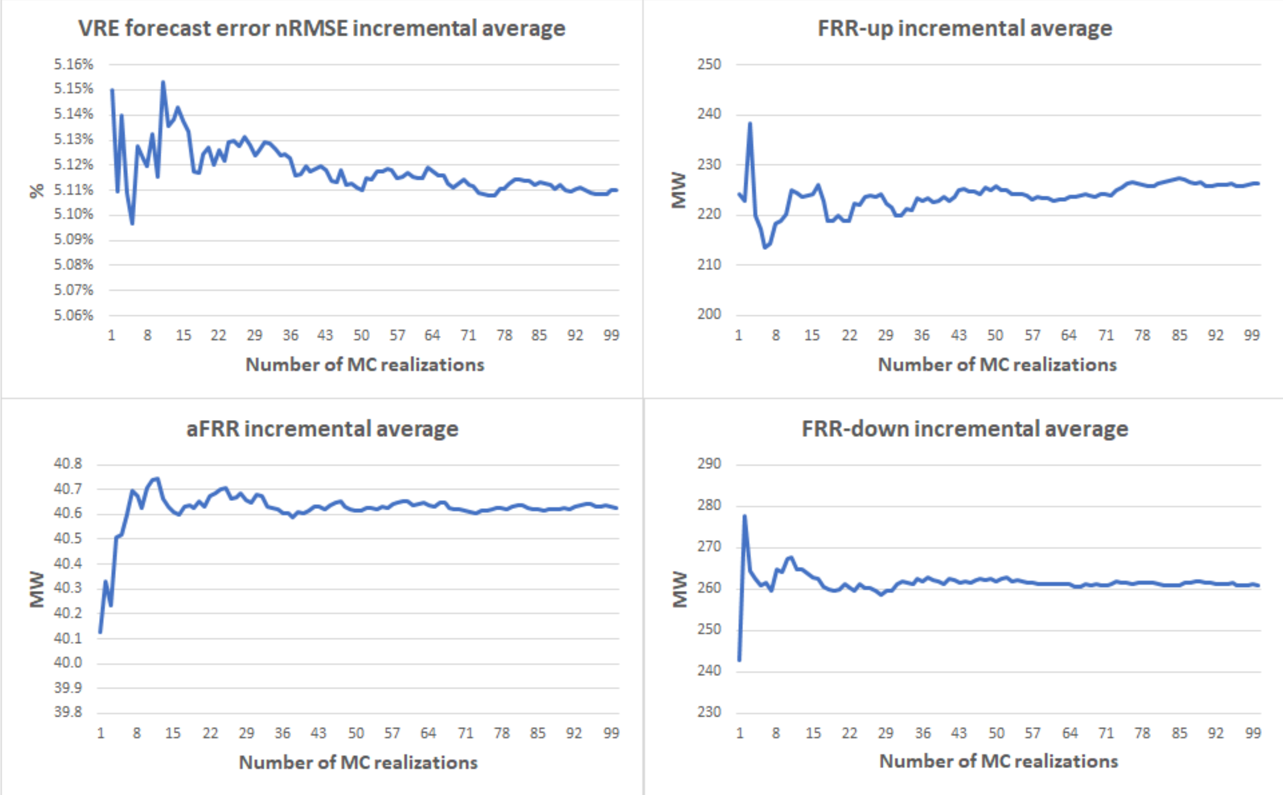

Figure 4.29 – Model convergence - Green scenario (2025)

Forecasted peak load in 2030 is expected to be around 1686 MW according to provided data by the MEPSO, while in case of Green scenario in 2030 total installed VRE capacity is 1040 MW. Secondary and tertiary reserve dimensioning results are presented in following table.

Table 4.8 – Secondary and tertiary reserve forecast – Green scenario (2030)

Product	EXP	MIN	MAX	P95	P50
FRR-up	**250**	179	321	300	249
FRR-down	**289**	234	382	341	288
aFRR-up	**50**	48	52	52	50
aFRR-down	**50**	48	52	52	50
mFRR-up	**200**	130	270	249	199
mFRR-down	**240**	185	334	291	238

Symmetric aFRR is around 50 MW which is higher than the value obtained by using of empirical formula (48.4 MW). Again, it can be concluded that downward FRR is greater than upward FRR due to positively shifted distribution for load forecast error.

The convergence of the obtained results is depicted on following diagrams (Figure 4.30). It can be seen that incremental average converges to the expected value practically for 35 MC years. Aggregated "natural" VRE forecast error for the observed scenario and year is also depicted on the same figure.

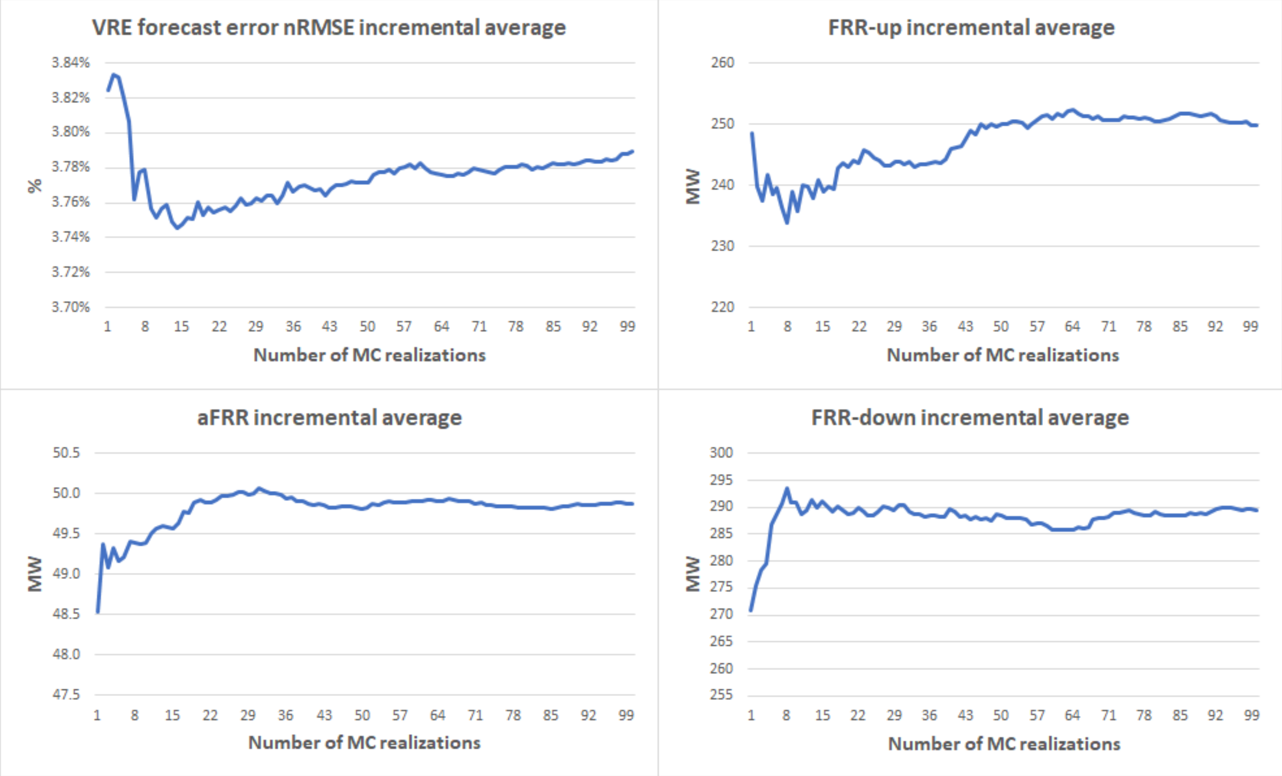

Figure 4.30 – Model convergence - Green scenario (2030)

Finally, the results for 2040 are presented in Table 4.9. This case assumes peak load in MEPSO control area of 2092 in 2040 and total VRE installed capacity of 2133 MW. It can be seen that total required FRR is significantly higher, while aFRR almost two times higher compared to 2030, which is higher than the value calculated using empirical formula (58.4 MW).

Table 4.9 – Secondary and tertiary reserve forecast – Green scenario (2040)

Product	EXP	MIN	MAX	P95	P50
FRR-up	**343**	268	444	401	340
FRR-down	**391**	335	488	442	389
aFRR-up	**92**	88	99	97	92
aFRR-down	**92**	88	99	97	92
mFRR-up	**251**	177	352	309	249
mFRR-down	**299**	240	397	351	298

The convergence of the obtained results is depicted on following diagrams (Figure 4.31). It can be seen that incremental average converges to the expected value practically for 35 MC years. Aggregated “natural” VRE forecast error for the observed scenario and year is also depicted on the same figure.

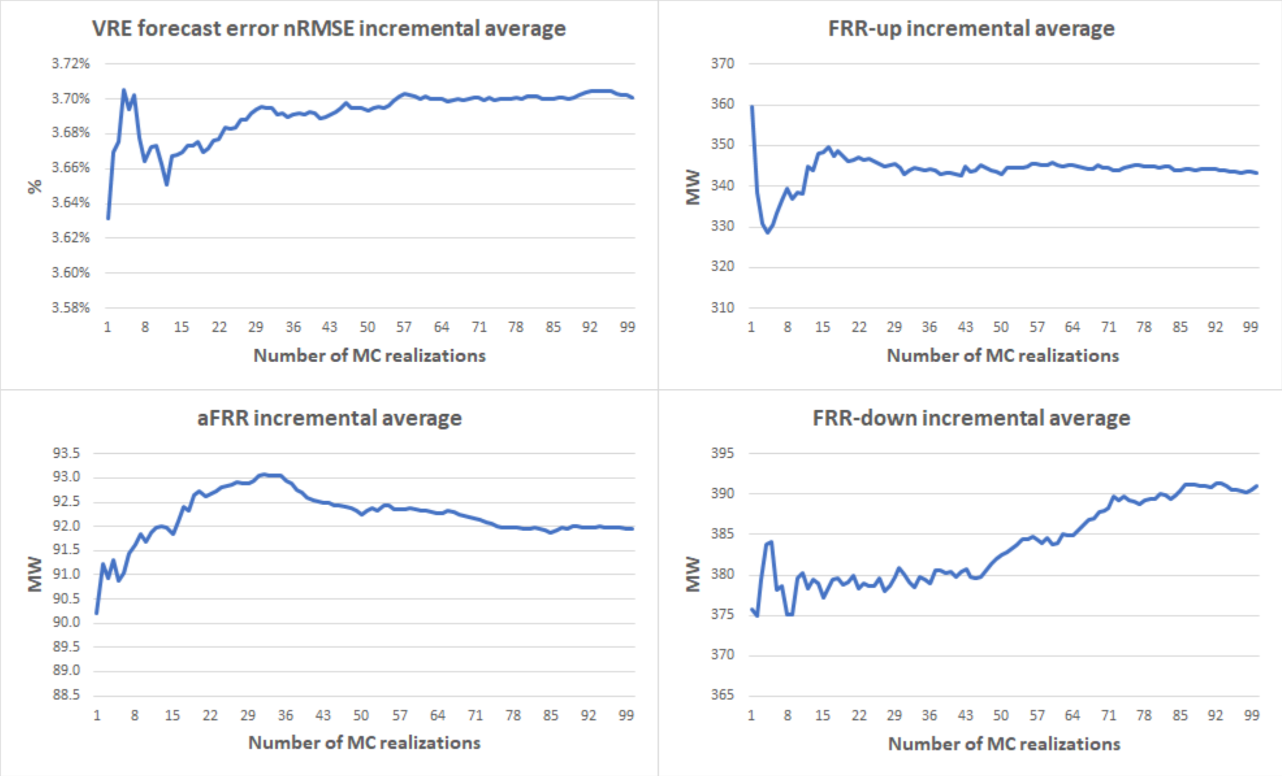

Figure 4.31 – Model convergence - Green scenario (2040)

4.2.2 Rapid scenario

Balancing reserve dimensioning (aFRR and mFRR) results Rapid scenario of development are presented in this subchapter, for all three analyzed years 2025, 2030 and 2040.

In 2025 forecasted peak load in MEPSO market area is around 1562 MW (average on 35 climatic years, data provided by the MEPSO) while total VRE (wind and solar) installed capacity is 1363 MW. The results of secondary (aFRR) and tertiary (mFRR) reserve dimensioning, as well as the total required FRR level are presented in Table 4.10. The expected value for the reserve (i.e. the average over all simulated MC years) is given in the first column. It can be seen that total FRR in upward direction is 236 MW, while FRR downward is 271 MW. On the other hand, symmetric aFRR (upward and downward) is around 60 MW, which is a little higher compared to calculated value for Green scenario. All other typical values are presented in the table, such as minimum and maximum value among all simulated MC years, as well as the median (P50) and P95 value.

Table 4.10 – Secondary and tertiary reserve forecast – Rapid scenario (2025)

Product	EXP	MIN	MAX	P95	P50
FRR-up	**236**	172	342	284	235
FRR-down	**271**	229	325	310	269
aFRR-up	**60**	57	64	63	60
aFRR-down	**60**	57	64	63	60
mFRR-up	**177**	113	281	225	176
mFRR-down	**211**	164	268	251	208

The convergence of the obtained results is depicted on following diagrams (Figure 4.32). It can be seen that incremental average converges to the expected value practically for 35 MC years. Aggregated “natural” VRE forecast error for the observed scenario and year is also depicted on the same figure.

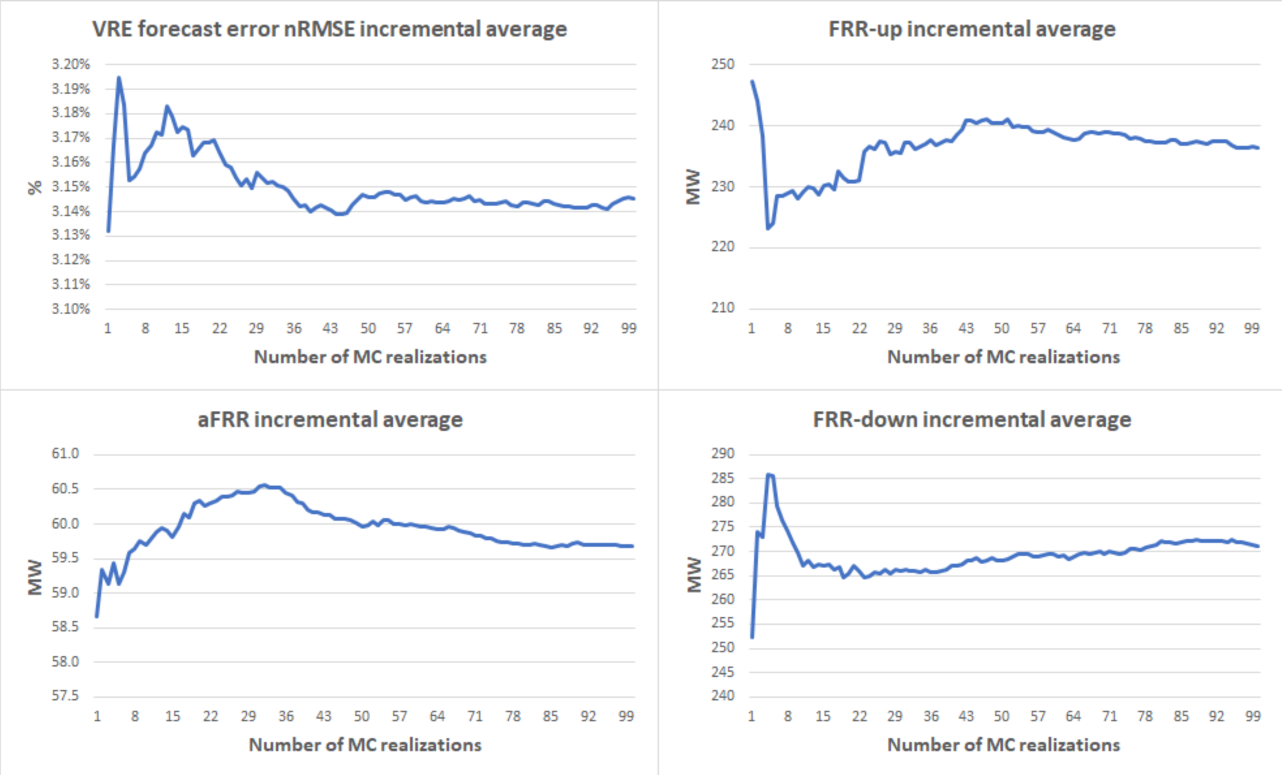

Figure 4.32 – Model convergence - Rapid scenario (2025)

Forecasted peak load in 2030 is expected to be around 1686 MW, according to provided data by the MEPSO, while in case of Rapid scenario in 2030 total installed VRE capacity is 3172 MW. Secondary and tertiary reserve dimensioning results are presented in following table (Table 4.11).

Table 4.11 – Secondary and tertiary reserve forecast – Rapid scenario (2030)

Product	EXP	MIN	MAX	P95	P50
FRR-up	**415**	363	477	455	413
FRR-down	**407**	382	449	438	405
aFRR-up	**149**	141	158	155	149
aFRR-down	**149**	141	158	155	149
mFRR-up	**266**	213	329	310	266
mFRR-down	**258**	228	300	287	257

The convergence of the obtained results is depicted on following diagrams (Figure 4.33). It can be seen that incremental average converges to the expected value practically for 35 MC years. Aggregated "natural" VRE forecast error for the observed scenario and year is also depicted on the same figure.

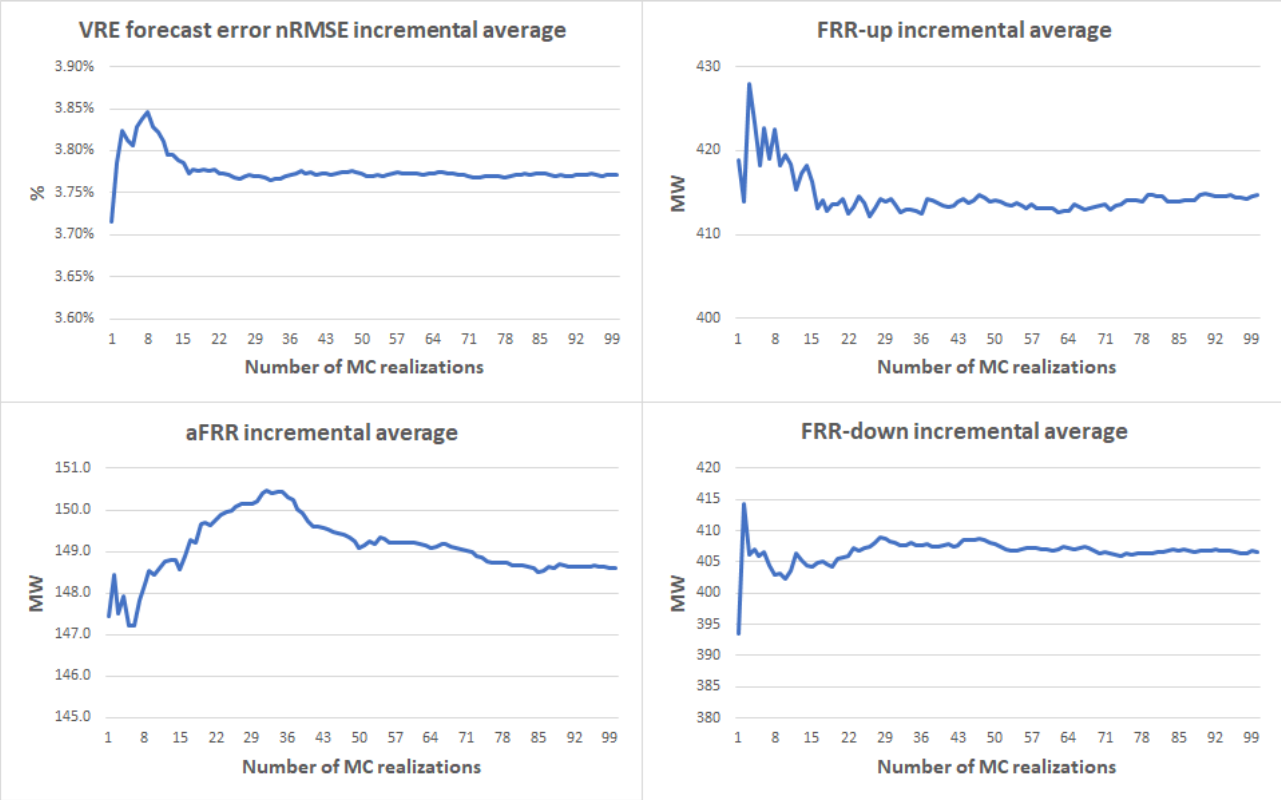

Figure 4.33 – Model convergence - Rapid scenario (2030)

Finally, the results for 2040 are presented in Table 4.12. This case assumes peak load in MEPSO control area of 2092 in 2040 and total VRE installed capacity of 5450 MW. It can be seen that total required FRR is higher compared to 2030.

Table 4.12 – Secondary and tertiary reserve forecast – Rapid scenario (2040)

Product	EXP	MIN	MAX	P95	P50
FRR-up	**574**	522	663	633	574
FRR-down	**556**	515	628	590	554
aFRR-up	**265**	253	281	275	266
aFRR-down	**265**	253	281	275	266
mFRR-up	**309**	256	391	367	307
mFRR-down	**291**	249	359	332	288

The convergence of the obtained results is depicted on following diagrams (Figure 4.34). It can be seen that incremental average converges to the expected value practically for 35 MC years. Aggregated “natural” VRE forecast error for the observed scenario and year is also depicted on the same figure.

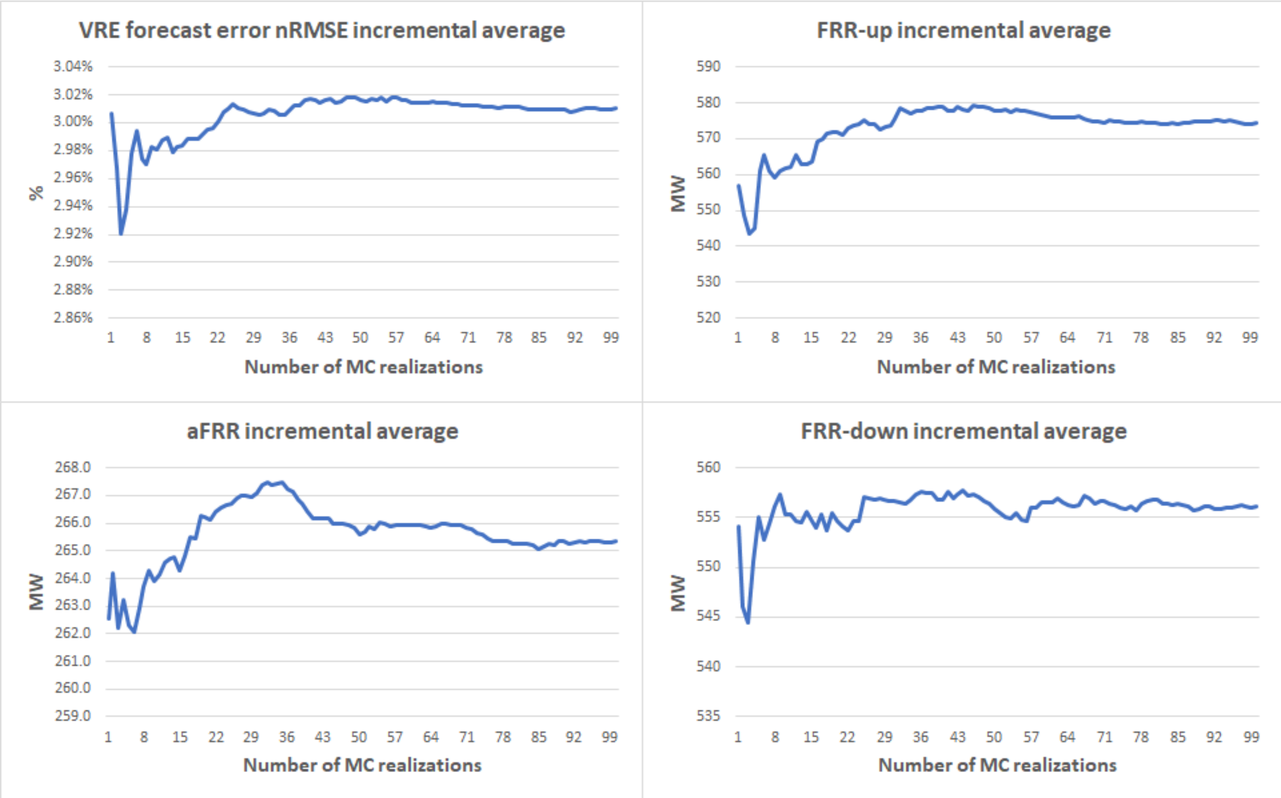

Figure 4.34 – Model convergence - Rapid scenario (2040)

4.2.3 Slow scenario

Finally, balancing reserve dimensioning (aFRR and mFRR) results for Slow scenario of VRE development are presented in this subchapter, for all three analyzed years 2025, 2030 and 2040.

In 2025 forecasted peak load in MEPSO control area is around 1562 MW (average on 35 climatic years, data provided by the MEPSO) while total VRE (wind and solar) installed capacity is only 145 MW. The results of secondary (aFRR) and tertiary (mFRR) reserve dimensioning, as well as the total required FRR level are presented in Table 4.13. The expected value for the reserve (i.e. the average over all simulated MC years) is given in the first column. It can be seen that total FRR in upward direction is 229 MW, while FRR downward is 259 MW. On the other hand, symmetric aFRR (upward and downward) is around 41 MW. All other typical values are presented in the table, such as minimum and maximum value among all simulated MC years, as well as the median (P50) and P95 value.

Table 4.13 – Secondary and tertiary reserve forecast – Slow scenario (2025)

Product	EXP	MIN	MAX	P95	P50
FRR-up	**229**	146	378	295	224
FRR-down	**259**	221	341	303	256
aFRR-up	**41**	39	42	41	41
aFRR-down	**41**	39	42	41	41
mFRR-up	**188**	105	337	256	183
mFRR-down	**218**	180	300	262	215

The convergence of the obtained results is depicted on following diagrams (Figure 4.35). It can be seen that incremental average converges to the expected value practically for 35 MC years. Aggregated “natural” VRE forecast error for the observed scenario and year is also depicted on the same figure.

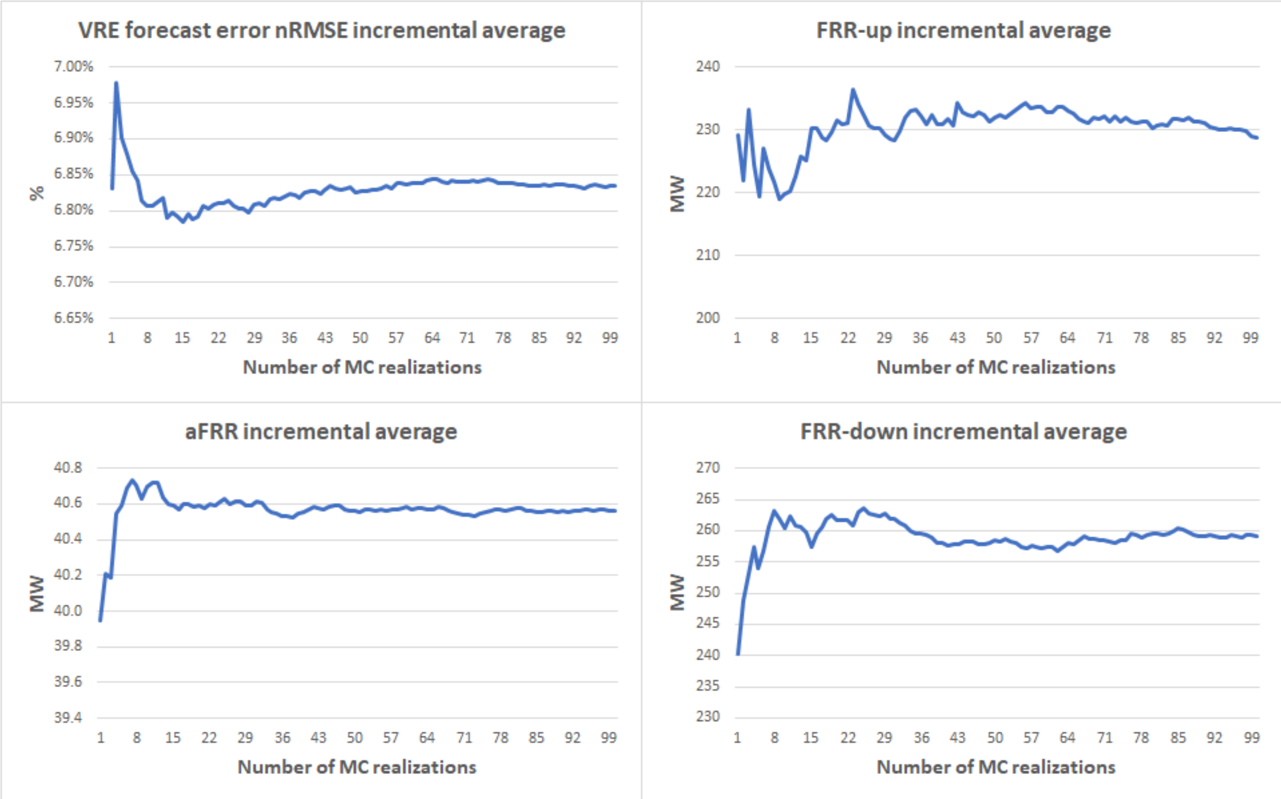

Figure 4.35 – Model convergence - Slow scenario (2025)

Forecasted peak load in 2030 is expected to be around 1686 MW, according to provided data by the MEPSO, while in case of Slow scenario in 2030 total installed VRE capacity is 485 MW. Secondary and tertiary reserve dimensioning results are presented in following table (Table 4.14).

Table 4.14 – Secondary and tertiary reserve forecast – Slow scenario (2030)

Product	EXP	MIN	MAX	P95	P50
FRR-up	**247**	165	349	309	248
FRR-down	**281**	238	331	320	280
aFRR-up	**45**	44	46	46	45
aFRR-down	**45**	44	46	46	45
mFRR-up	**203**	120	303	264	204
mFRR-down	**236**	193	286	275	234

The convergence of the obtained results is depicted on following diagrams (Figure 4.36). It can be seen that incremental average converges to the expected value practically for 35 MC years. Aggregated “natural” VRE forecast error for the observed scenario and year is also depicted on the same figure.

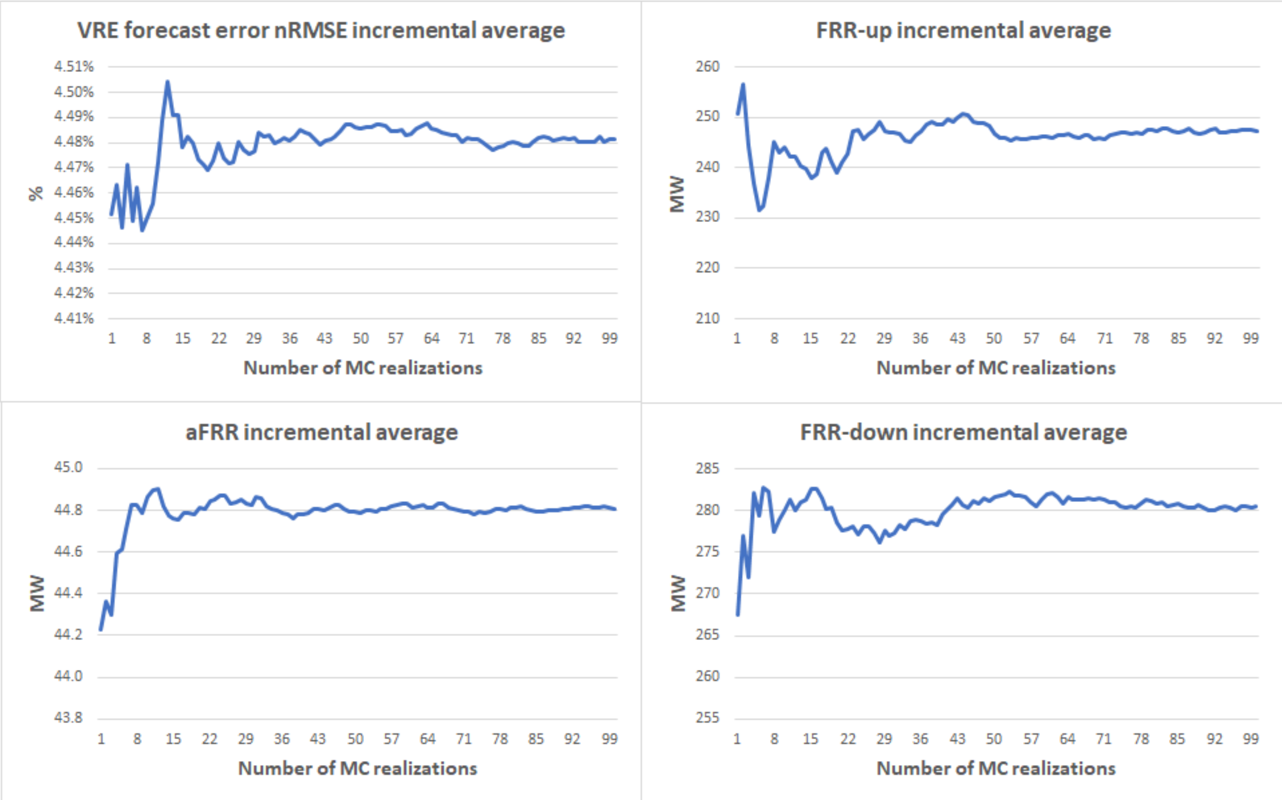

Figure 4.36 – Model convergence - Slow scenario (2030)

Finally, the results for 2040 are presented in (Table 4.15). This case assumes peak load in MEPSO control area of 2092 in 2040 and total VRE installed capacity of 1252 MW. It can be seen that total required FRR is significantly higher, while aFRR is a little higher (62 MW) than the value calculated using empirical formula (58.4 MW).

Table 4.15 – Secondary and tertiary reserve forecast – Slow scenario (2040)

Product	EXP	MIN	MAX	P95	P50
FRR-up	**299**	233	390	356	296
FRR-down	**355**	288	463	401	352
aFRR-up	**62**	60	65	64	62
aFRR-down	**62**	60	65	64	62
mFRR-up	**237**	169	328	294	234
mFRR-down	**294**	229	398	339	290

The convergence of the obtained results is depicted on following diagrams (Figure 4.37). It can be seen that incremental average converges to the expected value practically for 35 MC years. Aggregated “natural” VRE forecast error for the observed scenario and year is also depicted on the same figure.

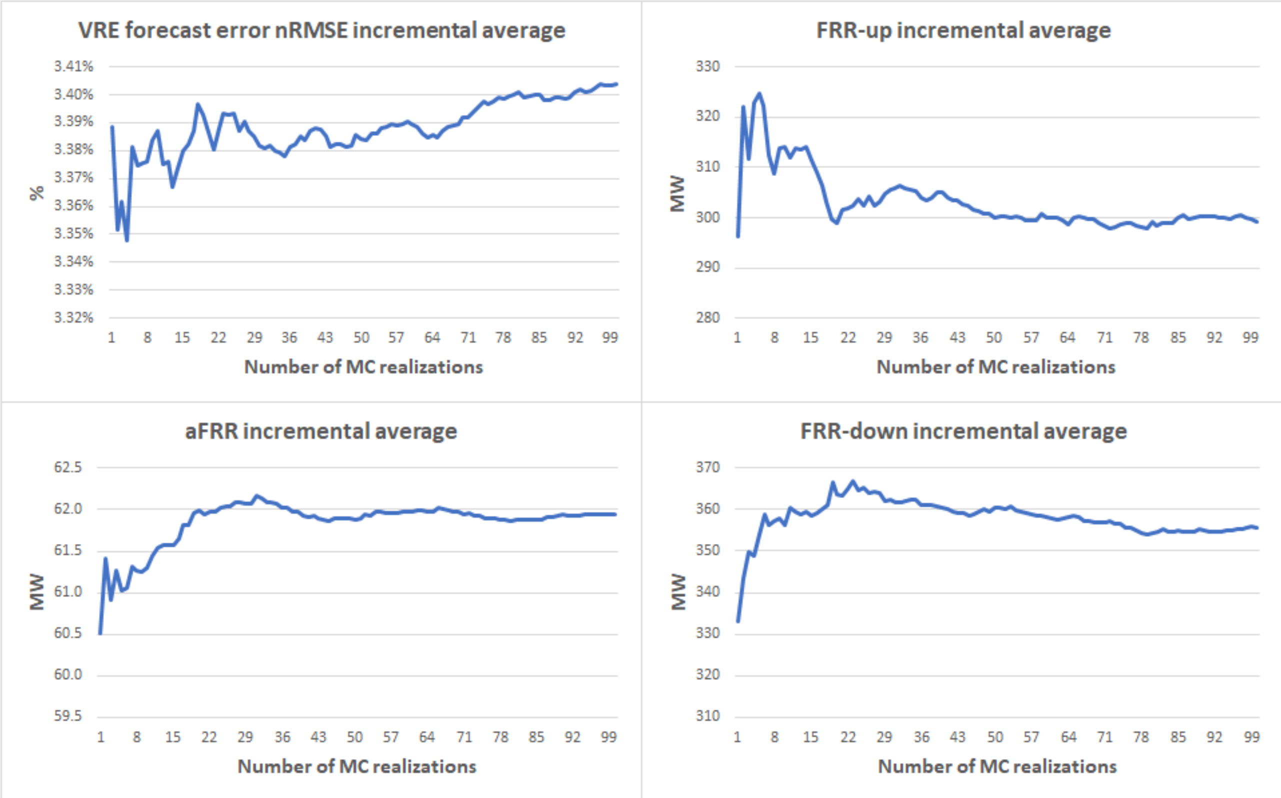

Figure 4.37 – Model convergence - Slow scenario (2040)

4.3 Mid-term reserve provision analysis

In order to test if the system is capable to provide required secondary and tertiary reserve levels in the near future i.e. in year 2025, preliminary market analyses in ANTARES have been carried out. To do so, Rapid scenario with 1363 MW of VRE installed capacity was selected as the most extreme.

Market analysis has been carried out based on developed Pan-European model that will be used for CBA analysis within this study. All input data were provided by the MEPSO and are in accordance with ENTSO-E studies TYNDP 2022 and ERAA 2021. MEPSO market area was modeled according to provided scenario specific data.

Calculated required secondary and tertiary reserve (in both directions), with assumed forecast error nRMSE level of 6%, was modeled as a spinning reserve via Binding Constraints (see Appendix). In addition, cross-zonal cooperation with EMS control area was considered due to participation in SMM block. By this approach up to 30% of required reserve (aFRR/mFRR) can be imported, of course if corresponding cross-zonal capacity (CZC) is allocated. On the other hand, it was assumed that all thermal and hydro units (except small and Run of River) can participate in both aFRR and mFRR provision, according to the MEPSO Grid Code. On the other hand, regarding downward mFRR reserve, it was assumed that shutdown of hydro units can provide additional downward capacity, while in case of thermal units, only difference between maximum generation capacity and actual generation was considered as a reserve.

The results of preliminary market simulation showed that required level of secondary and tertiary reserve can be provided by power plants within MEPSO control area in almost all hours in the year. In fact, in case of climatic year 2008 (the most critical among selected three typical ENTSO-E TYNDP 2022 years), there are some hours when the required reserve cannot be covered by the local hydro and thermal power plants. As a consequence, one part of the capacity was imported from the EMS control area, allocating the necessary cross-zonal transfer capacity.

Therefore, it can be concluded that the system can deal with planned level of VRE integration up to 2025, even in case of more aggressive Rapid scenario. During the hours with a lack of reserve in the system we can rely on cooperation within SMM block.

In case of other two analyzed climatic years (1995 and 2009), there are no problems with reserve provision, i.e. the entire capacity can be provided from internal generation capacities. Therefore, it can be concluded that climatic conditions have influence to reserve provision. Therefore, by analyzing all 35 climatic years, the more critical conditions can be found. In addition, simulating different forced outage patterns of thermal units, on large number of Monte Carlo years (for instance 700), the obtained results may be more various.

Following four diagrams show reserve capacity provision for all 700 simulated Monte Carlo years in 2025, in case of Rapid scenario of RES development in MEPSO market area.

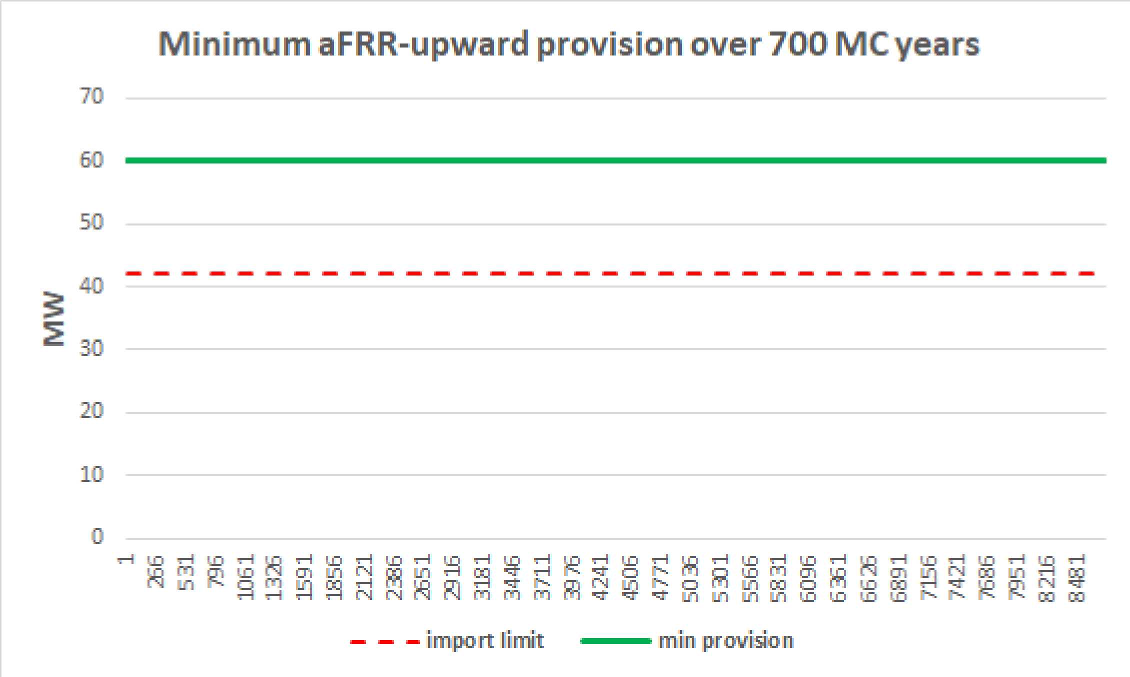

Figure 4.38 – Upward secondary reserve provision - Rapid scenario (2025)

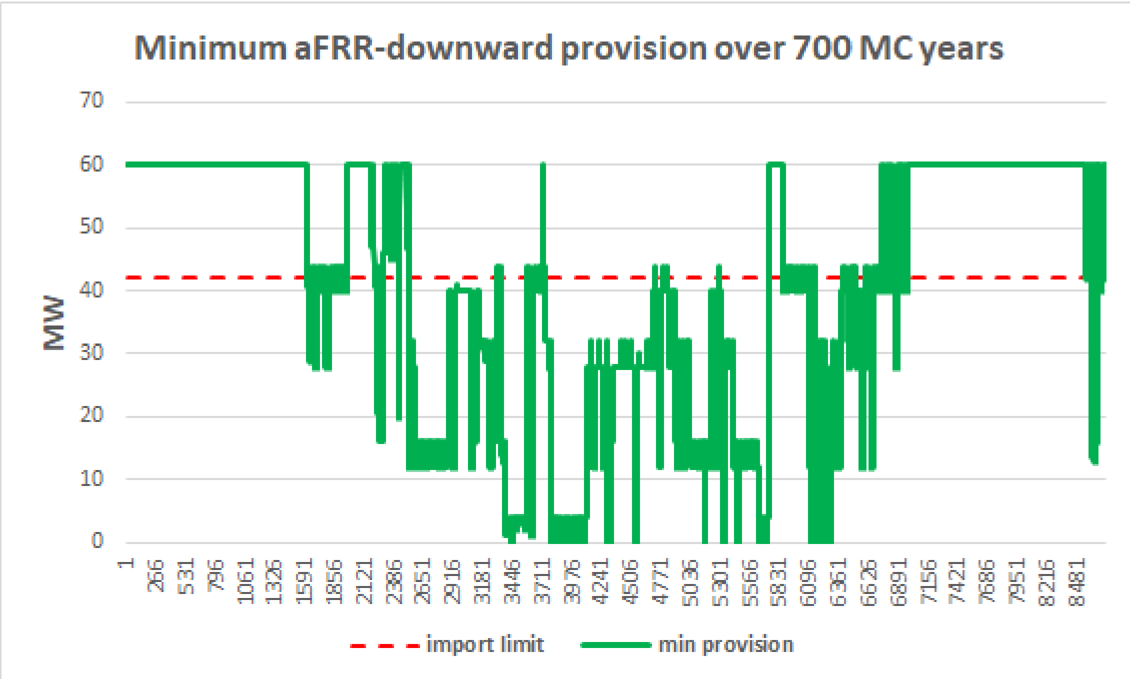

Figure 4.39 – Downward secondary reserve provision - Rapid scenario (2025)

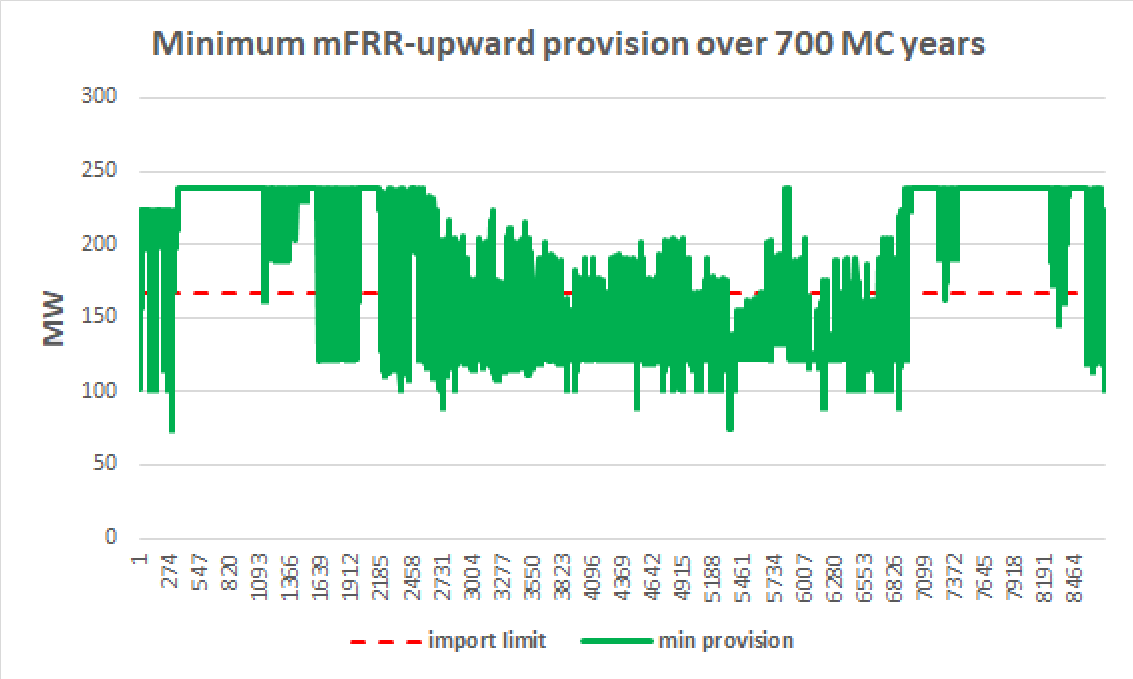

Figure 4.40 – Upward tertiary reserve provision - Rapid scenario (2025)

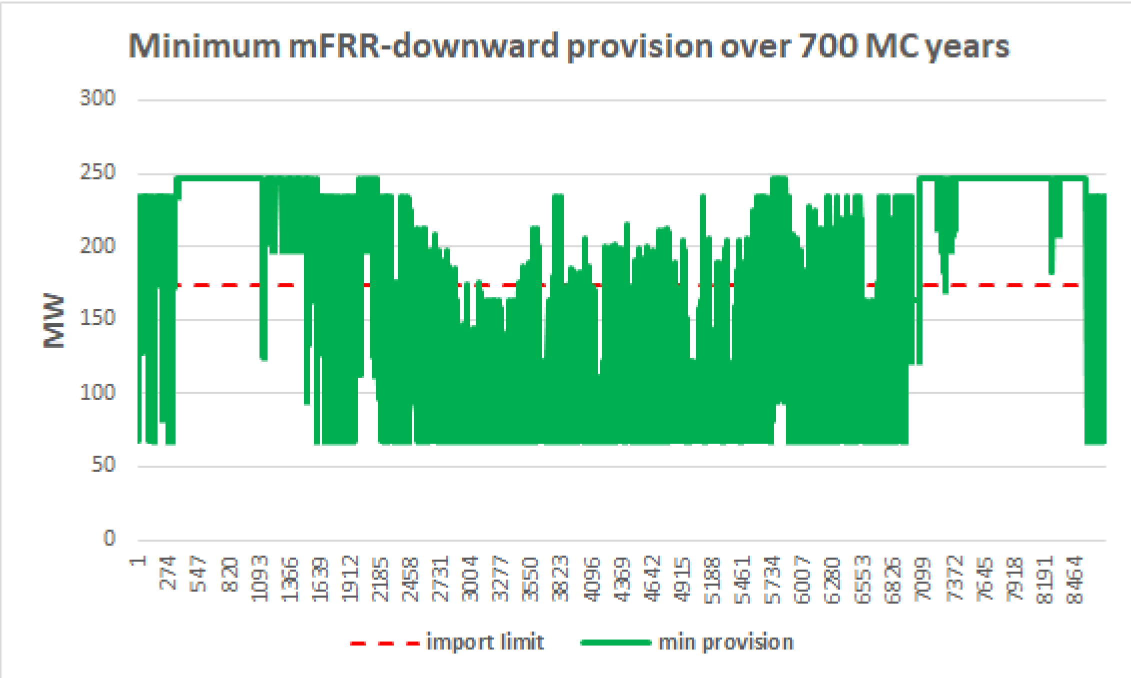

Figure 4.41 – Downward tertiary reserve provision - Rapid scenario (2025)

It can be concluded that a lack of reserve capacity occurs mainly during the summer, i.e. in the period when maintenance of thermal units is scheduled. This is especially indicative when we observe average results (over all 700 MC years) for reserve capacity provision. All values on diagrams that are below the red line indicates that more than 30% of reserve requirement by analyzed product must be allocated cross-border.

On the other hand, some additional information from the operational practice can be introduced on short-term horizon in order to model more properly the operation of the system. For instance, excluding the units which provide secondary reserve form tertiary, including of hydro power plants maintenance, etc., which can lead to more critical results.

5 CONCLUSIONS

The main conclusions related to balancing reserve sizing methodology, provided input data as well as the obtained results are presented in this chapter.

Since there is no strictly defined methodology for balancing reserve (secondary and tertiary) sizing in case of high VRE penetration (i.e. on long-term planning horizon) the best practice from European TSO's as well as the consultant's experience in VRE integration studies were used in order to develop the methodology for balancing reserve sizing in MEPSO control area. The methodology was developed completely in line with SOGL and relays on ENTSO-E SAFA document, i.e. on recommendations adapted to North Macedonia. However, it should be emphasized that there is no still explicit methodology for secondary reserve (aFRR) sizing on European level. Therefore, all results related to the share of aFRR and mFRR component within total FRR should be interpreted according to assumed rule for aFRR sizing in MEPSO control area. In order to establish the methodology for aFRR sizing in MEPSO control area, continuous calculations and testing of hypotheses are needed on short-term planning horizon. However, in order to do so, it is very important to collect and store all historic data related to system imbalances, reserve activations and forecast errors.

The key assumption used in methodology is the analysis of future system imbalances, which are forecasted depending on the pattern of provided historic time-series (forecast errors) and as well as all scenario specific assumptions (forecasted hourly time-series for load, wind and solar, generation mix, etc.). It should be emphasized that total system imbalance was calculated taking into account all individual sources of imbalances (load, renewables and thermal power plants). In addition, system imbalance decomposition to 1-hour component (due to forecast errors) and 15-min component (due to ramping) was used in order to obtain time series with 15-min resolution. Forecast error component (i.e. 1-hour component) was estimated by generating synthetic time-series in ANTARES software tool, based on historic data for existing wind and solar power plants, as well as data related to the electricity consumption from ENTSO-E Transparency platform. Finally, since future system imbalance forecasting can lead to uncertainties, a Monte Carlo approach was adopted in order to get more realistic results. It should be emphasized here that the quality of obtained results is directly connected to the quality of provided input data.

The main drivers for increase of required secondary and tertiary reserve are increase of forecast error (in sense of absolute value) due to increase of VRE installed capacity as well as an increase of ramping needs. Since the impact of assumed VRE forecast error can be significant as installed capacity increases, the sensitivity analysis with different levels of VRE nRMSE, greater and lower of calculated "natural" forecast error, has been conducted in order to reflect enhancement of forecast procedure in the future as well as the other effects that were neglected such as correlation between forecast errors of individual power plants.

An increase of required level of secondary and tertiary reserve with installed VRE capacity has relatively low slope in case with relatively low installed VRE capacities, since the load forecast error and ramping have more dominant influence to system imbalance. Therefore, it can be concluded that installing of additional 500 MW in VRE has no significant impact on balancing requirements regardless of VRE forecast error level (nRMSE). The similar situation is with FRR components, i.e. secondary (aFRR) and tertiary (mFRR) reserve, with increase of aFRR needs by only 4 MW.

On the other hand, the situation is more complex with increase of VRE installed capacity, above 500 MW. For instance, required level of total secondary and tertiary reserve in case of Rapid scenario 2025, with VRE installed capacity of 1363 MW leads to increase of reserve requirements between 16 MW and 283 MW, depending on the VRE forecast error level. If we assume VRE nRMSE level of 6% in 2025 as the most reasonable assumption, required additional capacity for balancing is around 65 MW (around 21 MW for aFRR and 44 for mFRR).

On the other hand, preliminary market analysis in ANTARES, for Rapid scenario and target year 2025, shows that required level of secondary and tertiary reserve capacity can be provided if all hydro and thermal units are included in these services as well as taking into account the support from other members of SMM block (from EMS and CGES control area) during critical hours and all scenario specific assumptions, such as commissioning of new gas fired units and decommissioning of old lignite fired power plants. However, it should be noted that under specific conditions, for instance in case of climatic year 2008 and randomly generated forced outages of thermal units it can happen that a lack of reserve can be greater than 30% of required reserve level for the observed product (aFRR or mFRR upward and downward). On the other hand, it should be emphasized that calculated reserve levels are more conservative since the impact of the control block was not considered. In order to reduce the level of required reserve common dimensioning within SMM block should be carried out, which is out of the scope of this study and implies the cooperation of all block members.

Furter increase of VRE installed capacity leads to increased needs for balancing capacity. The dependency can be expressed approximately as a linear function with fixed slope of 14%, 19%, 25%, 31% and 37% depending on VRE forecast error level (4% to 12%). The assessment of Macedonian power system capability to provide required level of upward and downward margin for all other scenarios and target years will be carried out in the next phase of the study, as a regular output of market simulations.

All results presented here which depict the impact of VRE on secondary and tertiary reserve required level depends on many input assumptions and quality of provided input data. However, the goal of the study is to estimate an expected level of required reserve for analyzed scenarios as well as to develop the methodology for reserve sizing. Therefore, all results presented here are general results for future system state calculated on long-term planning horizon. All analyses should be repeated with more precise data on mid and short-term horizon in order to estimate more realistic values. In other words, at least, 15-min data should be provided for VRE and load realizations, while in case of open-loop ACE, 1-min data should be provided as well as in order to get a better quality of performed calculations. In addition, the analyses should be repeated sequentially after addition of a few MW in VRE, for instance when additional X MW of VRE capacity are installed. Using this method, the input assumptions will be corrected. Finally, time granularity related to input data is also of interest.

It should be also emphasized that according to the analysis of provided input data, it can be concluded that load forecast was always overestimated in the past. In other words, load forecast error probability density function was positively shifted which causes increased requirements for secondary and tertiary reserve in downward direction compared to the situation in reality (i.e. analyzed ACE open-loop form history). Since the load forecast error level has a significant influence on FRR requirements some improvements of the load forecast should be done in the future as well. Similar is the situation with forecast errors for renewables (due to low installed capacity in the present, since only one wind power plant and distributed solar PV panels exist).

Therefore, in order to get more accurate results related for reserve sizing in the future, it is recommended that all necessary data from history should be stored by the MEPSO and accompany quality analysis of data should be performed. In order to achieve that, the following information should be stored:

- 15-min (or hourly) load forecast and realization
- 15-min (or hourly) wind and solar forecast and realization
- 1-min (or 15-min) Area Control Error (ACE)
- 15-min (or hourly) balancing reserve activation
- Unavailable power due to forced outages of thermal power plants

All these data should be statistically analyzed and processed in order to obtain all necessary information for balancing reserve sizing on short-term horizon by the MEPSO in the future.

Finally, here are listed some planning and operational measures that can decrease required balancing reserve level:

- Better quality of load, wind and solar forecasts
- Common dimensioning in SMM control block
- Moving to 15-min dispatch interval in the future

Measures that can increase available capacity for balancing reserve are:

- Installation of additional battery storage systems (for PV peak shaving)
- Demand side response
- Construction of pumped storage power plant Cebren

However, the impact of individual measures can be evaluated only by conducting additional sensitivity analyses for specific scenario of VRE development and applied operational measure.

6 REFERENCES

[1] **"TYNDP 2022 – Scenario Building Guidelines"**, ENTSO-E; April 2022

[2] **"TYNDP 2022 – Scenario Report"**, ENTSO-E; April 2022

[3] **"Balancing power and variable renewables: Three links"**, Lion Hirth, nkaZiegenhagen, April 2015.

[4] **"A new method for day-ahead sizing of control reserve in Germanyunder a 100% renewable energy sources scenario"**; D. Jost, M. Speckmann, F. Sandau; November 2014.

[5] **"Студија за проценка на вкупните трошоци за интегрирање на ОИЕ во ЕЕС на Македонија";** MEPSO, April 2017.

[6] **"A Probabilistic Methodology for Estimating Reserve Requirement and Optimizing Its Components in Systems With High Wind Penetration"**; Mohammed Saber Eltohamy; Hossam E. A. Talaat; Mohammed Said Abdel Moteleb; Said Fouad Mekhamer; Walid A. Omran; October 2022

[7] **"A Comparison of Wind Power and Load Forecasting Error Distributions"**, Bri-Mathias Hodge, Anthony Florita, Kirsten Orwig, Debra Lew, and Michael Milligan; NREL, May 2012

[8] **"Metrics for Evaluating the Accuracy of Solar Power Forecasting"**, J. Zhang, B.-M. Hodge, and A. Florita, S. Lu and H. F. Hamann, V. Banunarayanan, NREL, October 2013

[9] **"Wind Power Forecasting Error Distributions: An International Comparison"**; B.-M. Hodge, D. Lew, and M. Milligan, H. Holttinen, S. Sillanpää, E. Gómez-Lázaro, R. Scharff and L. Söder, X. G. Larsén, G. Giebel, D. Flynn, J. Dobschinski

[10] **"Statistical distribution for wind power forecast error and its application to determine optimal size of energy storage system"**; Junli Wu, Buhan Zhang, Hang Li, Zhongcheng Li, Yi Chen, Xiaogang Miao, September, 2013.

[11] **"Studija zajedničkog dimenzionisanja FRR rezerve u okviru SMM kontrolnog bloka "**; EMS, CGES, MEPSO, EKC, December 2022.

[12] **"Methodology for the dimensioning of the aFRR needs"**, Public Consultation, Elia, June 2020

[13] **"WB21-MKD-ENE-03 North Macedonia, Strengthening the Transmission Network in the Southeast Region of North Macedonia - Component 1- Final Report"**, November 2021

[14] **"Energy development Strategy in North Macedonia"**, December 2019

[15] **"GRID CODE – Rules for Electrical Transmission System Operation"**, MEPSO; December 2019

[16] **"Ten-Year Network Development Plan (TYNDP) 2022"**; ENTSO-E; 2022.

[17] **"ENTSO-E Transparency platform"**; https://transparency.entsoe.eu/

7 APPENDIX

7.1 Modeling of reserve in ANTARES software tool

In order to model correctly the reserve in market simulation with ANTARES software tool (secondary and tertiary for both directions upward and downward), the following set of linear constraints have been introduced:

$$\sum_{k\in\mathcal{G}} aFRR_{up,k} + \Delta P_{imp,aFRR_{up}} \geq aFRR_{up}$$

$$\sum_{k\in\mathcal{G}} aFRR_{down,k} + \Delta P_{imp,aFRR_{down}} \geq aFRR_{down}$$

$$\sum_{k\in\mathcal{G}} mFRR_{up,k} + \Delta P_{imp,mFRR_{up}} \geq mFRR_{up}$$

$$\sum_{k\in\mathcal{G}} mFRR_{down,k} + \sum_{k\in\mathcal{G}_H} v_k \cdot P_k^{min} + \Delta P_{imp,mFRR_{down}} \geq mFRR_{down}$$

$$F_{RS00\to MK00} + \Delta P_{imp,aFRR_{up}} + \Delta P_{imp,mFRR_{up}} \leq NTC_{RS00\to MK00}$$

$$F_{MK00\to RS00} + \Delta P_{imp,aFRR_{down}} + \Delta P_{imp,mFRR_{down}} \leq NTC_{MK00\to RS00}$$

$$aFRR_{up,k} + mFRR_{up,k} \leq u_k \cdot P_k^{max} - P_k$$

$$aFRR_{down,k} + mFRR_{down,k} \leq P_k - u_k \cdot P_k^{min}$$

$$0 \leq aFRR_{up,k} \leq P_k^{max} - P_k^{min}$$

$$0 \leq mFRR_{up,k} \leq P_k^{max} - P_k^{min}$$

$$0 \leq aFRR_{down,k} \leq P_k^{max} - P_k^{min}$$

$$0 \leq mFRR_{down,k} \leq P_k^{max} - P_k^{min}$$

$$0 \leq \Delta P_{imp,aFRR_{up}} \leq 0.3 \cdot aFRR_{up}$$

$$0 \leq \Delta P_{imp,mFRR_{up}} \leq 0.3 \cdot mFRR_{up}$$

$$0 \leq \Delta P_{imp,aFRR_{down}} \leq 0.3 \cdot aFRR_{down}$$

$$0 \leq \Delta P_{imp,mFRR_{down}} \leq 0.3 \cdot mFRR_{down}$$

$$u_k \cdot P_k^{min} \leq P_k \leq u_k \cdot P_k^{max}$$

$$0 \leq v_k \leq u_k$$

$$u_k, v_k \in \{0.1\}$$

$$\mathcal{G}_H \subset \mathcal{G}$$

7.2 Balancing reserve dimensioning detailed results

Reserve product	Scenario	Year	NRMSE (%)	Reserve [MW]
FRR-up	Green	2025	0%	230
FRR-down	Green	2025	0%	258
aFRR-up	Green	2025	0%	41
aFRR-down	Green	2025	0%	41
mFRR-up	Green	2025	0%	189
mFRR-down	Green	2025	0%	217
FRR-up	Green	2025	4%	227
FRR-down	Green	2025	4%	259
aFRR-up	Green	2025	4%	41
aFRR-down	Green	2025	4%	41
mFRR-up	Green	2025	4%	186
mFRR-down	Green	2025	4%	219
FRR-up	Green	2025	6%	227
FRR-down	Green	2025	6%	262
aFRR-up	Green	2025	6%	41
aFRR-down	Green	2025	6%	41
mFRR-up	Green	2025	6%	186
mFRR-down	Green	2025	6%	222
FRR-up	Green	2025	8%	228
FRR-down	Green	2025	8%	266
aFRR-up	Green	2025	8%	41
aFRR-down	Green	2025	8%	41
mFRR-up	Green	2025	8%	187
mFRR-down	Green	2025	8%	226
FRR-up	Green	2025	10%	233
FRR-down	Green	2025	10%	272
aFRR-up	Green	2025	10%	41
aFRR-down	Green	2025	10%	41
mFRR-up	Green	2025	10%	192
mFRR-down	Green	2025	10%	231
FRR-up	Green	2025	12%	241
FRR-down	Green	2025	12%	278
aFRR-up	Green	2025	12%	41
aFRR-down	Green	2025	12%	41
mFRR-up	Green	2025	12%	201
mFRR-down	Green	2025	12%	237
FRR-up	Green	2030	0%	250
FRR-down	Green	2030	0%	280
aFRR-up	Green	2030	0%	50
aFRR-down	Green	2030	0%	50
mFRR-up	Green	2030	0%	201

Reserve product	Scenario	Year	NRMSE (%)	Reserve [MW]
mFRR-down	Green	2030	0%	230
FRR-up	Green	2030	4%	251
FRR-down	Green	2030	4%	291
aFRR-up	Green	2030	4%	50
aFRR-down	Green	2030	4%	50
mFRR-up	Green	2030	4%	201
mFRR-down	Green	2030	4%	241
FRR-up	Green	2030	6%	272
FRR-down	Green	2030	6%	305
aFRR-up	Green	2030	6%	50
aFRR-down	Green	2030	6%	50
mFRR-up	Green	2030	6%	222
mFRR-down	Green	2030	6%	255
FRR-up	Green	2030	8%	309
FRR-down	Green	2030	8%	326
aFRR-up	Green	2030	8%	50
aFRR-down	Green	2030	8%	50
mFRR-up	Green	2030	8%	259
mFRR-down	Green	2030	8%	276
FRR-up	Green	2030	10%	358
FRR-down	Green	2030	10%	353
aFRR-up	Green	2030	10%	50
aFRR-down	Green	2030	10%	50
mFRR-up	Green	2030	10%	308
mFRR-down	Green	2030	10%	303
FRR-up	Green	2030	12%	410
FRR-down	Green	2030	12%	385
aFRR-up	Green	2030	12%	50
aFRR-down	Green	2030	12%	50
mFRR-up	Green	2030	12%	360
mFRR-down	Green	2030	12%	335
FRR-up	Green	2040	0%	307
FRR-down	Green	2040	0%	356
aFRR-up	Green	2040	0%	92
aFRR-down	Green	2040	0%	92
mFRR-up	Green	2040	0%	215
mFRR-down	Green	2040	0%	264
FRR-up	Green	2040	4%	353
FRR-down	Green	2040	4%	398
aFRR-up	Green	2040	4%	92
aFRR-down	Green	2040	4%	92
mFRR-up	Green	2040	4%	261
mFRR-down	Green	2040	4%	306
FRR-up	Green	2040	6%	444

Reserve product	Scenario	Year	NRMSE (%)	Reserve [MW]
FRR-down	Green	2040	6%	453
aFRR-up	Green	2040	6%	92
aFRR-down	Green	2040	6%	92
mFRR-up	Green	2040	6%	352
mFRR-down	Green	2040	6%	361
FRR-up	Green	2040	8%	556
FRR-down	Green	2040	8%	524
aFRR-up	Green	2040	8%	92
aFRR-down	Green	2040	8%	92
mFRR-up	Green	2040	8%	464
mFRR-down	Green	2040	8%	432
FRR-up	Green	2040	10%	676
FRR-down	Green	2040	10%	606
aFRR-up	Green	2040	10%	92
aFRR-down	Green	2040	10%	92
mFRR-up	Green	2040	10%	584
mFRR-down	Green	2040	10%	514
FRR-up	Green	2040	12%	800
FRR-down	Green	2040	12%	695
aFRR-up	Green	2040	12%	92
aFRR-down	Green	2040	12%	92
mFRR-up	Green	2040	12%	708
mFRR-down	Green	2040	12%	603
FRR-up	Slow	2025	0%	230
FRR-down	Slow	2025	0%	258
aFRR-up	Slow	2025	0%	41
aFRR-down	Slow	2025	0%	41
mFRR-up	Slow	2025	0%	189
mFRR-down	Slow	2025	0%	218
FRR-up	Slow	2025	4%	229
FRR-down	Slow	2025	4%	259
aFRR-up	Slow	2025	4%	41
aFRR-down	Slow	2025	4%	41
mFRR-up	Slow	2025	4%	189
mFRR-down	Slow	2025	4%	218
FRR-up	Slow	2025	6%	229
FRR-down	Slow	2025	6%	259
aFRR-up	Slow	2025	6%	41
aFRR-down	Slow	2025	6%	41
mFRR-up	Slow	2025	6%	188
mFRR-down	Slow	2025	6%	218
FRR-up	Slow	2025	8%	228
FRR-down	Slow	2025	8%	259
aFRR-up	Slow	2025	8%	41

Reserve product	Scenario	Year	NRMSE (%)	Reserve [MW]
aFRR-down	Slow	2025	8%	41
mFRR-up	Slow	2025	8%	188
mFRR-down	Slow	2025	8%	219
FRR-up	Slow	2025	10%	228
FRR-down	Slow	2025	10%	260
aFRR-up	Slow	2025	10%	41
aFRR-down	Slow	2025	10%	41
mFRR-up	Slow	2025	10%	188
mFRR-down	Slow	2025	10%	219
FRR-up	Slow	2025	12%	228
FRR-down	Slow	2025	12%	261
aFRR-up	Slow	2025	12%	41
aFRR-down	Slow	2025	12%	41
mFRR-up	Slow	2025	12%	187
mFRR-down	Slow	2025	12%	220
FRR-up	Slow	2030	0%	250
FRR-down	Slow	2030	0%	278
aFRR-up	Slow	2030	0%	45
aFRR-down	Slow	2030	0%	45
mFRR-up	Slow	2030	0%	205
mFRR-down	Slow	2030	0%	233
FRR-up	Slow	2030	4%	248
FRR-down	Slow	2030	4%	280
aFRR-up	Slow	2030	4%	45
aFRR-down	Slow	2030	4%	45
mFRR-up	Slow	2030	4%	203
mFRR-down	Slow	2030	4%	235
FRR-up	Slow	2030	6%	247
FRR-down	Slow	2030	6%	283
aFRR-up	Slow	2030	6%	45
aFRR-down	Slow	2030	6%	45
mFRR-up	Slow	2030	6%	203
mFRR-down	Slow	2030	6%	238
FRR-up	Slow	2030	8%	250
FRR-down	Slow	2030	8%	289
aFRR-up	Slow	2030	8%	45
aFRR-down	Slow	2030	8%	45
mFRR-up	Slow	2030	8%	205
mFRR-down	Slow	2030	8%	244
FRR-up	Slow	2030	10%	257
FRR-down	Slow	2030	10%	295
aFRR-up	Slow	2030	10%	45
aFRR-down	Slow	2030	10%	45
mFRR-up	Slow	2030	10%	212

Reserve product	Scenario	Year	NRMSE (%)	Reserve [MW]
mFRR-down	Slow	2030	10%	250
FRR-up	Slow	2030	12%	267
FRR-down	Slow	2030	12%	304
aFRR-up	Slow	2030	12%	45
aFRR-down	Slow	2030	12%	45
mFRR-up	Slow	2030	12%	222
mFRR-down	Slow	2030	12%	259
FRR-up	Slow	2040	0%	301
FRR-down	Slow	2040	0%	348
aFRR-up	Slow	2040	0%	62
aFRR-down	Slow	2040	0%	62
mFRR-up	Slow	2040	0%	239
mFRR-down	Slow	2040	0%	286
FRR-up	Slow	2040	4%	303
FRR-down	Slow	2040	4%	359
aFRR-up	Slow	2040	4%	62
aFRR-down	Slow	2040	4%	62
mFRR-up	Slow	2040	4%	241
mFRR-down	Slow	2040	4%	297
FRR-up	Slow	2040	6%	328
FRR-down	Slow	2040	6%	376
aFRR-up	Slow	2040	6%	62
aFRR-down	Slow	2040	6%	62
mFRR-up	Slow	2040	6%	266
mFRR-down	Slow	2040	6%	314
FRR-up	Slow	2040	8%	373
FRR-down	Slow	2040	8%	401
aFRR-up	Slow	2040	8%	62
aFRR-down	Slow	2040	8%	62
mFRR-up	Slow	2040	8%	311
mFRR-down	Slow	2040	8%	339
FRR-up	Slow	2040	10%	429
FRR-down	Slow	2040	10%	432
aFRR-up	Slow	2040	10%	62
aFRR-down	Slow	2040	10%	62
mFRR-up	Slow	2040	10%	367
mFRR-down	Slow	2040	10%	370
FRR-up	Slow	2040	12%	494
FRR-down	Slow	2040	12%	471
aFRR-up	Slow	2040	12%	62
aFRR-down	Slow	2040	12%	62
mFRR-up	Slow	2040	12%	432
mFRR-down	Slow	2040	12%	409
FRR-up	Rapid	2025	0%	233

Reserve product	Scenario	Year	NRMSE (%)	Reserve [MW]
FRR-down	Rapid	2025	0%	260
aFRR-up	Rapid	2025	0%	60
aFRR-down	Rapid	2025	0%	60
mFRR-up	Rapid	2025	0%	173
mFRR-down	Rapid	2025	0%	200
FRR-up	Rapid	2025	4%	249
FRR-down	Rapid	2025	4%	279
aFRR-up	Rapid	2025	4%	60
aFRR-down	Rapid	2025	4%	60
mFRR-up	Rapid	2025	4%	189
mFRR-down	Rapid	2025	4%	220
FRR-up	Rapid	2025	6%	298
FRR-down	Rapid	2025	6%	307
aFRR-up	Rapid	2025	6%	60
aFRR-down	Rapid	2025	6%	60
mFRR-up	Rapid	2025	6%	239
mFRR-down	Rapid	2025	6%	247
FRR-up	Rapid	2025	8%	364
FRR-down	Rapid	2025	8%	345
aFRR-up	Rapid	2025	8%	60
aFRR-down	Rapid	2025	8%	60
mFRR-up	Rapid	2025	8%	304
mFRR-down	Rapid	2025	8%	285
FRR-up	Rapid	2025	10%	437
FRR-down	Rapid	2025	10%	390
aFRR-up	Rapid	2025	10%	60
aFRR-down	Rapid	2025	10%	60
mFRR-up	Rapid	2025	10%	377
mFRR-down	Rapid	2025	10%	330
FRR-up	Rapid	2025	12%	516
FRR-down	Rapid	2025	12%	440
aFRR-up	Rapid	2025	12%	60
aFRR-down	Rapid	2025	12%	60
mFRR-up	Rapid	2025	12%	456
mFRR-down	Rapid	2025	12%	381
FRR-up	Rapid	2030	0%	264
FRR-down	Rapid	2030	0%	300
aFRR-up	Rapid	2030	0%	149
aFRR-down	Rapid	2030	0%	149
mFRR-up	Rapid	2030	0%	116
mFRR-down	Rapid	2030	0%	151
FRR-up	Rapid	2030	4%	433
FRR-down	Rapid	2030	4%	419
aFRR-up	Rapid	2030	4%	149

Reserve product	Scenario	Year	NRMSE (%)	Reserve [MW]
aFRR-down	Rapid	2030	4%	149
mFRR-up	Rapid	2030	4%	284
mFRR-down	Rapid	2030	4%	271
FRR-up	Rapid	2030	6%	609
FRR-down	Rapid	2030	6%	543
aFRR-up	Rapid	2030	6%	149
aFRR-down	Rapid	2030	6%	149
mFRR-up	Rapid	2030	6%	461
mFRR-down	Rapid	2030	6%	394
FRR-up	Rapid	2030	8%	798
FRR-down	Rapid	2030	8%	681
aFRR-up	Rapid	2030	8%	149
aFRR-down	Rapid	2030	8%	149
mFRR-up	Rapid	2030	8%	649
mFRR-down	Rapid	2030	8%	533
FRR-up	Rapid	2030	10%	991
FRR-down	Rapid	2030	10%	827
aFRR-up	Rapid	2030	10%	149
aFRR-down	Rapid	2030	10%	149
mFRR-up	Rapid	2030	10%	842
mFRR-down	Rapid	2030	10%	678
FRR-up	Rapid	2030	12%	1185
FRR-down	Rapid	2030	12%	976
aFRR-up	Rapid	2030	12%	149
aFRR-down	Rapid	2030	12%	149
mFRR-up	Rapid	2030	12%	1036
mFRR-down	Rapid	2030	12%	827
FRR-up	Rapid	2040	0%	350
FRR-down	Rapid	2040	0%	417
aFRR-up	Rapid	2040	0%	265
aFRR-down	Rapid	2040	0%	265
mFRR-up	Rapid	2040	0%	85
mFRR-down	Rapid	2040	0%	151
FRR-up	Rapid	2040	4%	719
FRR-down	Rapid	2040	4%	653
aFRR-up	Rapid	2040	4%	265
aFRR-down	Rapid	2040	4%	265
mFRR-up	Rapid	2040	4%	454
mFRR-down	Rapid	2040	4%	388
FRR-up	Rapid	2040	6%	1035
FRR-down	Rapid	2040	6%	880
aFRR-up	Rapid	2040	6%	265
aFRR-down	Rapid	2040	6%	265
mFRR-up	Rapid	2040	6%	770

Reserve product	Scenario	Year	NRMSE (%)	Reserve [MW]
mFRR-down	Rapid	2040	6%	614
FRR-up	Rapid	2040	8%	1363
FRR-down	Rapid	2040	8%	1125
aFRR-up	Rapid	2040	8%	265
aFRR-down	Rapid	2040	8%	265
mFRR-up	Rapid	2040	8%	1098
mFRR-down	Rapid	2040	8%	860
FRR-up	Rapid	2040	10%	1696
FRR-down	Rapid	2040	10%	1379
aFRR-up	Rapid	2040	10%	265
aFRR-down	Rapid	2040	10%	265
mFRR-up	Rapid	2040	10%	1431
mFRR-down	Rapid	2040	10%	1114
FRR-up	Rapid	2040	12%	2033
FRR-down	Rapid	2040	12%	1638
aFRR-up	Rapid	2040	12%	265
aFRR-down	Rapid	2040	12%	265
mFRR-up	Rapid	2040	12%	1768
mFRR-down	Rapid	2040	12%	1373